GRADO EN INGENIERÍA EN TECNOLOGÍAS INDUSTRIALES

TRABAJO FIN DE GRADO

Simulación de Evacuación de Campings Turísticos mediante Pathfinder

Autor: Pablo Murillo Pascual

Director: Borja Rengel Darnaculleta

Firma del Autor:

VºBº del Director:

Simulación de Evacuación de Campings Turísticos: Análisis comparativo de dos campings mediante Pathfinder

RESUMEN DEL PROYECTO

1. Introducción

Los incendios forestales en la interfaz urbano forestal (IUF) representan una de las amenazas naturales más graves para la vida humana en el sur de Europa. En 2023, el Sistema Europeo de Información sobre Incendios Forestales (EFFIS) registró más de 500 000 hectáreas quemadas en la Unión Europea (San-Miguel-Ayanz et al., 2024). El incendio de Mati (Grecia, 2018) causó 104 muertes en una zona costera de uso turístico, constituyendo el episodio más letal en Europa desde 1900. España fue el Estado miembro más afectado en 2022, con cerca de 245 000 hectáreas destruidas (Salas, 2024).

En este contexto, los campings turísticos constituyen una tipología de ocupación especialmente vulnerable. Concentran centenares de personas en espacios abiertos, generalmente rodeados de vegetación combustible, con un número reducido de salidas vehiculares. Sus ocupantes son turistas que desconocen la geografía local, pueden no hablar el idioma del país, y en muchos casos viajan en grupos familiares con distintos niveles de movilidad (Labhiri et al., 2024). En España, el Real Decreto 393/2007 (Ministerio del Interior, 2007) obliga a los establecimientos susceptibles de generar situaciones de emergencia a redactar Planes de Autoprotección con rutas de evacuación y puntos de reunión, pero estos planes raramente se validan mediante simulación cuantitativa.

La simulación de evacuación peatonal mediante modelos basados en agentes permite evaluar los planes de emergencia antes de que se produzca un siniestro real. El software Pathfinder (Thunderhead Engineering, 2024) es uno de los simuladores más utilizados en la comunidad de seguridad contra incendios y ha sido aplicado recientemente a infraestructuras turísticas en el marco del proyecto europeo WUITIPS (UCPM-2027, Acuerdo de subvención 101101169). El precedente más directo es la tesis de Labhiri (2024), que modeló la evacuación del Camping Punta Milà (Cataluña) mediante un enfoque combinado Pathfinder-SUMO. El presente estudio extiende ese trabajo en tres direcciones: modela dos campings con geometrías contrastadas para permitir un análisis comparativo; diseña una campaña de siete escenarios que aísla de forma controlada el efecto del momento del día, la disponibilidad de salidas, el protocolo de punto de reunión y el movimiento en grupos familiares; e identifica y corrige un problema de conversión de unidades en los parámetros log-normales de tiempo previo al movimiento documentado en Labhiri (2024), validado mediante pruebas de Kolmogorov-Smirnov.

El objetivo general del estudio es evaluar el rendimiento de evacuación de dos campings turísticos españoles bajo una gama de escenarios de emergencia y derivar recomendaciones operativas para los responsables de planificación. Los objetivos específicos son: (1) construir modelos Pathfinder validados de ambos campings; (2) parametrizar el comportamiento de los ocupantes con distribuciones empíricamente fundamentadas; (3) diseñar y ejecutar una campaña sistemática de escenarios; (4) extraer y comparar indicadores cuantitativos de evacuación; y (5) formular recomendaciones operativas basadas en la evidencia.

2. Metodología

El estudio analiza dos campings turísticos españoles seleccionados por ofrecer un contraste geométrico claro. Parque Ardales (PA, Málaga) es un camping extenso y alargado, emplazado en el entorno del embalse del Guadalhorce, con 500 ocupantes y una configuración de salidas que en la práctica se reduce a una sola. Cabo Mayor (CM, Santander) es un camping compacto de geometría más rectangular, con 650 ocupantes y dos salidas funcionales hacia la Avenida del Faro. La inversión de la relación habitual entre extensión y capacidad, PA es más grande, pero aloja menos ocupantes, hace que la comparación sea analíticamente valiosa.

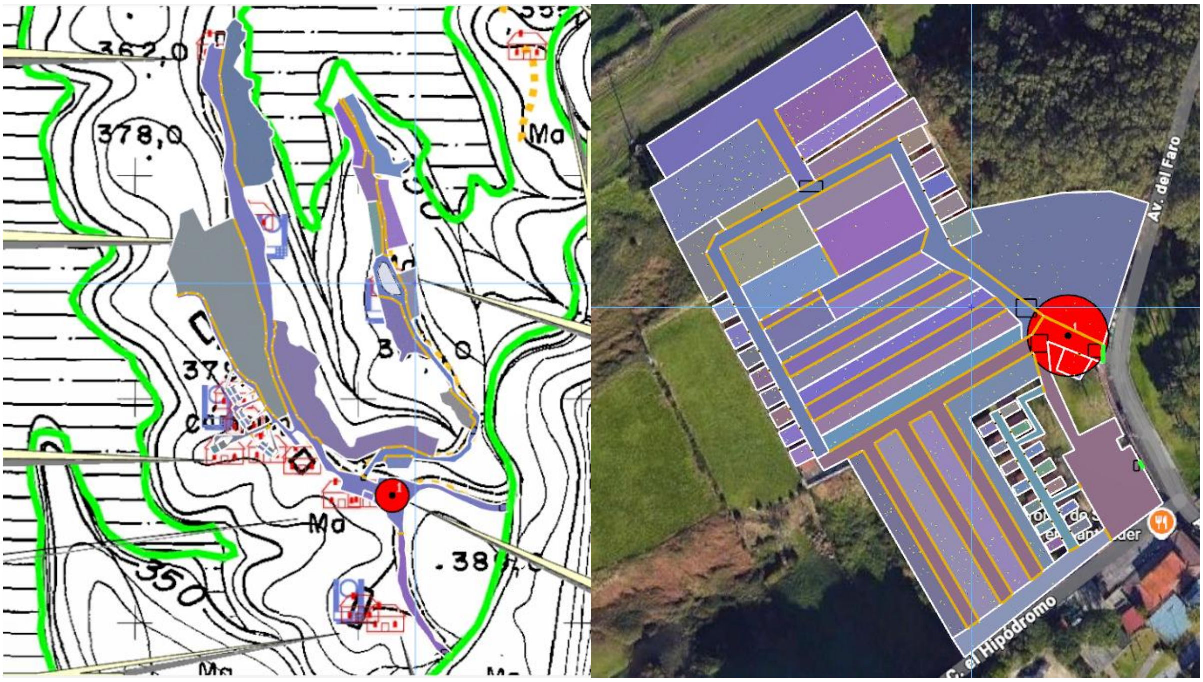

Fig. 1. Malla de navegación de Pathfinder de Parque Ardales superpuesta sobre el plano topográfico a escala del Plan de Autoprotección (Ayuntamiento de Ardales, 2012) y Cabo Mayor superpuesta sobre la imagen satelital de Google Maps.

Los modelos se construyeron en Pathfinder 2026.1.211 superponiendo la malla de navegación sobre imágenes de fondo a escala: el Plan de Autoprotección del Ayuntamiento de Ardales (2012) para PA, y una imagen satelital de Google Maps para CM. La calibración de escala se realizó mediante coordenadas UTM conocidas en PA y mediante una dimensión física verificable (la piscina del camping) en CM. Las puertas de los alojamientos privados en CM se configuraron como unidireccionales para impedir que el algoritmo de búsqueda de rutas utilizara el interior de los bungalós como atajo, una decisión que incrementó el tiempo total de evacuación en aproximadamente un 43 % respecto a la configuración bidireccional y se justifica por ser la representación físicamente realista.

Los ocupantes se distribuyeron en tres perfiles demográficos (adulto, niño, anciano) en proporciones aproximadas del 50 %, 40 % y 10 %, respectivamente. Las velocidades de marcha y anchuras de hombros se modelaron mediante distribuciones Normal truncadas, verificadas mediante la prueba de Kolmogorov-Smirnov (KS) sobre las muestras de salida de Pathfinder (adulto diurno: n = 332, D = 0,036, no rechazada al 5 %). Los límites de truncado se fijaron en los percentiles 5.º y 95.º, siguiendo la convención antropométrica de Pheasant y Haslegrave (2006).

Los tiempos previos al movimiento (pre-movement times) se modelaron mediante distribuciones log-normales derivadas de la norma PD 7974-6:2019 (BSI, 2019), categoría B para escenarios diurnos (ocupantes despiertos) y categoría Ciii para nocturnos (ocupantes dormidos). Los parámetros requirieron una conversión de unidades de minutos a segundos: para una distribución log-normal, el parámetro Localización es la media del logaritmo natural de la variable, por lo que el cambio de unidad actúa de forma aditiva mediante ln(60), mientras que el parámetro Escala (desviación típica del logaritmo) es invariante bajo esa transformación. Los parámetros resultantes son: Localización = 6,7435, Escala = 0,1487 para escenarios diurnos (límites 600-1200 s, 10-20 min); y Localización = 7,4367, Escala = 0,1487 para nocturnos (límites 1200-2400 s, 20-40 min). La corrección fue validada con KS sobre las salidas de Pathfinder (D = 0,031 para CM diurno, n = 650; D = 0,052 para PA nocturno, n = 500; ninguno rechazado al 5 %).

La campaña de simulación consta de siete escenarios por camping (Tabla 1), que varían de forma controlada el momento del día, la estrategia de evacuación (directa frente a muster), la disponibilidad de salidas y el movimiento en grupos familiares. Cada escenario se ejecutó cinco veces con semillas aleatorias independientes, totalizando 70 simulaciones en modo Steering. Se definieron cinco Regiones de Medida (MR) por camping en los puntos de convergencia de flujos y aproximaciones a las salidas, con áreas entre 7 y 55 m² en PA y entre 7 y 49 m² en CM.

Escenario	Momento	Estrategia	Salidas disponibles	Movimiento	Referencia
S1	Día	Directa	Ambas	Individual	Línea base
S2	Día	Muster	Ambas	Individual	Protocolo muster
S3	Día	Directa	Solo Salida 1	Individual	Cierre Sal. 2
S4	Día	Directa	Solo Salida 2	Individual	Cierre Sal. 1
S5	Noche	Directa	Ambas	Individual	Nocturno
S6	Noche	Muster	Ambas	Individual	Noche + muster
S7	Día	Directa	Ambas	Grupos familiares	Grupos

Tabla 1. Diseño de escenarios (idéntico en ambos campings).

3. Resultados

La Tabla 2 resume los indicadores principales de evacuación para los siete escenarios en ambos campings.

Escen.	TotalT PA (min)	TotalT CM (min)	MeanCompT PA (min)	MeanCompT CM (min)	Reparto salidas PA / CM
S1	30,6	23,6	20,3	16,3	499/1 · 78/22 %
S2	32,2	25,1	21,7	18,3	500/0 · 99,8/0,2 %
S3	32,3	23,5	21,0	16,4	0/500 · 100/0 %
S4	31,6	24,6	20,4	16,8	500/0 · 0/100 %
S5	52,7	44,1	36,7	31,2	499/1 · 78/22 %
S6	55,8	47,5	38,9	34,8	500/0 · 100/0 %
S7	34,9	24,4	24,2	18,9	499/1 · 79/21 %

Tabla 2. Resultados maestros de evacuación (medias de 5 ejecuciones por escenario).

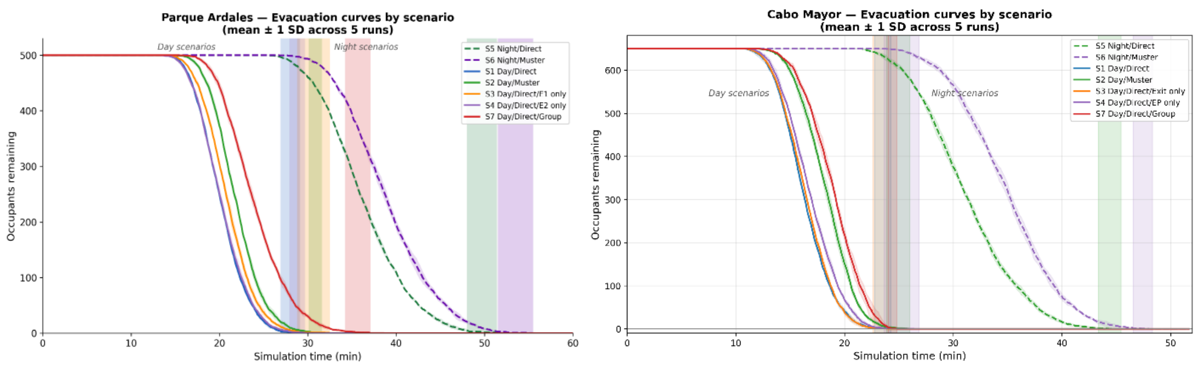

Fig. 3. Curvas de evacuación de Parque Ardales (izquierda) y Cabo Mayor (derecha): ocupantes restantes en función del tiempo de simulación, media ± 1 desviación típica de 5 ejecuciones por escenario. Los escenarios diurnos (S1-S4, S7) se agrupan a la izquierda; los nocturnos (S5-S6) se desplazan hacia la derecha.

Penalización nocturna. El momento del día es el factor dominante en ambos campings. La transición de día a noche añade +22,1 min (+72 %) en PA y +20,5 min (+87 %) en CM. La diferencia de magnitud relativa refleja que, en CM, las distancias de recorrido son un tercio de las de PA (~119 m frente a ~358 m), por lo que el tiempo previo al movimiento, cuya mediana se duplica al pasar de la categoría B a la Ciii de la PD 7974-6:2019 (de 14,1 a 28,3 min), representa una fracción mayor del tiempo total.

Configuración de salidas. PA opera como un camping de salida única de facto: 499 de 500 ocupantes utilizan la Salida 2 en todos los escenarios de línea base, a pesar de que la Salida 1 posee una capacidad física equivalente (0,86 frente a 0,89 ocu/s). La asimetría es puramente geométrica. CM, en cambio, reparte el flujo en proporción 78/22 entre la salida vehicular y la peatonal en todos los escenarios de evacuación directa, lo que le confiere una redundancia estructural de la que PA carece.

Asimetría del cierre de salidas. En PA, cerrar la salida dominante (S3) impone una penalización de +1,7 min, mientras que cerrar la marginal (S4) cuesta +1,0 min, a pesar de que la ratio de uso previa al cierre es de 499:1. En CM, el patrón se invierte: cerrar la salida peatonal minoritaria (S3, 22 % de uso) no altera prácticamente el tiempo total (−0,1 min), mientras que cerrar la salida vehicular dominante (S4) añade +1,0 min. En ambos campings, el coste del cierre depende de la longitud del camino alternativo y del número de ocupantes desplazados, no del volumen de tráfico previo en la salida cerrada.

Colapso del muster en Cabo Mayor. Cuando se activa el protocolo de muster (S2, S6), el reparto 78/22 de CM colapsa a aproximadamente 100/0: tras concentrarse en el punto de reunión frente a la recepción, el camino más corto a cualquier salida conduce inequívocamente a la salida vehicular, dejando la salida peatonal inactiva. La densidad media pico en MR_Exit bajo muster (0,47 ocu/m²) es estadísticamente indistinguible de la registrada cuando la salida peatonal está físicamente bloqueada (0,49 ocu/m² en S3). Este fenómeno, denominado colapso del muster, es el resultado operativo más significativo del estudio: el protocolo de muster, tal como está implementado, elimina la principal ventaja estructural del camping sin aportar ningún beneficio compensatorio en tiempo.

Penalización por movimiento en grupos. El escenario S7 impone una penalización de +4,3 min (+14,1 %) en PA frente a +0,8 min (+3,3 %) en CM, una diferencia de 5,4× en términos absolutos. La razón es la distancia: los mismos parámetros de cohesión de grupo (distancia máxima líder-miembro de 2,0 m) acumulan un coste mayor en corredores más largos. El tiempo de congestión cinemática por ocupante es casi idéntico en ambos campings (~125 s en PA, ~120,5 s en CM), lo que confirma que la congestión no es un fenómeno espacial (cuellos de botella) sino cinético (desaceleración del adulto líder para mantener la cohesión con los miembros más lentos).

Densidades. En ninguna de las 70 simulaciones se supera el umbral operativo de 4 ocu/m² (Oberhagemann, 2012; Helbing y Mukerji, 2012). La densidad pico máxima registrada es 0,74 ocu/m² (CM S4, MR_Exit_Peatonal), un orden de magnitud por debajo del umbral. El déficit de velocidad cinemática es nulo en todos los escenarios sin grupos (S1-S6). Ambos campings operan en un régimen limitado por el tiempo de desplazamiento, no por las colas en las salidas.

4. Conclusiones

El estudio produce seis conclusiones principales. Primera: ambos campings operan en un régimen limitado por el tiempo de desplazamiento. El factor limitante de la evacuación no es la capacidad de las salidas sino la suma del tiempo previo al movimiento y el tiempo de recorrido; no se forma ninguna cola sostenida en ninguna salida en ninguna de las 70 simulaciones.

Segunda: el momento del día es el eje de variación dominante, con una penalización nocturna de +22,1 min en PA (+72 %) y +20,5 min en CM (+87 %), que supera con amplitud el efecto de cualquier otro factor de escenario. Este resultado es una consecuencia directa de la distribución log-normal de los tiempos previos al movimiento extraída de la norma PD 7974-6:2019.

Tercera: la asimetría del cierre de salidas se invierte entre campings. En PA, cerrar la salida menos utilizada cuesta más tiempo que cerrar la dominante; en CM ocurre lo contrario. El coste del cierre depende de la combinación entre el número de ocupantes desplazados y la calidad del camino alternativo disponible, no del volumen de tráfico previo en la salida cerrada.

Cuarta: el colapso del muster en Cabo Mayor es un hallazgo original del estudio. La posición geométrica del punto de reunión junto a la salida vehicular principal convierte el protocolo de muster en un mecanismo que elimina la redundancia de dos salidas del camping sin reducir el tiempo de evacuación. Las pruebas exploratorias de reubicación del punto de reunión confirmaron que la penalización del muster se debe al tiempo de espera, no al efecto de enrutamiento, por lo que la recomendación no es reubicar el punto de reunión para ganar tiempo, sino rediseñar el protocolo para preservar la distribución de flujo entre salidas.

Quinta: la penalización por movimiento en grupos escala con la distancia media de recorrido. La diferencia de 5,4× en la penalización absoluta entre PA y CM es proporcional a la diferencia de 3,0× en la distancia media de S1, con un mecanismo cinético que acumula retardo de forma lineal a lo largo del corredor de evacuación.

Sexta: la corrección de la conversión de unidades para los parámetros log-normales de tiempo previo al movimiento es una contribución metodológica con aplicabilidad general. La transformación $\mu_s = \mu_{min} + \ln(60)$, con σ invariante, reproduce en segundos la distribución que la norma PD 7974-6:2019 describe matemáticamente en minutos, y se aplica a cualquier estudio Pathfinder que extraiga tiempos previos al movimiento de dicha norma.

Las recomendaciones operativas principales son: (1) instalar sistemas de alerta acústica en todas las unidades de alojamiento para reducir el tiempo previo al movimiento nocturno, que es el factor de mayor palanca en ambos campings; (2) proteger la Salida 2 de PA de obstrucciones, pues el camping depende de ella en un 99,8 % de los casos; (3) rediseñar el protocolo de muster de CM para preservar la distribución de flujo entre salidas, ya sea adoptando un esquema de dos puntos de reunión por sectores o sustituyendo el muster centralizado por un recuento por salidas.

5. Referencias

British Standards Institution. (2019). PD 7974-6:2019. Application of fire safety engineering principles to the design of buildings. Part 6: Human factors. BSI.

Helbing, D., & Mukerji, P. (2012). Crowd disasters as systemic failures: Analysis of the Love Parade disaster. EPJ Data Science, 1(1), Article 7.

Labhiri, A. (2024). Informing wildfire evacuation guidelines in touristic areas [Master's thesis, Lund University].

Labhiri, A., Ronchi, E., & Rohaert, A. (2024). A scoping review of tourist evacuation behavior in wildfire scenarios. Safety Science, 175, Article 106516.

Ministerio del Interior. (2007). Real Decreto 393/2007, Norma Básica de Autoprotección. BOE, 72, 12841-12850.

Oberhagemann, D. (2012). Static and dynamic crowd densities at major public events (Technical Report TB 13-01). vfdb.

Pheasant, S., & Haslegrave, C. M. (2006). Bodyspace: Anthropometry, ergonomics and the design of work (3rd ed.). CRC Press.

Ronchi, E., & La Mendola, S. (2016). Sensitivity analysis of evacuation model results using the Kolmogorov-Smirnov test. Lund University.

Salas, J. (2024, March 12). Spain broke its own wildfire record in 2022. El País English.

San-Miguel-Ayanz, J., et al. (2024). Forest fires in Europe, Middle East and North Africa 2023 (JRC Technical Report). Publications Office of the EU.

Thunderhead Engineering. (2024). Pathfinder technical reference manual (Version 2024.1). Thunderhead Engineering Consultants, Inc.

Wildfire evacuation simulation of tourist campings: comparative analysis of two sites using pathfinder

PROJECT SUMMARY

1. Introduction

Wildfires at the wildland-urban interface (WUI) are one of the most severe natural hazards for human life in southern Europe. In 2023, the European Forest Fire Information System (EFFIS) recorded over 500,000 hectares of burned area across the European Union (San-Miguel-Ayanz et al., 2024). The 2018 Mati fire in Greece killed 104 people in a coastal tourist area, making it the deadliest wildfire event in Europe since 1900. Spain was the worst-affected EU member state in 2022, with nearly 245,000 hectares destroyed (Salas, 2024).

Tourist campings are a particularly vulnerable occupancy type in this context. They concentrate hundreds of people in open-air settings surrounded by combustible vegetation, with a limited number of vehicular exit gates. Their occupants are unfamiliar with the local geography, may not speak the local language, and frequently travel in family groups with varying mobility levels (Labhiri et al., 2024). In Spain, Real Decreto 393/2007 (Ministerio del Interior, 2007) requires establishments capable of generating emergency situations to develop Self-Protection Plans with evacuation routes and assembly points, but these plans are rarely validated through quantitative simulation.

Agent-based pedestrian evacuation simulation offers a means to close this gap. Pathfinder (Thunderhead Engineering, 2024) is one of the most widely used simulators in the fire safety engineering community and has been applied to tourist infrastructure in the context of the European WUITIPS project (UCPM-2027, Grant Agreement 101101169). The most directly relevant prior study is the thesis of Labhiri (2024), who modeled the evacuation of Camping Punta Milà (Catalonia) using a coupled Pathfinder-SUMO approach. The present study extends that work in three directions: it models two campings with contrasting geometries to enable comparative analysis; it designs a seven-scenario campaign that isolates in a controlled manner the effects of time of day, exit availability, muster protocol, and family-group movement; and it identifies and corrects a unit-conversion issue in the log-normal pre-movement parameters derived from Labhiri (2024), validated through Kolmogorov-Smirnov tests.

The overarching goal is to evaluate the evacuation performance of two Spanish tourist campings under a range of emergency scenarios and to derive evidence-based recommendations for emergency planners. The five specific objectives are: (1) construct validated Pathfinder models of both campings; (2) configure occupant behavior through empirically grounded parameter distributions; (3) design and execute a systematic scenario campaign; (4) extract and compare quantitative evacuation indicators; and (5) formulate operational recommendations.

2. Methodology

The study analyzes two Spanish tourist campings selected for their geometric contrast. Parque Ardales (PA, Málaga) is a large, elongated camping set within the Guadalhorce reservoir natural park, with 500 occupants and an exit configuration that reduces in practice to a single gate. Cabo Mayor (CM, Santander) is a compact, rectangular camping with 650 occupants and two functional exit gates onto the Avenida del Faro. The inversion of the usual relationship between site area and capacity, PA is larger but holds fewer occupants, makes the pairing analytically useful.

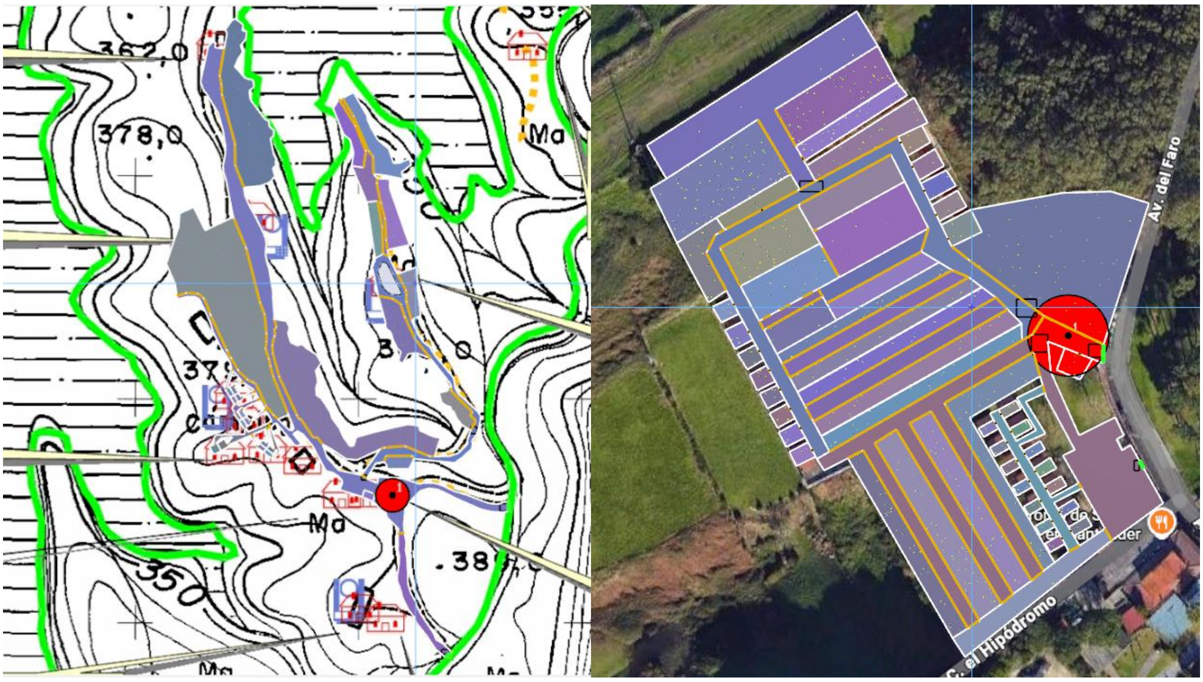

Fig. 1. Pathfinder navigation mesh of Parque Ardales overlaid on the scaled topographic plan (Ayuntamiento de Ardales, 2012) and Cabo Mayor overlaid on the Google Maps satellite image.

Models were constructed in Pathfinder 2026.1.211 by superimposing navigation meshes over scaled background images: the official Self-Protection Plan (Ayuntamiento de Ardales, 2012) for PA, and a Google Maps satellite image for CM. Scale calibration used UTM coordinates for PA and a known physical dimension (the swimming pool) for CM. Private accommodation doors at CM were configured as one-way to prevent the routing algorithm from treating bungalow interiors as shortcuts, a decision that increased total evacuation time by approximately 43% relative to the bidirectional configuration and represents the more physically realistic, conservative estimate.

Occupants were distributed across three demographic profiles (Adult, Child, Elderly) in approximate proportions of 50%, 40%, and 10%, respectively. Walking speed and shoulder width were modeled as truncated Normal distributions, verified by Kolmogorov-Smirnov tests on Pathfinder output samples (Adult_Day: $n = 332$, $D = 0.036$, not rejected at 5%). Truncation bounds were set at the 5th and 95th percentiles, following the anthropometric convention of Pheasant and Haslegrave (2006).

Pre-movement times were modeled as log-normal distributions derived from PD 7974-6:2019 (BSI, 2019), Category B for daytime scenarios (awake occupants) and Category Ciii for nighttime (sleeping occupants). Converting from minutes to seconds requires care: for a log-normal distribution, the Location parameter is the mean of the natural logarithm of the variable, so the unit change acts additively as ln(60), while the Scale parameter (standard deviation of the logarithm) is invariant under that transformation. The resulting parameters are: Location = 6.7435, Scale = 0.1487 for daytime (bounds 600-1200 s); Location = 7.4367, Scale = 0.1487 for nighttime (bounds 1200-2400 s). The correction was validated by KS tests on Pathfinder output (D = 0.031 for CM daytime, n = 650; D = 0.052 for PA nighttime, n = 500; neither rejected at 5%).

The simulation campaign comprises seven scenarios per camping (Table 1), varying time of day, evacuation strategy (direct vs. muster-first), exit availability, and family-group movement. Each scenario was executed five times with independent random seeds, yielding 70 runs in Steering mode. Five Measurement Regions (MRs) per camping were placed at flow-convergence points and exit approaches, with areas between 7 and 55 m² at PA and between 7 and 49 m² at CM.

Scenario	Time of day	Strategy	Exits available	Movement	Role
S1	Day	Direct	Both	Individual	Baseline
S2	Day	Muster	Both	Individual	Muster protocol
S3	Day	Direct	Exit 1 only	Individual	Close Exit 2
S4	Day	Direct	Exit 2 only	Individual	Close Exit 1
S5	Night	Direct	Both	Individual	Nighttime
S6	Night	Muster	Both	Individual	Night + muster
S7	Day	Direct	Both	Family groups	Groups

Table 1. Scenario design (identical at both campings).

3. Results

Table 2 summarizes the principal evacuation indicators for all seven scenarios at both campings.

Scenario	TotalT PA (min)	TotalT CM (min)	MeanCompT PA (min)	MeanCompT CM (min)	Exit split PA / CM
S1	30.6	23.6	20.3	16.3	499/1 · 78/22%
S2	32.2	25.1	21.7	18.3	500/0 · 99.8/0.2%
S3	32.3	23.5	21.0	16.4	0/500 · 100/0%
S4	31.6	24.6	20.4	16.8	500/0 · 0/100%

S5	52.7	44.1	36.7	31.2	499/1 · 78/22%
S6	55.8	47.5	38.9	34.8	500/0 · 100/0%
S7	34.9	24.4	24.2	18.9	499/1 · 79/21%

Table 2. Master evacuation results (means across 5 runs per scenario).

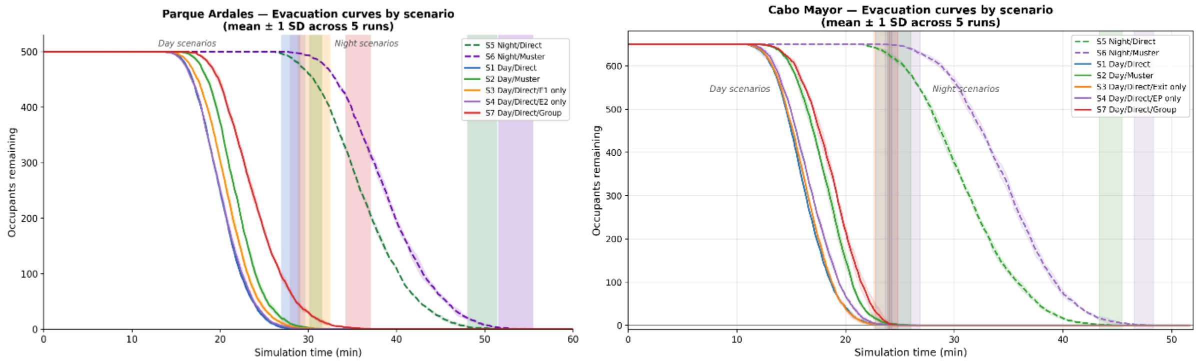

Fig. 3. Evacuation curves for Parque Ardales (left) and Cabo Mayor (right): occupants remaining versus simulation time, mean across 5 runs. Day scenarios cluster at left; night scenarios at right.

Night-time penalty. Time of day is the dominant axis of variation at both campings. The day-to-night transition adds +22.1 min (+72%) at PA and +20.5 min (+87%) at CM. The larger relative penalty at CM reflects the shorter baseline walking distances (~119 m vs. ~358 m): the pre-movement median, which doubles from 14.1 to 28.3 min when moving from PD 7974-6:2019 Category B to Ciii, accounts for a larger fraction of CM's shorter total evacuation time.

Exit configuration. PA operates as a de-facto single-exit camping: 499 of 500 occupants use Exit 2 in all baseline scenarios despite Exit 1 possessing equivalent physical capacity (0.86 vs. 0.89 occ/s). The asymmetry is purely geometric. CM, by contrast, distributes its 650 occupants in a stable 78/22 split between the vehicular and pedestrian gates in all direct evacuation scenarios, providing structural redundancy that PA entirely lacks.

Exit-closure asymmetry. At PA, closing the dominant exit (S3) imposes a +1.7 min penalty while closing the marginal exit (S4) costs +1.0 min, despite the pre-closure usage ratio being 499:1. At CM the pattern inverts: closing the minority pedestrian gate (S3, 22% usage) barely changes total time (−0.1 min), while closing the dominant vehicular gate (S4) adds +1.0 min. At both sites the closure penalty tracks the interaction between displaced-occupant count and alternative-path quality, not pre-closure traffic volume.

Muster collapse at Cabo Mayor. When the muster protocol is activated (S2, S6), the 78/22 CM split collapses to approximately 100/0: after assembling at the reception muster point, the shortest onward path to any exit unambiguously favors the vehicular gate, leaving the pedestrian gate idle. The mean peak density at MR_Exit under muster (0.47 occ/m²) is statistically indistinguishable from the value when the pedestrian gate is physically locked

(0.49 occ/m² in S3). This muster-collapse phenomenon is the most operationally significant finding of the study: the muster protocol, as implemented, eliminates the camping's principal structural safety advantage without delivering any compensating time benefit.

Group-movement penalty. Scenario S7 imposes a +4.3 min penalty (+14.1%) at PA but only +0.8 min (+3.3%) at CM, a 5.4× ratio in absolute terms. The mechanism is distance: the same group-cohesion parameters (maximum leader-member distance of 2.0 m) accumulate a larger time cost over longer corridors. Mean kinematic congestion time per occupant is nearly identical at both sites (~125 s at PA, ~120.5 s at CM), confirming that congestion is kinematic rather than spatial, adult leaders decelerate to maintain proximity to slower children and elderly members rather than forming spatial queues at bottlenecks.

Density regime. No run across the 70-simulation campaign records a density at or above the 4 occ/m² operational threshold (Oberhagemann, 2012; Helbing & Mukerji, 2012). The highest single-run peak is 0.74 occ/m² (CM S4 Run 5, MR_Exit_Peatonal), an order of magnitude below the threshold. Zero kinematic congestion is recorded in any of the 60 ungrouped runs (S1-S6). Both campings operate firmly in a travel-time-limited regime.

4. Conclusions

Six principal conclusions emerge from the seventy-run simulation campaign. First, both campings operate in a travel-time-limited regime: no sustained queuing forms at any exit in any run, and the binding constraint on evacuation time is the combination of pre-movement delay and walking distance, not exit capacity.

Second, time of day is the dominant axis of variation, with a night-time penalty of +22.1 min at PA (+72%) and +20.5 min at CM (+87%) that dwarfs the effect of every other scenario factor. This is a direct consequence of the log-normal pre-movement distribution derived from PD 7974-6:2019, whose night median is approximately twice the day median.

Third, exit-closure asymmetry inverts between sites. The direction of the penalty depends on the interaction between displaced-occupant count and alternative-path quality, not on traffic volume alone. Geometric route analysis, rather than exit-usage statistics, is the appropriate tool for assessing closure vulnerability.

Fourth, the muster-collapse phenomenon at Cabo Mayor is an original finding: the muster protocol converts a genuine dual-exit camping into a de-facto single-exit system, eliminating redundancy without reducing time. Exploratory testing confirmed that the penalty is driven by the muster wait time rather than by routing distortion, so the recommendation is to redesign the protocol to preserve dual-exit load distribution rather than to relocate the assembly point.

Fifth, the group-movement penalty scales with mean walking distance, producing a 5.4× absolute difference between PA and CM that is proportional to the 3.0× difference in baseline distances. The per-occupant kinematic congestion time is site-invariant (~122 s), confirming a cinematic rather than spatial congestion mechanism.

Sixth, the unit-conversion correction for log-normal pre-movement parameters ($\mu_s = \mu_{min} + \ln(60)$, σ invariant) is a methodological contribution with applicability to any Pathfinder study drawing pre-movement times from PD 7974-6:2019.

The principal operational recommendations are: (1) install audible alarm systems in all accommodation units to reduce nighttime pre-movement time, the factor with the largest single leverage on evacuation duration at both sites; (2) protect Exit 2 at Parque Ardales from obstruction, as the camping depends on it in 99.8% of all simulated scenarios; and (3) redesign the Cabo Mayor muster protocol to preserve dual-exit load distribution, either by adopting a sector-based two-point muster scheme or by replacing the centralized assembly step with a per-exit headcount.

5. References

British Standards Institution. (2019). PD 7974-6:2019. Application of fire safety engineering principles to the design of buildings. Part 6: Human factors. BSI.

Helbing, D., & Mukerji, P. (2012). Crowd disasters as systemic failures: Analysis of the Love Parade disaster. EPJ Data Science, 1(1), Article 7.

Labhiri, A. (2024). Informing wildfire evacuation guidelines in touristic areas [Master's thesis, Lund University].

Labhiri, A., Ronchi, E., & Rohaert, A. (2024). A scoping review of tourist evacuation behavior in wildfire scenarios. Safety Science, 175, Article 106516.

Ministerio del Interior. (2007). Real Decreto 393/2007, Norma Básica de Autoprotección. BOE, 72, 12841-12850.

Oberhagemann, D. (2012). Static and dynamic crowd densities at major public events (Technical Report TB 13-01). vfdb.

Pheasant, S., & Haslegrave, C. M. (2006). Bodyspace: Anthropometry, ergonomics and the design of work (3rd ed.). CRC Press.

Ronchi, E., & La Mendola, S. (2016). Sensitivity analysis of evacuation model results using the Kolmogorov-Smirnov test. Lund University.

Salas, J. (2024, March 12). Spain broke its own wildfire record in 2022. El País English.

San-Miguel-Ayanz, J., et al. (2024). Forest fires in Europe, Middle East and North Africa 2023 (JRC Technical Report). Publications Office of the EU.

Thunderhead Engineering. (2024). Pathfinder technical reference manual (Version 2024.1). Thunderhead Engineering Consultants, Inc.

Table of Contents

Chapter 1. Introduction

1.1 Motivation

Wildfire risk in southern Europe has intensified markedly over the past two decades. The year 2023 was one of the worst for wildfires in the European Union since systematic monitoring began in 2000, with approximately 500,000 hectares of land burned across EU member states (San-Miguel-Ayanz et al., 2024). The largest single fire event ever recorded by the European Forest Fire Information System (EFFIS) occurred near Alexandroupolis, Greece, consuming approximately 96,000 hectares in August 2023. The previous year, 2022, had already been the second worst on record, with Spain alone accounting for over 245,000 hectares of burned area (Salas, 2024). These figures represent not only ecological and economic losses, estimated at over 2.5 billion euros annually across the EU (Joint Research Centre, 2023), but also a direct threat to human life: at least 41 people died in forest fires in the EU in 2023, and the 2018 Mati fire in Greece killed 104 people in a single event, many of them trapped while attempting to evacuate.

Within this broader crisis, the intersection of wildfire risk and tourism creates a specific and under-studied vulnerability. Mediterranean Europe's most regions prone to fire are also its most popular tourist destinations: coastal areas of Spain, Portugal, Greece, and southern France draw tens of millions of visitors each summer, precisely during peak fire season. Tourist campings are particularly exposed because they concentrate hundreds of transient occupants in open air settings, often surrounded by vegetation that constitutes available fuel. Unlike permanent residents, camping tourists are typically unfamiliar with the local geography, may not speak the local language, may not have immediate access to a vehicle, and have no prior experience of evacuation from the site (Labhiri et al., 2024). These characteristics make tourist campings qualitatively different from the residential communities that dominate the wildland and urban interface (WUI) evacuation literature.

Despite this vulnerability, the evacuation planning framework for tourist campings in Spain remains largely paper-based. Real Decreto 393/2007 (Ministerio del Interior, 2007) establishes the Norma Básica de Autoprotección, which requires establishments that may generate emergency situations, including campings, to develop self-protection plans (Planes de Autoprotección). These plans designate evacuation routes, assembly points, and staff responsibilities, but they are rarely validated through quantitative analysis. The Plan de Autoprotección of Camping Parque Ardales (Ayuntamiento de Ardales, 2012), which serves as one of the primary inputs to this study, is representative of this approach: it specifies exit locations and a muster point at the open area in front of reception, but provides no estimate of evacuation time, no analysis of bottleneck formation, and no assessment of how the plan would perform under nighttime conditions or with a blocked exit.

Agent-based pedestrian simulation offers a means to close this gap. By constructing a geometric model of the camping, populating it with occupants whose walking speeds, pre-movement times, and demographic characteristics follow empirically grounded distributions, and running the model under a systematic set of scenarios, it is possible to test an evacuation plan before a real emergency occurs. The simulation identifies vulnerabilities that paper-based planning cannot reveal, such as de-facto single-exit dependencies, routing distortions due to muster points, and the quantitative dominance of nighttime pre-movement delays over all geometric factors. This study applies that approach to two Spanish tourist campings with contrasting geometries, producing the first systematic comparative analysis of camping evacuation performance in the published literature.

1.2 Context

This study is situated at the intersection of two converging developments: a growing European policy commitment to wildfire evacuation preparedness, and an emerging body of academic research on pedestrian simulation applied to tourist infrastructure.

At the policy level, the European Union Civil Protection Mechanism (UCPM) has progressively expanded its scope to include wildfire preparedness as a core priority. The UCPM-2027 program (Grant Agreement 101101169), in which the supervisor of this thesis has participated, has developed methodological frameworks specifically oriented toward the modeling of evacuation in tourist campings using Pathfinder, the agent-based pedestrian simulator employed in this study. The associated WUITIPS project aims to produce standardized tools and protocols for WUI evacuation planning at the European scale. This institutional context signals that camping evacuation simulation is not an isolated academic exercise but a component of a broader European effort to reduce wildfire risk in tourist areas.

At the academic level, the most directly relevant precedent is the work of Labhiri (2024), who modeled the evacuation of the Punta Milà campsite in Catalonia using a coupled Pathfinder-SUMO approach that integrated pedestrian movement with vehicular traffic. Labhiri's study established the feasibility of applying agent-based simulation to camping evacuation, identified key behavioral variables affecting tourist evacuation decisions, and developed a set of occupant archetypes based on a scoping literature review. The present study extends Labhiri's work in three directions. First, it models two campings with contrasting geometries, enabling a comparative analysis that a single-site study cannot provide. Second, it designs a seven-scenario campaign that systematically isolates the effects of time of day, exit availability, muster protocol, and group movement as individually controlled variables, whereas Labhiri's scenario design varied multiple factors simultaneously (evacuation mode, behavioral archetypes, time of day, and group composition). Third, it identifies and corrects a unit-conversion issue in the specification of log-normal pre-movement parameters when transferring PD 7974-6:2019 distributions into Pathfinder (BSI, 2019), a correction that is documented in Annex C and validated through Kolmogorov-Smirnov tests.

Beyond Labhiri, the broader literature on WUI evacuation modeling provides the conceptual framework for this study. Ronchi et al. (2019) identify three fundamental modeling layers for wildfire evacuation: fire-spread propagation, pedestrian behavior, and vehicular traffic. Folk et al. (2019) propose a conceptual model of human behavior in response to WUI fires that informs the occupant behavior parameters adopted in Chapter 5. Lovreglio et al. (2023) demonstrate the application of Pathfinder to the evacuation of humanitarian settlements, an infrastructure type that shares several characteristics with campings (temporary occupancy, open-air layout, transient population). No published study, however, has performed a systematic comparative analysis of evacuation performance across multiple camping sites with different geometric configurations, which constitutes the principal research gap that this study addresses.

1.3 Objectives

The overarching goal of this study is to evaluate the evacuation performance of two Spanish tourist campings under a range of emergency scenarios using agent-based pedestrian simulation, and to derive evidence-based recommendations for emergency planners. This goal is decomposed into five specific objectives:

1. **Construct validated Pathfinder models of two tourist campings with contrasting geometries.** Parque Ardales (Málaga, 500 occupants) is a large, elongated camping in an isolated natural park with limited exit options. Cabo Mayor (Santander, 650 occupants) is a compact, urban-adjacent camping with a genuine dual-exit configuration. The geometric contrast enables a comparative analysis that isolates the effect of site layout on evacuation performance (Chapter 5).
2. **Configure occupant behavior through empirically grounded parameter distributions.** Walking speeds, pre-movement times, shoulder widths, and demographic profiles (Adult, Child, Elderly) are specified using distributions drawn from PD 7974-6:2019 (BSI, 2019), Pheasant and Haslegrave (2006), and Labhiri (2024), with all parameters validated against Pathfinder output via Kolmogorov-Smirnov tests (Chapter 5, Annex C).
3. **Design a systematic scenario campaign.** Seven scenarios (S1-S7) are defined for each camping, varying time of day (day vs. night), exit availability (both exits, exit 1 closed, exit 2 closed), muster protocol (direct evacuation vs. muster-then-evacuate), and group movement (individual vs. family groups). Each scenario is executed five times with different random seeds to capture stochastic variability (Chapter 5).
4. **Extract and compare quantitative evacuation indicators across both sites.** Total evacuation time, mean completion time, exit-usage distribution, measurement-region density, and velocity-deficit metrics are analyzed for each scenario at each camping, and cross-camping comparisons are drawn to identify regime differences, site-specific vulnerabilities, and generalizable patterns (Chapter 6).
5. **Formulate operational recommendations for emergency planners.** The simulation evidence is translated into prioritized, actionable recommendations for each camping and into generalizable principles applicable to tourist campings more broadly (Chapter 7).

1.4 Document Structure

The remainder of this document is organized as follows.

Chapter 2 (Description of Technologies) presents Pathfinder, the agent-based pedestrian evacuation simulator used throughout this study, including its two simulation modes (SFPE and Steering), its occupant-behavior configuration capabilities, and the auxiliary tools (Python, Google Maps, OpenStreetMap) employed for data processing and geometry capture.

Chapter 3 (State of the Art) reviews the academic literature on pedestrian evacuation modeling, pre-movement time distributions, WUI evacuation research, and tourist-specific evacuation behavior. It identifies the research gap that this study addresses and positions the work relative to Labhiri (2024) and the broader WUITIPS/UCPM-2027 program.

Chapter 4 (Project Definition) formalizes the justification, objectives, methodology, project timeline, and cost estimate for the study.

Chapter 5 (Model Development) describes the construction and configuration of both Pathfinder models in detail: site selection and characterization, geometry calibration, occupant-profile specification, pre-movement and muster-time distributions, simulation-mode selection, density-measurement framework, scenario design, and verification procedures. This chapter constitutes the methodological core of the thesis.

Chapter 6 (Results and Analysis) presents the simulation results for Parque Ardales (Section 6.1), Cabo Mayor (Section 6.2), and a comparative analysis of both campings (Section 6.3). Each site section reports master evacuation times, analyzes the effect of each scenario factor, examines exit-usage patterns and density regimes, and synthesizes the findings.

Chapter 7 (Conclusions and Future Work) distills the six principal findings of the study, translates them into prioritized operational recommendations for each camping and for tourist campings more broadly, enumerates the limitations of the study, and proposes seven lines of future research.

Chapter 8 (Bibliography) compiles all references cited in the text in APA 7 format.

The document concludes with six annexes: Annex A (alignment with the United Nations Sustainable Development Goals), Annex B (project timeline), Annex C (pre-movement parameter derivation and validation), Annex D (complete occupant-profile parameter tables), Annex E (detailed per-run simulation results), and Annex F (Python analysis scripts).

Chapter 2. Description of the Technologies

2.1 Pathfinder

2.1.1 Overview

Pathfinder is a commercial agent-based pedestrian evacuation simulator developed by Thunderhead Engineering (Thunderhead Engineering, 2024). It is designed for modeling the movement of large numbers of occupants through complex geometries under emergency conditions, and is widely used in the fire safety engineering community for building code compliance, performance-based design, and research applications. The version used in this project is Pathfinder 2026.1.211. Pathfinder models are stored as .pth files and can be freely duplicated via File, then Save As to create scenario variants from a common baseline, a workflow used extensively in this project to generate the seven scenarios per camping from a single calibrated model.

2.1.2 Model Construction

The modeling environment is organized around a continuous triangulated navigation mesh that represents all walkable floor area. Geometry is constructed by drawing rooms, which define navigable areas, and connecting them through doors, which define the passages between rooms and the exits to the exterior. The construction process begins with the importation of a scaled background image (a site plan, satellite image, or architectural drawing) over which the geometry is traced by hand. Scale calibration is performed by fixing an anchor point to known coordinates and setting the distance between two reference points, after which Pathfinder's coordinate readout reflects real-world dimensions.

Rooms are drawn as polygonal areas and can represent any navigable space: an accommodation unit, a corridor, an open parcel, or an internal road. Doors placed on shared edges between rooms allow occupant flow between them; doors placed on exterior boundary edges of rooms function as exits (Thunderhead Engineering, 2024). Each door has configurable properties accessible through the property panel: width, flow rate, state, and wait time. The state of a door can be set to Open, Closed, or One-way by selecting the door and clicking the link next to State in the property panel, which opens the Edit Door State dialog. This dialog also supports timed state changes, allowing doors to open or close at specified simulation times. Room properties include optional speed modifiers and capacity limits, though neither was used in the present study.

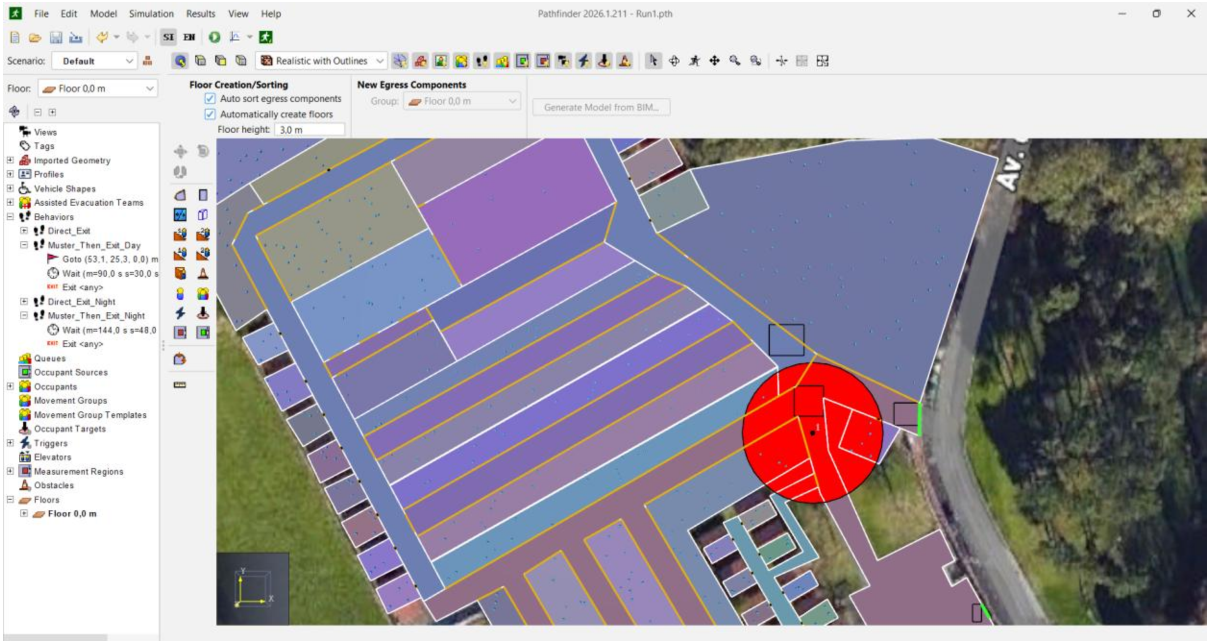

Figure 2.1. The Pathfinder geometry editor showing the navigation mesh of one of the camping models overlaid on the scaled background image. Rooms (navigable areas) are shown in color; doors connecting rooms are visible as highlighted edges.

2.1.3 Occupant Configuration

Occupants are placed in rooms via Model → Add Occupants (or by right-clicking a room and selecting Add Occupants) and are assigned to demographic profiles that govern their physical and behavioral attributes. Profiles are managed in the Profiles group of the Navigation View and define statistical distributions for three physical parameters: walking speed, shoulder width, and height. The speed distribution can be specified as Uniform, Normal, Log-Normal, or other types; this project uses truncated Normal distributions for speed and shoulder width, as documented in Chapter 5.

Pre-movement time, the delay between the start of the simulation and the moment an occupant begins moving, is configured in the Behavior system. Behaviors are user-defined action scripts located in the Behaviors group of the Navigation View. A behavior consists of a sequence of action types, including Goto Any Exit, Goto Specific Exit(s), Goto Waypoint, and Wait. The pre-movement delay is set through the Delay Before Reaction field in the occupant profile, which accepts distribution types including Log-Normal with Location, Scale, Min, and Max parameters. Muster behavior is implemented by chaining actions: Goto Waypoint (directing occupants to the assembly point), followed by a Wait action (representing the assembly time), followed by Goto Any Exit.

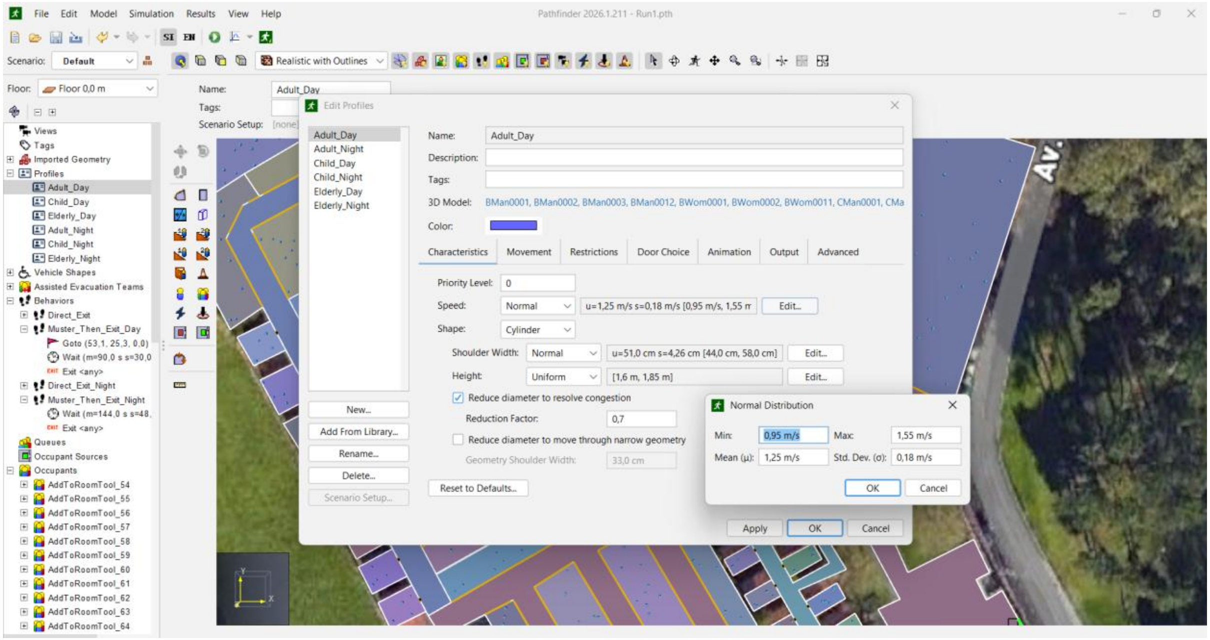

Figure 2.2. The occupant profile dialog showing the speed distribution configuration. The profile defines a truncated Normal distribution with mean, standard deviation, and minimum/maximum bounds.

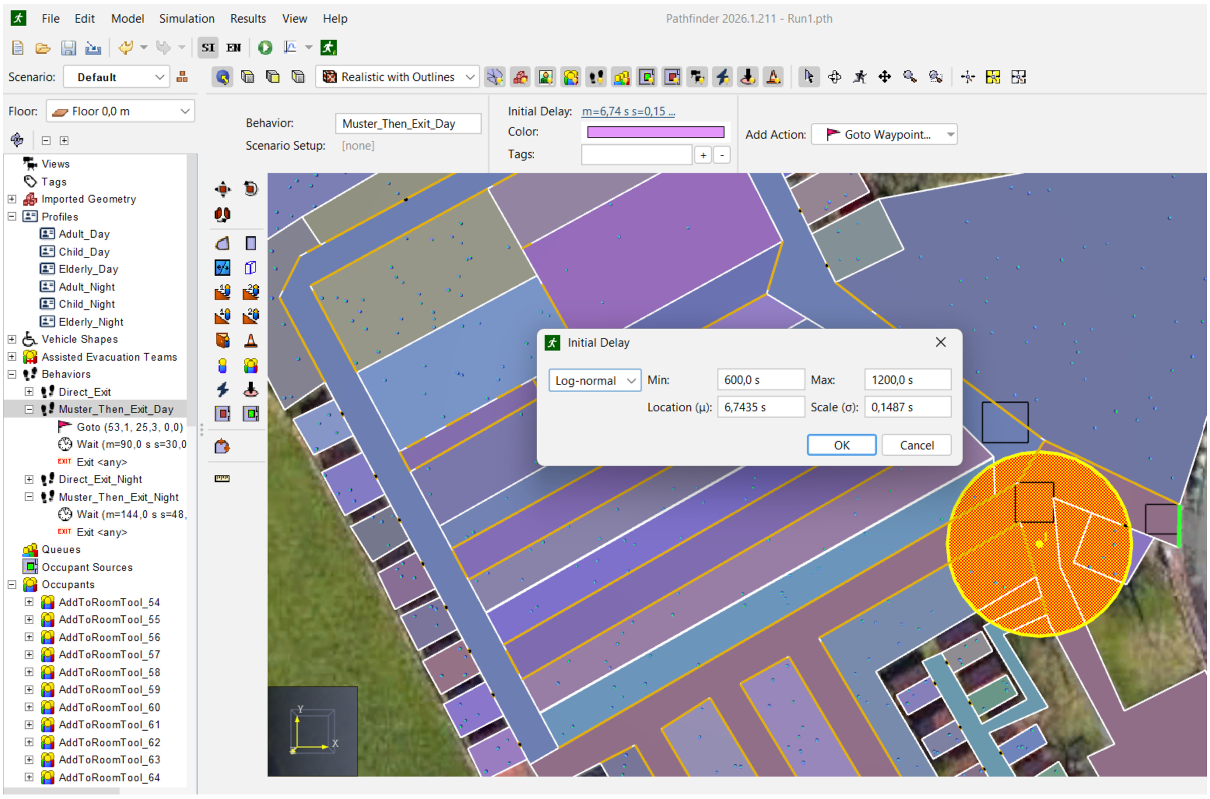

Figure 2.3. The behavior editor in the Navigation View, showing a muster behavior composed of a Goto Waypoint action, a Wait action, and a Goto Any Exit action.

Pathfinder also supports Movement Groups (Thunderhead Engineering, 2026), which allow occupants to be organized into cohesive units that move together under the guidance of a designated leader. Group parameters include maximum inter-member distance and leader assignment. This functionality is used in the S7 group-movement scenario of this project.

2.1.4 Simulation Modes

Pathfinder offers two simulation modes, selectable via Simulation → Simulation Parameters. The SFPE mode implements the hydraulic flow methodology of the SFPE Handbook (Gwynne & Boyce, 2016), in which occupant speed is determined by local crowd density and doors impose flow-rate limits. Occupants in SFPE mode do not resolve individual interactions: they follow a common route and cannot overtake one another. The Steering mode uses an agent-based approach in which each occupant navigates independently, avoiding collisions with other occupants and with the geometry in real time, allowing overtaking, lateral spreading, and local route variation. Both modes operate on the same navigation mesh and occupant configuration; switching between them requires only changing the mode setting, which permits direct comparison on identical models. This project uses Steering mode exclusively for the 70-run simulation campaign; the selection rationale and a quantitative mode comparison are documented in Chapter 5.

2.1.5 Simulation Execution and Stochastic Control

Simulations are launched via Simulation → Run Simulation or the toolbar play button. Because Pathfinder draws occupant attributes (speed, pre-movement time, body dimensions) from statistical distributions, each run produces a different realization of the population. To generate independent stochastic repetitions, occupants must be re-randomized between runs by right-clicking the occupant group and selecting Randomize, which assigns new random seeds to all distribution draws. Without this step, consecutive runs of the same model produce identical results. This project executed five independent runs per scenario, for a total of 70 runs across both campings.

2.1.6 Output and Measurement Tools

Pathfinder produces both aggregate and spatially resolved output. At the aggregate level, the results viewer (opened automatically after a simulation, or by loading the .pfr results file) provides exit-usage summaries, room clearing times, doorway flow rates, and per-occupant travel distances as exportable CSV files. Screenshots of the simulation state at any time step can be created via File → Create Screenshot, and animation movies via File → Create Movie.

For spatially resolved density analysis, Pathfinder provides two complementary tools. Measurement regions are user-defined polygons placed over the navigation mesh (managed in the Measurement Regions group of the Navigation View) within which the simulator records occupant count, density, and velocity at each time step, producing time-series data exportable as CSV. The density reported for a measurement region is the mean of the per-occupant local densities computed using the body-ellipse method of Fruin (1971), as documented in the Pathfinder Technical Reference Manual (Thunderhead Engineering, 2024, §7.2.3). Floor contour density maps provide a complementary spatial visualization by interpolating density across the entire navigation mesh, producing color-coded maps at any simulation time step. Both tools are used extensively in Chapter 6.

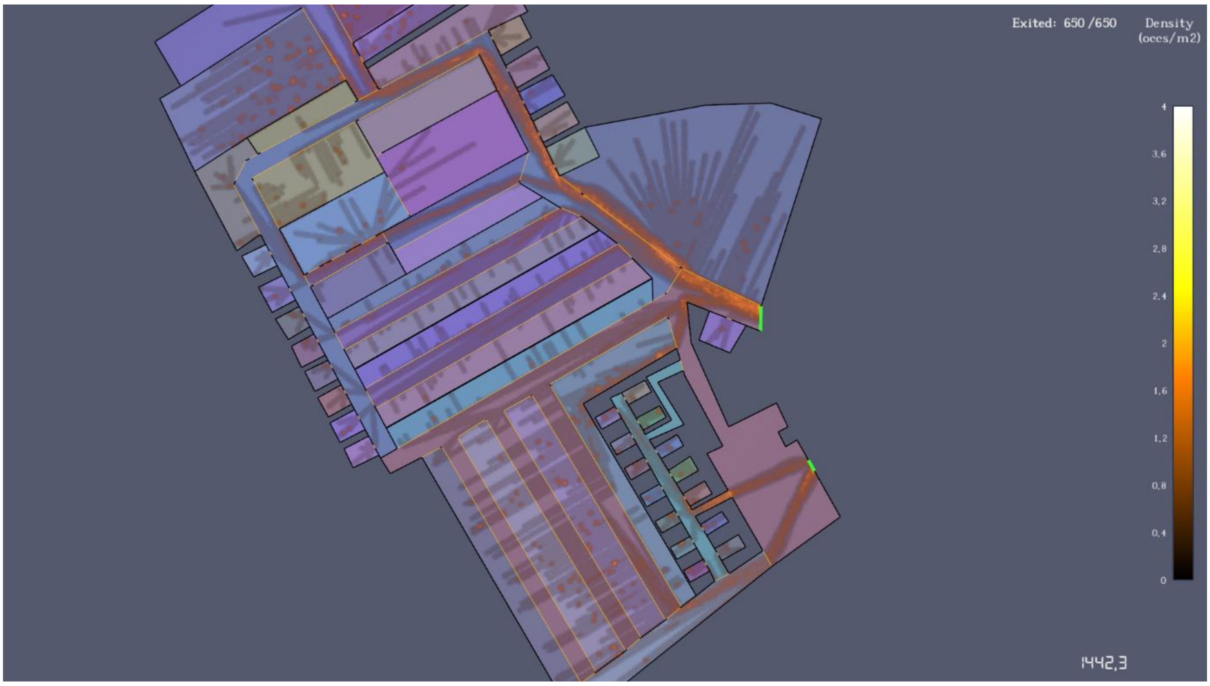

Figure 2.4. The Pathfinder results viewer showing a density contour map. The color scale represents occupant density across the navigation mesh.

2.2 Python

The post-processing of simulation outputs was performed using Python 3.x with four principal libraries. Pandas (McKinney, 2010) was used for reading, filtering, and aggregating the CSV files exported by Pathfinder, including the per-run measurement-region time series and the per-occupant exit summaries. NumPy provided the numerical operations underlying the statistical calculations, including scenario-mean and standard-deviation aggregation across five runs. Matplotlib (Hunter, 2007) generated all figures in this thesis at 300 DPI resolution, including evacuation curves, density time series, exit-usage bar charts, and contour-map comparisons. SciPy.stats supplied the Kolmogorov-Smirnov test implementation used to validate the pre-movement and speed distributions against Pathfinder's output.

The decision to process results externally rather than relying on Pathfinder's built-in analysis tools was driven by the scale of the simulation campaign. With 70 runs producing measurement-region time series at 1.0-second intervals across 10 measurement regions, the dataset comprised approximately 14 million data points. Extracting scenario-level statistics (mean peak density, time to peak, congestion duration), computing cross-run variability, and producing the comparative figures of Chapter 6 required scripted batch processing that exceeded the capabilities of the interactive results viewer.

2.3 Supporting Tools

Several additional tools supported the project workflow. Google Maps provided the satellite imagery used as the scaled background for the Cabo Mayor model. Microsoft Word, using the ICAI thesis template, was used for document preparation. The bibliography follows APA 7th edition formatting. All tools beyond Pathfinder and Python are standard and require no further description.

Chapter 3. State of the Art

3.1 Pedestrian Evacuation Modeling

Pedestrian evacuation simulation provides a low-cost, low-risk method for assessing emergency plans and predicting evacuation outcomes under hypothetical scenarios, without the ethical and practical constraints of live drills involving large populations. Simulation tools can be broadly classified along two axes: the level of resolution (macroscopic versus microscopic) and the type of movement representation (flow-based versus agent-based). Macroscopic models treat the crowd as a continuous fluid and calculate evacuation times from aggregate flow rates and densities; they are computationally efficient and well suited for rapid estimation, but they cannot represent individual behavioral variability or emergent phenomena such as spontaneous bottleneck formation. Microscopic, agent-based models simulate each individual as an autonomous agent with its own attributes (walking speed, pre-movement time, destination preference) and movement decisions, enabling a richer representation of heterogeneous populations and complex crowd dynamics at the cost of greater computational demand (Lovreglio et al., 2023).

The theoretical foundations of pedestrian movement modeling draw on several disciplinary traditions. Fruin (1971) established the empirical relationships between pedestrian density, flow rate, and walking speed that remain the basis of flow-based calculation methods, and introduced the body ellipse concept for estimating the space occupied by an individual in a crowd. Pheasant and Haslegrave (2006) compiled the anthropometric data, shoulder width, stature, and body depth distributions stratified by age and sex, that underpin the physical dimensions assigned to simulated agents. On the agent-based side, Helbing and Molnár (1995) proposed the social-force model, in which pedestrian motion is governed by the superposition of a desired velocity and repulsive interaction forces between agents and between agents and walls. While this project does not implement a social-force model directly, the concept is relevant as theoretical context for the steering algorithms used in modern evacuation software.

Pathfinder, developed by Thunderhead Engineering, is one of the most widely used agent-based pedestrian evacuation simulators in the fire safety engineering community (Thornton et al., 2011). It models each occupant as an individual agent navigating a continuous triangulated mesh that represents the walkable floor area of the modeled environment. Agents interact with each other and with the geometry through collision avoidance, queue formation at constrictions, and responses to changes in exit availability. Pathfinder offers two distinct simulation modes. The SFPE mode implements the flow-based hydraulic methodology codified in the SFPE Handbook (Gwynne & Boyce, 2016), in which occupant movement speed is determined by local crowd density according to the empirical speed-density relationships established by Fruin (1971). In this mode, agents do not interact individually; flow rates at exits and corridors are calculated from aggregate density. The Steering mode uses an individual agent-based approach in which each occupant makes autonomous navigation decisions in real time, responding to the local environment and to the positions of other agents. Steering produces more realistic representations of crowd dynamics in scenarios involving wide open spaces, lateral overtaking, and heterogeneous populations, and is the mode adopted as primary for this project (the selection reasoning and a quantitative mode comparison are documented in Chapter 5).

Although Pathfinder was originally developed for building evacuation analysis, several recent studies have demonstrated its applicability to larger and more complex environments. Lovreglio et al. (2023) applied Pathfinder to the evacuation of the Kutupalong refugee camp in Cox's Bazar, Bangladesh, a scenario that, in terms of spatial scale, layout complexity, and population heterogeneity, shares important characteristics with large campsite evacuations. Their study found that results are particularly sensitive to pre-movement delays, route availability, and occupant density, conclusions directly relevant to the present work. Bellas et al. (2026) demonstrated the coupling of Pathfinder with fire dynamics data from the Fire Dynamics Simulator (FDS) to simulate evacuation in a leisure and spa resort, a facility type that, like a campsite, involves a diverse population in a non-standard built environment. These precedents, combined with the methodological framework developed within the EU-funded WUITIPS/UCPM-2027 project specifically for campsite modeling with Pathfinder (discussed in §3.4), provide a solid basis for applying this tool to the present study.

3.2 Pre-Movement Time Distributions

Among all the parameters that influence the outcome of a pedestrian evacuation simulation, pre-movement time, the interval between the moment an alarm is issued and the moment an individual begins moving toward an exit, is consistently identified as one of the most influential determinants of total evacuation time. In the fire engineering literature, pre-movement time is conventionally decomposed into a recognition phase (from alarm perception to acknowledgment of the need to act) and a response phase (from acknowledgment to the initiation of directed movement). In outdoor WUI scenarios, this decomposition is less straightforward than in buildings because the "alarm" may take various forms: a formal public address announcement, a visual cue such as smoke, a warning from another person, or a message received via mobile phone. Nevertheless, the aggregate pre-movement interval remains the single parameter with the greatest leverage on simulated evacuation times, as demonstrated by the sensitivity analyses of Ronchi and La Mendola (2016), who showed that varying the pre-movement distribution shape and parameters produces larger changes in egress outcomes than equivalent variations in walking speed or exit width.

The normative framework most widely used to estimate pre-movement times in fire safety engineering is PD 7974-6:2019 (BSI, 2019), the British Standard on human factors in fire safety. Its Table E.2 classifies occupancy scenarios along two dimensions: the scenario category, which captures the alertness and familiarity of the occupants, and the management level, which captures the quality of the fire safety systems and staff training. Scenario categories range from A (occupants who are awake, familiar with the building, and trained in emergency procedures) through Ciii (occupants who are asleep and unfamiliar with the environment). Management levels range from M1 (comprehensive alarm systems, trained staff, regular drills) through M3 (minimal fire safety management with no trained staff). For each combination, the standard provides estimated pre-movement times at the 1st percentile (the fastest responders) and the 99th percentile (the slowest), defining the bounds of the distribution.

Pre-movement times are typically represented by a log-normal distribution rather than a normal or uniform one. The rationale, as discussed by Ronchi and La Mendola (2016), is that the factors delaying evacuation initiation, such as social influence, information seeking, and psychological denial, produce a positively skewed distribution: most occupants begin moving within a relatively narrow time window, but a long tail of late responders extends the right side of the distribution significantly. The log-normal distribution captures this asymmetry naturally. Its mathematical properties are well established (Johnson et al., 1994): if a random variable X follows a log-normal distribution, then ln(X) is normally distributed with mean μ and standard deviation σ, where μ (termed Location in Pathfinder) controls the median of the distribution and σ (termed Scale) controls its spread. Crucially, σ is a dimensionless shape parameter that does not change under multiplicative unit conversion, a property that becomes relevant in Section 3.5 when discussing the parameter calibration adopted from Labhiri (2024).

The distinction between day and night pre-movement times is of particular importance for campsite evacuations. Gwynne and Boyce (2016), in the SFPE Handbook chapter on engineering data, document that sleeping occupants take substantially longer to initiate movement than awake ones, with delays that can exceed a factor of two. In the PD 7974-6:2019 framework, this is captured by the difference between Category B (awake and unfamiliar) and Category Ciii (sleeping and unfamiliar). For a campsite with basic fire safety management (a level between M2 and M3, reflecting the presence of some staff training but the absence of comprehensive alarm systems and the impossibility of assuming that all tourists are trained), the standard suggests pre-movement bounds of approximately 10-20 minutes for awake occupants and 20-40 minutes for sleeping ones. These are the intervals adopted by Labhiri (2024) and, with a correction to the distribution parameters, by this project. The full calibration is documented in Chapter 5, with the mathematical derivation in Annex C.

No camping-specific empirical data on pre-movement times currently exists in the published literature. The estimates used in this project, and in all prior campsite evacuation studies, are derived from the PD 7974-6:2019 framework by analogy with the closest available occupancy categories. This is an acknowledged limitation of the field, and one that can only be resolved through future observational or experimental studies of actual campsite evacuations. Within the constraints of the available data, the approach adopted here, log-normal distributions bounded by the 1st and 99th percentiles of PD 7974-6 Category B and Ciii at management level M2-M3, represents the best available estimate and is consistent with the approach used by the only directly comparable prior study (Labhiri, 2024).

3.3 Camping and Tourist-Infrastructure Evacuation

The majority of the existing literature on WUI fire evacuation behavior focuses on permanent residents of threatened communities. The decisions, actions, and constraints faced by tourists during an evacuation differ substantially from those of local residents. Tourists lack knowledge of the local road network and alternative evacuation routes, may not speak the local language, are in an unfamiliar psychological state that may affect their perception of risk, and may be dependent on public transport or have limited vehicle access (Labhiri et al., 2024). These differences are compounded in camping settings, where the open-air layout, the absence of compartmentalization, and the heterogeneous accommodation types (tents, caravans, bungalows, mobile homes) produce a population with widely varying physical vulnerabilities, mobility levels, and response times.

Labhiri et al. (2024) conducted the most comprehensive scoping review to date specifically addressing the evacuation behavior of tourists in wildfire scenarios, analyzing 23 peer-reviewed studies identified from a pool of 524 papers indexed in Scopus and Web of Science. Their synthesis identifies ten key variables that shape tourist evacuation decision-making and behavior, which can be grouped into three thematic clusters. The first cluster concerns familiarity and information: risk perception, which is often systematically lower among tourists than among residents; safety culture, shaped largely by the information provided at check-in and the visibility of emergency signage; past experience with evacuations, which positively influences both the decision to evacuate and the speed of response; and access to timely, clear, and credible emergency information, typically delivered by campsite staff or public address systems rather than through media or social networks. The second cluster addresses social and demographic factors: individual socio-demographic characteristics such as age, physical mobility, and language barriers; collective behavior, particularly the tendency to evacuate in family groups, a phenomenon documented more broadly by Moussaïd et al. (2010) as affiliative behavior; and the pattern of interaction with authorities, which tends toward higher compliance among tourists than among residents, though some individuals may delay evacuation to photograph or film the event. The third cluster captures attachment and motivation: property attachment, which operates differently for tourists than for permanent residents; the length of stay, which correlates with both familiarity and reluctance to leave; and transportation mode, which determines evacuation autonomy.

Beyond individual variables, Labhiri et al. (2024) propose a typology of tourist evacuation archetypes that captures qualitatively distinct patterns of behavior. Two are particularly relevant to campsite scenarios. Threat deniers are tourists who, despite receiving an alarm or perceiving danger cues, choose not to evacuate or delay their departure significantly, driven by low-risk perception and high property attachment. Responsibility deniers acknowledge the danger but assume that campsite staff or emergency services will manage their evacuation, producing highly variable delays contingent on the actions of others. These archetypes provide a conceptual basis for defining differentiated pre-movement time distributions for distinct segments of the campsite population, an approach implemented by Labhiri (2024) in her Scenario 4 and acknowledged as a possible extension of the present work in Chapter 7.

Tourist campings also introduce specific physical challenges for pedestrian movement during an evacuation. Internal circulation routes are often narrow, shared between pedestrians and vehicles, and designed for comfort rather than emergency egress. The simultaneous movement of cars, caravans, and pedestrians toward the same limited number of exits creates traffic-pedestrian conflicts that are difficult to manage under time pressure. The typically low number of access and exit points, often only one or two vehicular gates, means that these exits can rapidly become bottlenecks during a mass evacuation. The day-night dimension adds further complexity: during daytime, occupants may be dispersed across the site or its surroundings, making their exact location at the moment of alarm uncertain; at night, occupants are sleeping in accommodation units with poor acoustic insulation, meaning that alarm propagation may be uneven across the site and pre-movement times are substantially longer (Gwynne & Boyce, 2016).

Despite these recognized challenges, the published literature on campsite-specific evacuation simulation remains extremely limited. Beyond Labhiri (2024), discussed in detail in Section 3.5, and the methodological framework developed within the WUITIPS/UCPM-2027 project (Section 3.4), no peer-reviewed study has applied agent-based pedestrian simulation to a tourist camping. The closest analogues are Lovreglio et al. (2023), who modeled a large humanitarian settlement with similar characteristics of spatial scale and population heterogeneity, and Bellas et al. (2026), who coupled Pathfinder with fire dynamics data to simulate evacuation in a leisure resort. Neither addresses the specific combination of WUI fire context, tourist occupant profile, and open-air camping geometry that defines the present study.

3.4 Wildfire-Driven Evacuation

Wildfire evacuation at the wildland-urban interface is inherently a problem with multiple layers. Folk et al. (2019) proposed a provisional conceptual model of human behavior in response to WUI fires that identifies three interacting systems: fire propagation, which determines the spatial and temporal evolution of the threat; human behavior, which governs the decisions of individuals to evacuate, shelter, or defend; and traffic dynamics, which constrain the physical movement of people and vehicles through the road network. The interactions among these layers produce emergent behaviors, such as traffic jams that trap evacuees in the path of advancing fire, that cannot be predicted from any single layer in isolation. The 2018 Mati wildfire near Athens, in which motorists were accidentally directed toward the flames and became trapped in narrow streets, is a stark illustration of this coupling.

Ronchi et al. (2019) formalized this multi-layer perspective into an open framework for modeling WUI fire evacuations, coupling fire spread models, pedestrian simulation, and traffic simulation into a unified computational pipeline. Wahlqvist et al. (2021) developed the WUI-NITY platform as a practical implementation of this concept, integrating microscopic fire spread data with pedestrian and traffic models to produce spatially and temporally resolved evacuation predictions. More recently, Ronchi et al. (2023) addressed the verification challenges specific to WUI evacuation models, noting that the scarcity of empirical validation data for large-scale outdoor evacuations remains one of the principal limitations of the field. The present project addresses one layer of this framework, pedestrian evacuation, without coupling to fire-spread or traffic models. This choice is deliberate: isolating the pedestrian component allows a controlled comparative analysis of camping-specific variables (exit configuration, muster protocol, time of day, group movement) that would be confounded by fire-scenario variability. The absence of fire-spread coupling is acknowledged as a limitation in Chapter 7, and the total evacuation times reported in Chapter 6 should be interpreted as lower bounds corresponding to the Required Safe Egress Time (RSET) component of the fire safety timeline, not as predictions of survival outcomes in a specific fire scenario.

The EU-funded WUITIPS project (UCPM-2027, Grant Agreement 101101169) represents the most directly relevant institutional precedent for this thesis. The project developed methodological frameworks specifically oriented to the simulation of tourist infrastructure evacuations in WUI contexts, including campsite modeling with Pathfinder. Its final workshop, held in Brussels in February 2025, presented pedestrian density simulations of Camping Le Bois Fleuri (France) and fire-attack simulations of Camping Punta Milà (Spain), the latter being the site modeled by Labhiri (2024). The director of the present thesis participated in the WUITIPS project, providing a direct methodological link between the European research effort and this study.

The Spanish regulatory framework for emergency preparedness in tourist campings is established by Real Decreto 393/2007, which approves the Norma Básica de Autoprotección (NBA). This regulation requires establishments that may generate emergency situations, including tourist campings above a certain capacity threshold, to develop and maintain a formal Self-Protection Plan (*Plan de Autoprotección*). Such a plan must include a risk assessment identifying potential emergency scenarios, a description of the physical environment with evacuation routes, emergency exits, and assembly points, an emergency action protocol specifying staff roles, a communication plan for alerting occupants and coordinating with external services, and a maintenance and training program. For this project, the Self-Protection Plan of Camping Parque Ardales (Ayuntamiento de Ardales, 2012) constitutes the primary source of geometric and operational data for the PA model, providing the site layout, exit locations, and designated assembly point. The regulatory framework also serves as a benchmark against which the simulation results and operational recommendations of Chapter 7 can be evaluated, ensuring that the project's outputs are actionable within the existing Spanish regulatory structure.

3.5 Labhiri (2024): Methodological Precedent

The most directly relevant prior study to this project is the master's thesis by Labhiri (2024), completed within the International Master of Science in Fire Safety Engineering (IMFSE) program at Lund University and Université Libre de Bruxelles, and developed in the context of the WUITIPS/UCPM-2027 project. Labhiri modeled the emergency evacuation of Camping Punta Milà (l'Escala, Girona), a large Mediterranean campsite with approximately 900 occupants, using Pathfinder for the pedestrian component and SUMO for the vehicular component. Her study defined seven scenarios spanning day and night conditions, direct and muster evacuation protocols, and a differentiated archetype scenario in which distinct pre-movement distributions were assigned to different tourist behavioral profiles. Each scenario was executed with 10 simulation runs to capture stochastic variability, and the results were analyzed in terms of total pedestrian evacuation time, active movement time, and the interaction between pedestrian and vehicular flows at the campsite exit.

Labhiri's parameter calibration approach established the methodological template that this project adopts and refines. Pre-movement times were derived from PD 7974-6:2019, Table E.2, by classifying the campsite occupancy as Category B (awake and unfamiliar with the environment) for day scenarios and Category Ciii (sleeping and unfamiliar) for night scenarios. The management level was placed between M2 and M3, reflecting the presence of some staff training but the impossibility of assuming that all tourists possess fire safety knowledge. This classification yielded pre-movement bounds of 600-1200 seconds (10-20 minutes) for day scenarios and 1200-2400 seconds (20-40 minutes) for night scenarios, interpreted as the 1st and 99th percentiles of a log-normal distribution following the recommendation of Ronchi and La Mendola (2016). Walking speeds were assigned as uniform distributions stratified by demographic profile: adult (0.95-1.55 m/s), child (0.60-1.20 m/s), and elderly (0.50-1.10 m/s), with night speeds reduced by a factor of 0.75 to account for reduced visibility (Labhiri, 2024, Section 5.5). Body dimensions were sourced from Korhonen et al. (2008).

The conversion of the log-normal pre-movement parameters from the theoretical distribution (whose percentile bounds are expressed in minutes in PD 7974-6:2019) to the input format required by Pathfinder (which expects Location and Scale in seconds) requires care. For a log-normal distribution, the Location parameter μ corresponds to the mean of the natural logarithm of the variable, and the Scale parameter σ corresponds to the standard deviation of the natural logarithm. If the original derivation is performed in minutes, obtaining μ_{min} and σ_{min}, the standard mathematical transformation to seconds is $\mu_s = \mu_{min} + \ln(60)$, because $\ln(X \times 60) = \ln(X) + \ln(60)$; the Scale parameter σ, being the standard deviation of $\ln(X)$ and therefore dimensionless, is invariant under the change of units. Labhiri's Appendix I reports the derivation from the 1st and 99th percentile bounds and arrives at Location = 159 s and Scale = 9 s for the day scenario. This project applies the standard transformation, obtaining Location = 6.7435 and Scale = 0.1487 for day (and Location = 7.4367, Scale = 0.1487 for night). The corrected parameters reproduce the distribution that Labhiri's Appendix I describes mathematically: a log-normal bounded between 600 and 1200 seconds with the 1st and 99th percentiles at those bounds. Kolmogorov-Smirnov tests on Pathfinder output samples confirm the match, with $D = 0.031$ ($n = 650$, day) and $D = 0.052$ ($n = 500$, night), neither rejected at $\alpha = 0.05$. The complete derivation is documented in Annex C of this thesis and represents one of the original methodological contributions of this project.

Beyond the pre-movement parameters, the present project departs from Labhiri's methodology in several respects that reflect both the specific characteristics of the two campings studied and practical constraints encountered during model construction. First, walking speed and shoulder width are implemented as truncated-normal rather than uniform distributions. This change was motivated by the finding that Pathfinder 2026.1 enforces a Location ≥ 0 constraint in its speed profile field, which prevents the use of log-normal distributions for profiles with median speeds below 1.0 m/s (child and elderly). Truncated-normal distributions, validated against Pathfinder output via Kolmogorov-Smirnov tests (Adult_Day, $n = 332$, $D = 0.036$, not rejected), provide a better representation of the expected bell-shaped variability around a central speed than the uniform distributions used by Labhiri. Second, the muster wait-time distribution was adjusted downward relative to Labhiri's values to reflect the smaller occupancy of the two campings studied here (500 and 650 versus 900) and the compact geometry of the assembly areas, while maintaining Labhiri's night-to-day ratio of 1.6. Third, this project does not include a vehicular evacuation component: the scope is limited to pedestrian movement, consistent with the project brief and with the objective of isolating the pedestrian dynamics that campsite operators can influence through layout and protocol design. Fourth, an additional scenario axis, family-group movement using Pathfinder's Movement Group functionality (Thunderhead Engineering, 2026), was introduced to explore the effect of affiliative behavior (Moussaïd et al., 2010) on evacuation performance, an axis not present in Labhiri’s study.

3.6 Identified Research Gap

The review presented in this chapter reveals three converging gaps in the existing literature that this project is designed to address.

First, no published study has conducted a comparative evacuation analysis of two geometrically contrasting campings. Labhiri (2024) modeled a single site (Camping Punta Milà), and the WUITIPS project produced demonstrations on individual campings without cross-site comparison. A single-site study can characterize the evacuation dynamics of that particular geometry, but it cannot distinguish which findings are site-specific and which generalize to the broader class of tourist camping evacuations. By pairing Parque Ardales, a compact, elongated camping with a de-facto single exit, against Cabo Mayor, a wider-footprint camping with two functional exits, this project creates the conditions for identifying structural patterns, such as the relationship between geometry and exit-closure penalty or the interaction between muster protocol and exit-routing equilibrium, that would remain invisible in a single-site analysis.

Second, no prior study has systematically explored the effects of exit-closure and muster-protocol variations in a camping context. Labhiri’s scenario design varied time of day, evacuation mode (pedestrian versus vehicular), and behavioral archetypes, but did not include scenarios in which individual exits were selectively closed or in which the muster protocol was tested against a direct-evacuation baseline under otherwise identical conditions. These are precisely the operational variables that campsite managers and civil protection authorities can control, and their quantification through simulation is a direct input to evidence-based emergency planning.

Third, while Labhiri (2024) included group-movement scenarios at Punta Milà, no prior study has isolated the group-movement effect as a single controlled variable or compared its magnitude across campings with different geometric configurations. In Labhiri's design, group scenarios were combined with the pedestrian-only evacuation mode, confounding the group effect with the removal of the vehicular component. This project introduces a dedicated group-movement scenario (S7) that differs from the individual-movement baseline (S1) only in the activation of Pathfinder's Movement Group functionality (Thunderhead Engineering, 2026), enabling a clean measurement of the group-cohesion penalty. By running S7 at both campings, the project further tests whether the group penalty is geometry-dependent, a question that a single-site study cannot address.

These three gaps define the scope and the original contribution of this thesis. The methodology for addressing them, including the construction of two validated Pathfinder models, the calibration of occupant parameters, and the design of a seven-scenario campaign across four variation axes, is documented in Chapter 5. The results are presented in Chapter 6, and the operational recommendations derived from them are consolidated in Chapter 7.

Chapter 4. Definition of the Project

4.1 Justification

Wildfires at the wildland-urban interface (WUI) represent one of the most severe natural hazards for human life and infrastructure in southern Europe. The European Forest Fire Information System (EFFIS) recorded over 500,000 hectares of burned area across the EU in 2023, with fires in Rhodes, the Canary Islands, and Sicily striking tourist areas particularly hard (European Commission Joint Research Centre [JRC], 2023). Spain, where the Mediterranean climate and the extent of forested land create conditions especially favorable to rapid fire propagation, was the worst-affected EU member state in 2022, with nearly 245,000 hectares destroyed (JRC, 2022). These figures do not capture the full dimension of the risk: the 2018 Mati wildfire near Athens killed 104 people in a coastal resort popular with holidaymakers, many of whom were trapped in their cars or drowned attempting to reach the sea, making it the deadliest wildfire event in Europe since 1900 (Balkan Insight, 2024).

Tourist campings located in or near forested areas constitute a particularly vulnerable category of occupancy within the WUI context. They concentrate a large number of people in open, dispersed spaces with limited exit infrastructure, typically only one or two vehicular gates. Their occupants are unfamiliar with the local geography, may not speak the local language, often travel in family groups with varying mobility levels, and may be asleep at the time of an alert. These characteristics, widely recognized in the human-factors literature on tourist evacuation behavior (Labhiri et al., 2024), compound the baseline difficulty of any WUI evacuation. In Spain, the Real Decreto 393/2007 requires campings to maintain Self-Protection Plans (*Planes de Autoprotección*) that include evacuation protocols, exit routes, and assembly points, yet these plans are typically drafted using simplified empirical methods without the support of quantitative simulation.

Pedestrian evacuation simulation using agent-based models has become a well-established tool for evaluating emergency plans in the built environment (Ronchi & Nilsson, 2016). Software platforms such as Pathfinder (Thunderhead Engineering, 2024) allow systematic exploration of evacuation scenarios that cannot be tested through live drills: night-time evacuations, exit closures, muster protocols, and group movement dynamics. However, the application of these tools to open-air tourist infrastructure, and to campings in particular, remains scarce in the scientific literature. Labhiri (2024) and the ongoing EU UCPM-2027 project (Grant Agreement 101101169), in which the director of this thesis has participated, represent the earliest efforts to develop a methodological framework specifically oriented to camping evacuation modeling with Pathfinder.

This project addresses the identified gap by simulating the emergency pedestrian evacuation of two real Spanish campings of contrasting geometry and capacity: Parque Ardales (Málaga, 500 occupants, compact and elongated with a de-facto single exit) and Cabo Mayor (Santander, 650 occupants, wider footprint with two functional exits). A comparative study across seven scenarios per camping, varying the axes of time of day, evacuation protocol, exit availability, and family-group movement, allows the extraction of findings that are both site-specific and, where supported by the data, generalizable to the broader class of tourist camping evacuations. The project falls under the *Proyecto estudio* category of the ICAI Final Degree Project framework and integrates competencies from systems modeling, statistical analysis, safety engineering, and operational design.

4.2 Objectives

The project pursues five interrelated objectives that span the full lifecycle of a simulation-based engineering study, from literature review through actionable design recommendations.

1. Simulate the emergency pedestrian evacuation of two Spanish tourist campings of different capacity, Camping Parque Ardales (Málaga, 500 occupants) and Camping Cabo Mayor (Santander, 650 occupants), using Pathfinder (Thunderhead Engineering, 2024) as the primary modeling platform.
2. Model occupant behavior from initial locations (accommodation parcels and bungalows) to safe zones or camping exits, incorporating realistic parameters for pre-movement time, walking speed, demographic composition (adult, child, elderly), and occupant alertness state (day and night scenarios).
3. Define and evaluate multiple evacuation scenarios for each camping, varying the number and location of available exits, the alertness state of the occupants, the evacuation strategy (direct exit versus prior passage through a muster point), and the presence of family-group movement constraints.
4. Extract and compare the principal performance indicators across all scenarios and both campings: total evacuation time, mean completion time, exit-usage distributions, pedestrian density in circulation routes and at exits, and identification of congestion points.
5. Formulate evidence-based design recommendations for improving the evacuation of tourist campings, addressing exit configuration, signage, muster-point location, alert systems, and emergency protocol guidelines.

These objectives are addressed sequentially across the chapters of this thesis. Objective 1 provides the overarching scope and is implicit throughout. The literature foundations supporting Objective 2 are established in Chapter 3. The model construction, parameter calibration, and scenario design corresponding to Objectives 2 and 3 are documented in Chapter 5. The simulation results and comparative analysis of Objective 4 are presented in Chapter 6. The design recommendations of Objective 5 are consolidated in Chapter 7.

4.3 Methodology

This section outlines the methodological workflow followed throughout the project. Each stage is described at a high level; Chapter 5 provides the full technical documentation of every modeling decision, parameter, and validation step.

The project began with a familiarization phase in which Pathfinder 2026.1.211 (Thunderhead Engineering) was installed, configured, and tested through small-scale trial models. This phase served to establish working proficiency with the software's geometry editor, occupant profile system, behavioral triggers, measurement region configuration, and output formats. Concurrently, a literature review was conducted covering three domains: pedestrian evacuation modeling fundamentals, pre-movement time distributions and their normative basis in PD 7974-6:2019 (BSI, 2019), and the limited existing body of work on camping and tourist-infrastructure evacuation. The review identified the research gap this project addresses and established the empirical foundations for parameter calibration.

Two camping sites were then selected to form a geometrically contrasting pair suitable for comparative analysis. Parque Ardales (Málaga) is a compact, elongated camping with a de-facto single vehicular exit serving nearly all occupants, sourced from the publicly available Plan de Autoprotección (Ayuntamiento de Ardales, 2012). Cabo Mayor (Santander) is a wider-footprint camping with two functional exits and a more distributed internal layout, whose geometry was captured from Google Maps satellite imagery and operator-provided site information. Both sites were modeled in Pathfinder by importing scaled background images, calibrating spatial coordinates to UTM reference points, and constructing navigable meshes representing accommodation zones, circulation routes, exits, and assembly areas.

Occupant profiles were configured next. Three demographic categories, adult, child, and elderly, were defined with truncated-normal speed and shoulder-width distributions calibrated to the anthropometric and pedestrian-dynamics literature (Pheasant & Haslegrave, 2006; PD 7974-6:2019). Pre-movement times were assigned as log-normal distributions derived from PD 7974-6:2019 occupancy categories, incorporating a unit-conversion correction to the parameters published by Labhiri (2024) that constitutes one of the original methodological contributions of this project. Muster behavior was implemented through waypoint-based routing with a truncated-normal wait-time distribution at the assembly point. All distributions were validated against Pathfinder's output using Kolmogorov-Smirnov tests.

A structured scenario campaign was designed around four variation axes: time of day (day versus night, controlling the pre-movement distribution and walking speed), evacuation protocol (direct exit versus passage through a muster point), exit availability (all exits open versus closure of one exit), and family-group movement (S7, introducing leader-follower dynamics with realistic group compositions). This produced seven scenarios per camping, each executed five times with randomized seeds to capture stochastic variability, for a total of 70 simulation runs. All runs used the Steering movement mode, selected over SFPE on the basis of a validated baseline comparison showing less than 2% divergence in total evacuation time with identical exit splits.

Simulation outputs were processed using Python scripts to extract total and mean evacuation times, per-exit occupant counts, measurement-region density time series, and congestion indicators. The analysis proceeded in three stages: a camping-by-camping examination of each performance axis (Chapter 6, §6.1 and §6.2), a cross-camping comparative synthesis identifying patterns that generalize beyond the two specific sites (§6.3), and the formulation of operational design recommendations grounded in the simulation evidence (Chapter 7).

4.4 Project Planning

The project was developed over approximately nine months, from October 2025 to June 2026, corresponding to the 6 ECTS credits allocated to the Final Degree Project in the GITI curriculum (approximately 150 hours of student work). The work was organized into five sequential phases, with partial overlaps where the nature of the tasks permitted concurrent progress.

Phase 1 (October 2025 - February 2026) comprised tool familiarization with Pathfinder and the literature review on pedestrian evacuation modeling, pre-movement distributions, and camping-specific evacuation studies.

Phase 2 (March - April 2026) covered geometry capture and model construction for both campings, including background importation, UTM calibration, navigable-mesh construction, and occupant placement.

Phase 3 (May 2026, first half) addressed occupant profile calibration, scenario definition, and execution of the 70-run simulation campaign.

Phase 4 (May 2026, second half) comprised post-processing of simulation outputs, per-camping analysis, and cross-camping comparative synthesis.

Phase 5 (June 2026) was dedicated to the formulation of design recommendations and the drafting of the thesis document.

The detailed Gantt chart documenting the week-by-week allocation of tasks is provided in Anexo B.

Chapter 5. System / Model Development

This chapter documents the development of the two Pathfinder models that underpin the simulation campaign and the configuration choices common to both. It begins by characterizing the two campsites and justifying their selection as a contrasting pair (Section 5.1), then describes the construction of each model in turn, covering background importation, geometry, door connectivity, and occupant placement (Sections 5.2 and 5.3). Then, Section 5.4 sets out the configuration shared by both models, including the demographic profiles, the pre-movement and muster wait-time distributions, the selection of the Steering movement mode, the density evaluation framework, and the measurement regions. Section 5.5 defines the seven simulation scenarios, reports the initial verification of the models and includes the SFPE and Steering baseline comparison.

5.1 Site Selection and Characterization

The analysis is built on a deliberate comparison between two Spanish tourist campsites that differ markedly in spatial extent, occupant capacity, and exit configuration. The two sites were selected on the basis of two criteria: the availability of reliable geometric data, and the clear contrast they offer in scale and layout. Parque Ardales is the more spatially extensive of the two but holds fewer occupants, whereas Cabo Mayor is considerably more compact yet accommodates a larger population. This inversion of the usual relationship between area and capacity is the central reason the pairing is analytically useful: it allows the influence of site geometry on evacuation dynamics to be examined independently of raw occupant numbers.

5.1.1 Parque Ardales

Parque Ardales is a campsite located in the municipality of Ardales, in the province of Málaga (Andalucía), within the natural setting of the Guadalhorce reservoir system. The site occupies sloping terrain, with the accommodation and service areas situated on gradients of up to roughly twenty percent and the surrounding land predominantly wooded. This topography is relevant to the evacuation analysis because it produces long, channeled internal routes that connect the accommodation zones to the site exits.

The geometry of the model was reconstructed from the site's official self-protection plan (Ayuntamiento de Ardales, 2012), a municipal document that includes scaled topographic plans of the campsite. The plan confirms an accommodation stock of fourteen bungalows or apartments, complemented by parcels for tents and caravans, motorhome pitches, and service buildings including a reception, bar, supermarket, and restaurant. The document does not declare a single official maximum occupancy figure; the nominal capacity of 500 occupants adopted in this study is therefore an estimate derived from the physical pitch and accommodation stock represented in the plan, rather than a regulatory figure.

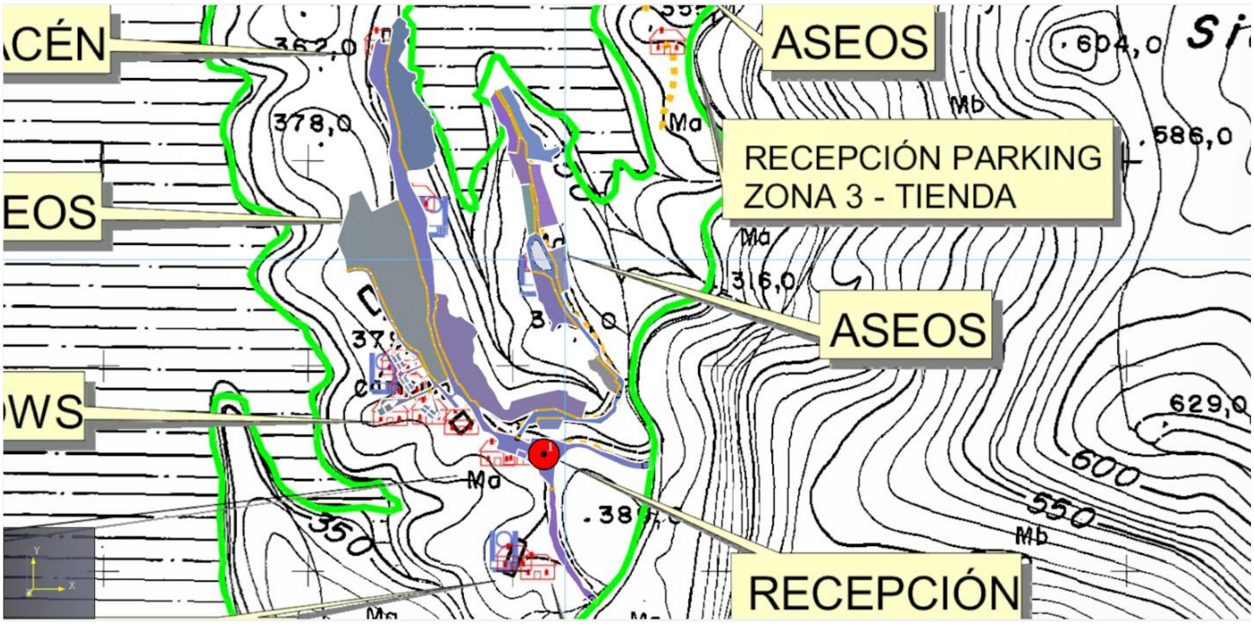

Figure 5.1. Pathfinder model of Parque Ardales overlaid on the scaled topographic plan from the site's self-protection plan (Ayuntamiento de Ardales, 2012). The navigable areas (paths and accommodation zones) are shown in purple over the original contour lines and zone labels.

The 500 occupants were distributed across the model according to the accommodation type, as summarized in Table 5.1. The largest single concentrations are in the parcels (electrified and non-electrified) and motorhome areas, with smaller numbers in the bungalows, campers, and reception. A residual group of occupants was placed on the internal roads (viales) to represent visitors in transit through the common areas at the moment the evacuation is triggered.

Zone	Occupants	Adult	Child	Elderly
Bungalows	70	35	28	7
Electrified parcels	100	50	40	10
Non-electrified parcels (1-4)	120	60	48	12
Motorhomes (1-4)	120	60	48	12
Small campers (1-2)	60	30	24	6
Reception (staff)	10	8	2	0
Internal roads (transit)	20	10	8	2
Total	**500**	**253**	**198**	**49**

Table 5.1. Occupant distribution at Parque Ardales by accommodation zone.

The demographic split across the site approximates a 50% adult, 40% child, and 10% elderly composition. The reception zone departs from this split, holding a higher proportion of adults because it represents campsite staff together with a small number of accompanying children; this is also why no elderly occupants are assigned there.

5.1.2 Cabo Mayor

Cabo Mayor is a campsite located in Santander (Cantabria), on the Carretera del Faro near the Cabo Mayor lighthouse, on the northern coast of Spain. In contrast to Parque Ardales, the site occupies relatively flat and compact terrain, bounded to the east by the Avenida del Faro. The campsite has two points of egress onto this road: a main vehicular exit and a secondary pedestrian exit.

No official self-protection document was available for this site. The model geometry was instead reconstructed from a satellite image obtained through Google Maps, used as the scaled background in Pathfinder, with a site plan provided directly by the campsite operators serving as a visual reference for the internal layout. Because no regulatory occupancy figure was available, the nominal capacity of 650 occupants was estimated by counting the bungalows and pitches visible in the plan and assigning a plausible occupancy to each.

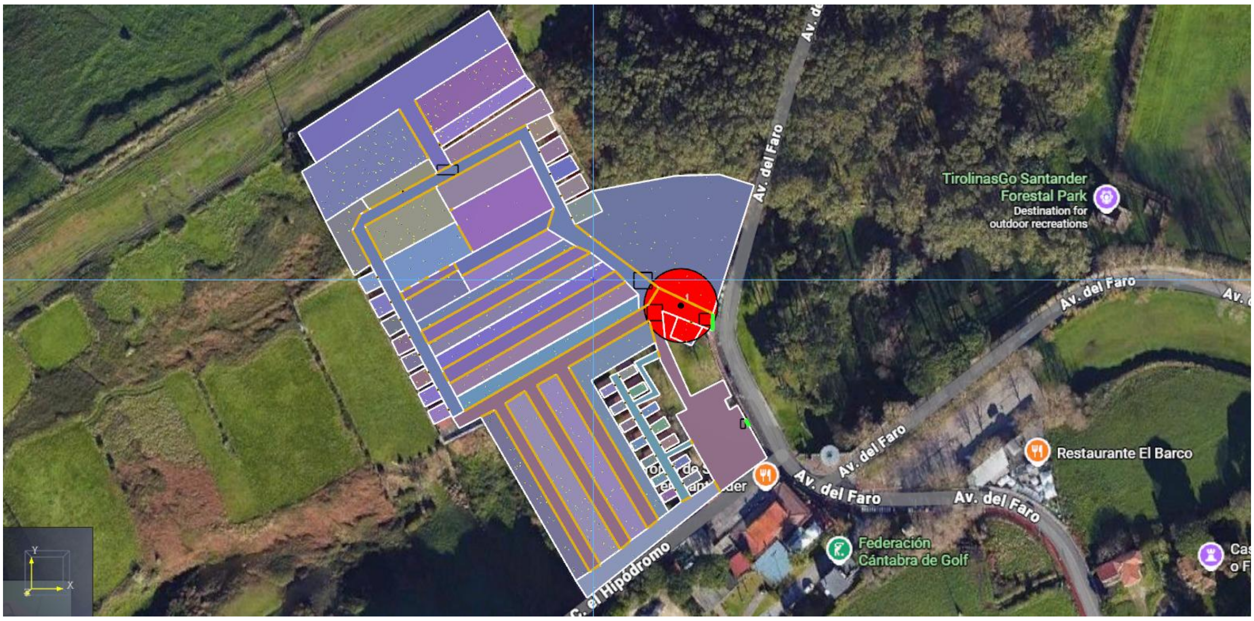

Figure 5.2. Pathfinder model of Cabo Mayor overlaid on the Google Maps satellite image used as the scaled background. The two exits onto the Avenida del Faro (main vehicular and secondary pedestrian) are visible at the eastern edge of the site.

The resulting distribution is summarized in Table 5.2. The accommodation stock comprises 27 four-person bungalows, a parcel of eleven two-person bungalows, a series of numbered parcels, three free-camping zones (Libre 1-3), and service areas including reception, a bar, a swimming pool, a terrace, toilet blocks, and a parking area. The larger parcels and free-camping zones account for the majority of the occupants.

Zone	Occupants	Adult	Child	Elderly
Four-person bungalows (×16): 2A + 2C	64	32	32	0
Four-person bungalows (×11): 2A + 1C + 1E	44	22	11	11
Parcel of eleven two-person bungalows	22	11	9	2
Parcels (1-12)	386	197	157	32
Free-camping zones (Libre 1-3)	90	45	36	9
Reception, bar, pool, terrace	30	17	12	1
Toilets (1-2), parking	14	8	6	0

Zone	Occupants	Adult	Child	Elderly
Total	**650**	**332**	**263**	**55**

Table 5.2. Occupant distribution at Cabo Mayor by accommodation type.

As at Parque Ardales, the site demographic composition approximates the 50/40/10 adult-child-elderly split, with minor deviations introduced by the fixed family compositions assigned to individual bungalows.

5.1.3 Justification of the Site Pairing

The two campsites were selected to function as a contrasting pair rather than as independent case studies. Their defining difference is the inversion between area and capacity: Parque Ardales is the larger site in physical extent but holds 500 occupants, whereas Cabo Mayor is the more compact site yet accommodates 650. This contrast is reinforced at the level of exit configuration. As the results in Chapter 6 establish, Parque Ardales behaves as a de-facto single exit site, with one exit absorbing almost the entire population, while Cabo Mayor possesses two genuinely usable exits under direct evacuation conditions. Pairing a large, sloping, single exit site with a compact, dual exit site allows the analysis to separate the effects attributable to site geometry from those attributable to occupant load, and to test whether the conclusions drawn for one site generalize to the other.

5.2 Pathfinder Model — Parque Ardales

5.2.1 Background Importation and Calibration

The Parque Ardales model was built on top of two georeferenced background images. The primary reference was Plan nº 4 (Installations) of the site's self-protection plan (Ayuntamiento de Ardales, 2012), a scaled topographic drawing that includes a UTM coordinate grid along its borders, with gridlines spaced at 200 m intervals. This image was extracted from the source document as a high-resolution PNG and imported into Pathfinder as a background image.

Calibration was performed using the known real distances encoded in the UTM grid rather than a graphic scale bar. An anchor point was placed on a clearly identifiable feature, the campsite reception, and assigned its true UTM coordinates (approximately X = 339,433 m, Y = 4,087,705 m). The scale was then fixed using two reference points separated by a known distance along the grid. After calibration, the cursor coordinate readout in Pathfinder reproduced the UTM values of independent grid intersections to within a few meters, confirming that any geometry drawn over the background would be rendered at true scale.

A second background image, a parcel distribution map of the site, was subsequently overlaid to aid in positioning the individual accommodation zones. Because this image was not natively georeferenced and was not oriented to true north, it was aligned to the already calibrated topographic plan using two common landmarks (the reception and the Zone 2 entrance), with an angular correction applied so that the two backgrounds coincided.

5.2.2 Geometry: Rooms, Roads, Corridors, and Exits

The campsite geometry was reconstructed by hand tracing the navigable areas over the calibrated backgrounds. Two of the four zones identified in the self-protection plan were modeled: Zone 1 and Zone 2, which together contain all of the campsite's accommodation. Zone 3 was deliberately excluded from the model, as it is a transit and circulation area in which camping is not permitted and which therefore holds no occupants to evacuate.

The navigable network was modeled using three categories of element. The internal roads (viales) were drawn as transit rooms with widths of roughly four to five meters, following the orange road layout of the plan; these form the primary evacuation arteries that channel occupants towards the exits. The bungalows were modeled as small individual rooms sized for approximately five occupants each, connected by doors to short corridors (pasillos) that in turn feed into the main road of Zone 1. The parcels (for tents, caravans, and motorhomes) were modeled as larger open areas; rather than enclosing them with walls, they were connected to the adjacent road along their full length using doors with maximum width, so that the boundary between parcel and road imposes no artificial constraint on occupant movement, reflecting the open nature of these pitches in reality.

Because the model was hand traced over the scaled plan, the geometry is not reproduced to millimeter accuracy. Straight segments were drawn in lengths of approximately four to five meters, reduced to around two meters along curved sections to follow the road geometry more faithfully. This level of fidelity is sufficient for the evacuation analysis, in which the relevant quantities are route lengths and flow capacities at the scale of meters rather than centimeters.

The model contains two exits onto the access road, both connecting to the Zone 1 entrance. Exit 1 is the southernmost connection between the road and the campsite, and corresponds to the site's nominal main entrance. Exit 2 is the second connection from the road. Although Exit 1 is the principal entrance in everyday use, the results in Chapter 6 show that Exit 2 is the more efficient egress route under evacuation conditions, and it absorbs almost the entire occupant population in the scenarios where both exits are available.

5.2.3 Door Connectivity and the Bungalow Door Width Finding

Door placement followed the physical connectivity of the site: bungalow doors connect to the corridors, corridors connect to the roads, and parcels connect to the roads through full length openings as described above.

During initial test runs, the bungalow doors revealed a modeling sensitivity worth documenting. With the doors set to an initial width of 0.90 m, a nominal standard doorway, some occupants became trapped at the threshold during the simulation, unable to resolve the movement through the opening. This is a known artifact of movement based on agents at constrictions whose width is close to the agents' shoulder width. The issue was resolved by widening the affected doors slightly, to 0.91 m and in some cases 1.01 m, which eliminated the blockage without materially altering the geometry. This adjustment is noted here because it is a concrete example of the kind of low-level calibration required to obtain physically plausible movement in a model built by hand.

5.2.4 Occupant Distribution

The placement of the 500 occupants across the model follows the accommodation breakdown already presented in Table 5.1. Each accommodation zone was populated using Pathfinder's room-based occupant distribution, with the demographic split (adult, child, elderly) assigned per zone according to the profile percentages. The bungalows, parcels, motorhome areas, and campers received their occupants directly; the reception was populated with staff and a small number of accompanying children; and a residual group was placed on the internal roads to represent occupants in transit at the moment of the alarm.

5.3 Pathfinder Model — Cabo Mayor

5.3.1 Background Importation and Calibration

The Cabo Mayor model was built over a satellite image of the site obtained through Google Maps, used as the scaled background in Pathfinder, with a site plan supplied directly by the campsite operators serving as a visual reference for the internal layout. Unlike Parque Ardales, no official document with a UTM coordinate grid was available for this site, so the scale was established using a known physical dimension visible in the satellite image.

Calibration followed the same procedure used for Parque Ardales. The graphic scale bar of the satellite image was used together with a measurement of the site's swimming pool, a feature whose length could be identified clearly and measured reliably on the image. An anchor point was placed on a fixed reference and the scale fixed against this known distance, so that the geometry drawn over the background would be rendered at true scale.

5.3.2 Geometry: Roads, Parcels, Free-Camping Zones, and Exits

The geometry of Cabo Mayor was reconstructed by hand tracing the navigable areas over the calibrated background. In contrast to the curved layout of Parque Ardales, Cabo Mayor occupies a terrain with predominantly rectilinear road network, so the traced segments are largely straight and required none of the short segment subdivision used to follow curves at the first site.

The navigable network was modeled using the same categories of element as at Parque Ardales. The internal roads (Vial 1 and Vial 2) were modeled as transit rooms forming the main circulation network. The 27 four person bungalows were modeled as individual rooms, as was the block of eleven two person bungalows. The service buildings (reception, bar, swimming pool, terrace, and toilet blocks) were modeled as rooms populated with their respective occupants.

A simplification was applied to the pitches. The site plan shows several hundred individually numbered parcels; because these are open air pitches with no physical barrier between them, modeling each one separately would have added substantial construction effort without affecting the evacuation dynamics. They were therefore grouped into larger parcel areas (Parcela 1-12), each holding between roughly twenty and fifty occupants, with the free camping zones (Libre 1-3) modeled in the same way as large open areas. As with Parque Ardales, these open areas connect to the adjacent roads along their full length, so that the boundary between parcels and roads imposes no artificial constraint on movement. One of these zones, Libre 2, was found during testing to function as a structural transit corridor, with substantially more occupants passing through it than were assigned to it; this is a genuine feature of the site geometry rather than a modeling error, and is documented as such.

The model has two exits onto the Avenida del Faro: a main vehicular exit, 7 m wide, and a secondary pedestrian exit, 3.4 m wide. Both are genuinely usable under direct evacuation conditions, a configuration that distinguishes Cabo Mayor from the de-facto single exit behavior of Parque Ardales and that is examined in detail in Chapter 6.

5.3.3 Door Connectivity and One-Way Doors on Private Accommodation

Door connectivity at Cabo Mayor incorporates a deliberate modeling decision that materially affects the results and therefore warrants explicit documentation. Following the supervisor's instruction, the doors of private accommodation (bungalows, reception, and toilet blocks) were configured as one-way, permitting movement only from the accommodation outwards, while the doors in transit zones were kept bidirectional.

The purpose of this configuration is to prevent occupants from using private accommodation as a shortcut. With fully bidirectional doors, Pathfinder's route-finding can treat the doorways of private units as reversible navigation nodes, allowing occupants originating elsewhere on the site to cut through bungalows or service buildings to reach an exit more directly. This is physically unrealistic: an occupant in a northern pitch would not traverse a stranger's bungalow during an evacuation. Making the private doors one-way removes these shortcuts and forces all traffic onto the legitimate road network.

The effect of this change was larger than a purely local connectivity adjustment might suggest. In Cabo Mayor scenario S1, switching the private doors from bidirectional to one-way increased the total evacuation time by approximately 43% (from roughly 16.98 min to 24.35 min before the pre-movement distribution was finalized). The change also altered the exit split, channeling a greater proportion of occupants towards the main vehicular exit, because some routes that previously reached the pedestrian exit by passing close to private units were no longer available. Rather than being an artifact, this outcome is the more physically realistic and conservative of the two: it reflects the fact that occupants are confined to the legitimate circulation network, and it yields longer, safer evacuation time estimates for design purposes. The magnitude of the effect illustrates that door directionality is a modeling choice with measurable consequences, not a trivial technical detail.

5.3.4 Occupant Distribution

The placement of the 650 occupants follows the accommodation breakdown presented in Table 5.2. The four person bungalows were populated with fixed family compositions (predominantly two adults with two children, or two adults with one child and one elderly occupant), the grouped parcels and free-camping zones received the bulk of the population, and the service buildings were populated with smaller numbers representing occupants present in the common areas at the moment of the alarm.

5.4 Common Configuration

The two models share an identical configuration of occupant behavior and movement parameters, so that any difference in their evacuation performance can be attributed to site geometry and scenario design rather than to differences in how the occupants themselves were modeled. This section documents that shared configuration: the demographic profiles governing movement speed and body size (5.4.1), the pre-movement time distributions (5.4.2), the muster wait-time distributions (5.4.3), the selection of the Steering movement mode (5.4.4), the density evaluation framework adopted for the analysis (5.4.5), and the measurement regions placed at each site (5.4.6).

5.4.1 Demographic Profiles: Speed, Shoulder Width, and Height

The occupant population at both sites was divided into three demographic profiles, adult, child, and elderly, in the proportions documented in Section 5.1 (approximately 50%, 40%, and 10% respectively). Each profile was assigned distributions for walking speed, shoulder width, and height rather than single deterministic values, so that the natural variability of a real population is represented and so that the five repetitions of each scenario sample a different realization of the population.

Walking speed and shoulder width were modeled using normal distributions. The decision to use a normal distribution rather than a log-normal one was made after testing: when a log-normal distribution was specified for the speed field, Pathfinder 2026.1 requires a non-negative Location parameter, but the child and elderly profiles have median speeds below 1 m/s, which corresponds to a negative log-Location and is rejected by the software. Inspection of the detailed per-occupant output confirmed that under these conditions the program did not reproduce the intended log-normal shape. A truncated Normal distribution, by contrast, reproduced the intended distribution faithfully: a Kolmogorov-Smirnov test on the realized adult daytime speeds ($n = 332$) returned $D = 0.036$ against the specified Normal, which does not reject the fit, while the same sample rejected a uniform distribution. The Normal distribution was therefore adopted for both speed and shoulder width.

The daytime speed parameters were set at 1.25 m/s (mean) for adults, 0.90 m/s for children, and 0.80 m/s for the elderly, each with a standard deviation of 0.18 m/s and truncated to a plausible physiological range. For the night scenarios, all speeds were scaled by a factor of 0.75 to represent reduced movement capability in darkness, following Labhiri (2024). Shoulder width and height parameters were assigned per profile from standard anthropometric data. The truncation limits for speed and shoulder width were set at the 5th and 95th percentiles, following the anthropometric convention of Pheasant and Haslegrave (2006), the source from which these body dimension ranges are drawn. Table 5.3 summarizes the daytime profile parameters.

Profile	Speed range (m/s)	Height range (m)	Shoulder range (m)	Night Speed range (m/s)
Adult	0.95-1.55	1.60-1.85	0.44-0.58	0.71-1.16
Child	0.60-1.20	1.30-1.60	0.39-0.45	0.45-0.9
Elderly	0.50-1.10	1.55-1.75	0.46-0.54	0.38-0.83

Table 5.3. Daytime movement parameters by occupant profile (truncated Normal distributions). Night-time speeds are obtained by scaling the mean and bounds by 0.75. Standard deviations for shoulder width and the full height ranges are reported in Annex D.

The distributions were verified against Pathfinder's output. A Kolmogorov-Smirnov test on the Adult_Day speed sample from the CM S1 baseline run ($n = 332$) yielded $D = 0.036$, not rejected at α = 0.05, confirming that Pathfinder correctly sampled the specified truncated-normal distribution. Equivalent tests on Child and Elderly profiles produced comparable results. Full KS statistics are reported in Annex C.

5.4.2 Pre-Movement Time Distributions

The pre-movement time, the interval between the alarm and the moment an occupant begins to move towards an exit, is one of the most influential parameters in any evacuation model, and at these sites it dominates the total evacuation time (as Chapter 6 establishes). It was modeled in Pathfinder's Behavior > Initial Delay field using a log-normal distribution, in line with the recommendation of PD 7974-6:2019 and the precedent set by Labhiri (2024).

Two behavioral states were distinguished. For daytime scenarios, the pre-movement distribution corresponds to category B of PD 7974-6:2019, representing occupants who are awake and broadly familiar with their surroundings. For nighttime scenarios, the distribution corresponds to category Ciii, representing sleeping occupants in unfamiliar surroundings, which produces substantially longer and more dispersed delays. The truncation limits were set at the 1st and 99th percentiles, following the convention of PD 7974-6:2019, the source of the distribution categories. The use of a different percentile convention here (1-99) from that used for the movement parameters (5-95) is deliberate: each variable adopts the convention of the standard from which it is drawn, rather than imposing a single arbitrary cut-off across variables of different origin.

The distribution parameters require care in the conversion between the units in which they are reported and the units Pathfinder expects. The pre-movement times are described in the literature in minutes, whereas Pathfinder's Initial Delay field operates in seconds. For a log-normal distribution, the Location and Scale parameters are defined on the logarithmic scale, where Location is the mean of the natural logarithm of the variable and Scale is its standard deviation. A change of time unit therefore acts additively on the Location parameter, through the logarithm of the conversion factor, and leaves the Scale parameter unchanged, since the standard deviation on the log scale is invariant under multiplication of the underlying variable by a constant. Applying this transformation to the minute descriptions yield the second based parameters used in this study: for daytime, Location = 6.7435 and Scale = 0.1487 (bounds 600-1200 s, 10-20 min); for night-time, Location = 7.4367 and Scale = 0.1487 (bounds 1200-2400 s, 20-40 min). The full derivation is given in Annex C.

The configured distributions were verified against the realized per-occupant output. A Kolmogorov-Smirnov test confirmed that the occupants' initial delays followed the intended log-normal distribution in both states: for the daytime distribution (Cabo Mayor S1, n = 650) the test returned D = 0.031, and for the night-time distribution (Parque Ardales S5, n = 500) it returned D = 0.052, both below the critical value at the 5% significance level and therefore not rejecting the log-normal fit. This confirms that the parameters adopted reproduce, in seconds, the same distribution that the source describes in minutes. The sensitivity of evacuation outcomes to the pre-movement distribution is discussed in the context of the results in Chapter 6, and the choice of distribution follows the recommendations of Ronchi and La Mendola (2016).

5.4.3 Muster Wait-Time Distributions

In the muster scenarios (S2 and S6), occupants do not evacuate directly to an exit but first travel to a designated assembly point, wait there for a period, and only then proceed to the exit. This wait represents the time spent gathering at the muster point before a coordinated movement to safety is initiated. It was modeled as an additional delay drawn from a truncated Normal distribution, distinct from the pre-movement delay.

The daytime muster wait was assigned a mean of 90 s and a standard deviation of 30 s; the nighttime muster wait a mean of 144 s and a standard deviation of 48 s. The night values preserve a night-to-day ratio of 1.6, consistent with the relationship adopted by Labhiri (2024) for muster behavior. The absolute values used here are somewhat lower than Labhiri's, a difference attributable to the smaller occupant populations and the more compact assembly areas of the two campsites studied, where the time required for occupants to converge on the muster point is correspondingly shorter.

A single muster point was defined at each site, located in an open area directly in front of the reception building, in the absence of any officially designated assembly point in the site documentation. As Chapter 6 shows, the geometric position of this muster point relative to the exits has a decisive effect on the muster scenario results, particularly at Cabo Mayor.

5.4.4 Selection of the Steering Movement Mode

Pathfinder offers two movement modes: an SFPE mode, which implements the hydraulic flow model of the SFPE Handbook, in which occupant speed is governed by local density and occupants follow routes based on queues without resolving individual interactions; and a Steering mode, in which each occupant independently steers around obstacles and other occupants, allowing overtaking, lateral spreading, and local route variation. Steering mode was selected as the primary movement mode for this study, and all 70 simulation runs were performed in it.

The justification rests on the nature of the environment being modeled. The two campsites are open air sites with wide internal roads, several meters across, rather than buildings with narrow corridors and doorways. In such an environment, faster occupants can overtake slower ones, and occupants distribute themselves laterally across the width of the road rather than forming a single file. The SFPE mode does not represent these behaviors: occupants follow a common route line and cannot pass one another, so the lateral space of a wide road is not used. This is visible directly in the simulation: in an SFPE run of the Parque Ardales model, occupants travel along the internal road in single file along a shared trajectory, without overtaking and without spreading across the available width, even where the road is wide enough to permit it (Figure 5.3). The Steering mode, by contrast, reproduces the overtaking and lateral spreading that would be expected of pedestrians on a wide open path, and therefore represents the movement dynamics of these sites more faithfully.

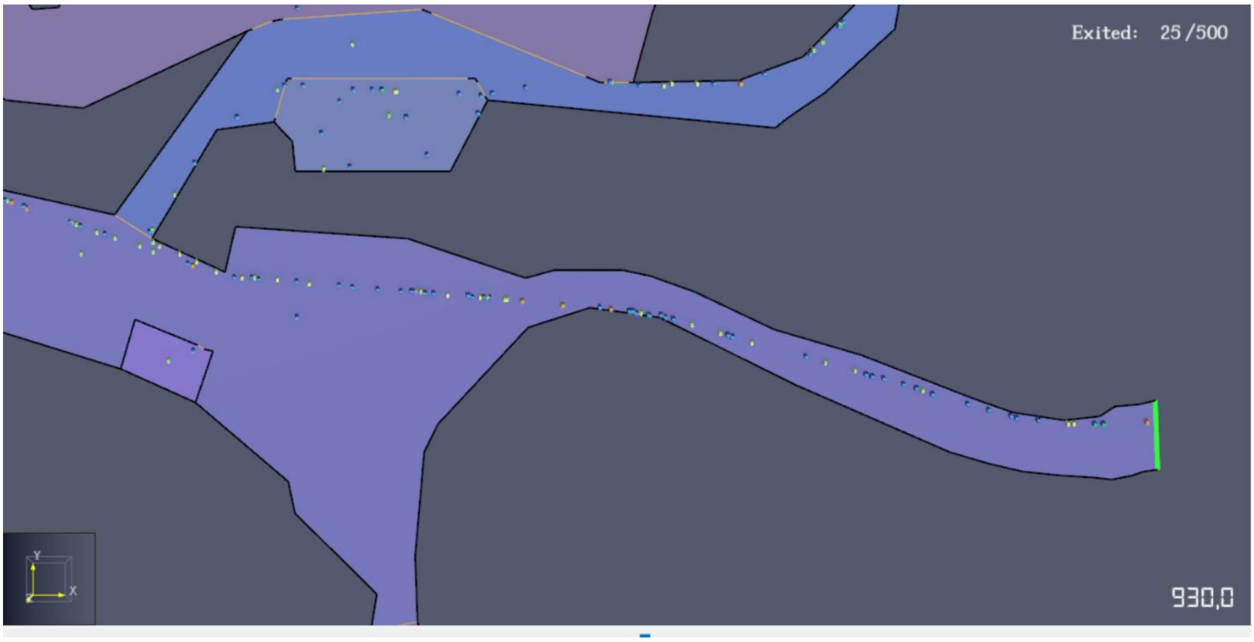

Figure 5.3. SFPE run of the Parque Ardales model. Occupants advance along the internal road in single file along a shared trajectory, without overtaking or lateral spreading, even where the road width would permit it. This single-file behavior is the principal reason SFPE mode was judged unsuitable for these open-air sites.

To confirm that the choice of mode did not introduce a gross distortion of the aggregate results, the two modes were compared on the same model and scenario (Parque Ardales, S1), with the same occupant configuration. The SFPE run produced a total evacuation time of 30.10 min and a mean completion time of 20.07, against 30.55 min and 20.28 min respectively for the Steering baseline, a difference in total time of under two percent. The exit split was identical between the two modes (499 occupants through Exit 2, one through Exit 1), confirming that the route choice behavior of the model is preserved across modes and that the choice of Steering affects the micro scale movement realism rather than the macroscopic evacuation outcome. Steering was therefore adopted as the more physically appropriate mode without any cost in the reliability of the aggregate results.

5.4.5 Density Evaluation Framework

The analysis of local crowding in Chapter 6 requires a defined framework for evaluating occupant density. Two distinct density quantities are produced by Pathfinder, and because they are computed differently and are not directly comparable in magnitude, both are defined here.

The first is the measurement region (MR) density, reported as a single value per measurement region over time. Pathfinder computes this as the mean of the per-occupant local densities of the occupants within the region, where each occupant's local density is estimated from the spacing to its neighbors using the body ellipse method of Fruin (1971), following the Pathfinder Technical Reference Manual (Thunderhead Engineering, 2024, §7.2.3). This is not the same as dividing the occupant count by the region area; consequently, the product of the reported density and the region area do not equal the occupant count, which is the expected behavior of this metric rather than an inconsistency. The second quantity is the floor contour density, a spatial field obtained by interpolating density across the navigation mesh, used to produce the density maps. Because one is a per-occupant local average over a polygon and the other a spatially interpolated field, the two are not directly comparable in magnitude, a distinction noted explicitly wherever both appear.

For the interpretation of these densities, an operational threshold of 4 occupants per square meter was adopted, following Oberhagemann (2012) and Helbing and Mukerji (2012), as the level above which crowd movement becomes critically constrained and the risk of dangerous crowd dynamics arises. This single, physically meaningful reference level was preferred over a graded Level-of-Service classification: the densities observed at both sites are, as Chapter 6 shows, an order of magnitude below this threshold, so a single threshold communicates the result more directly than a graded scale whose finer bands are never approached. All densities reported in Chapter 6 are therefore assessed against this level of 4 occupants per square meter.

5.4.6 Measurement Regions

To quantify local crowding along the evacuation routes, a set of measurement regions (MRs) was defined at each site. A measurement region is a polygon placed over the navigation mesh within which Pathfinder records occupant count, density, and velocity at each time step, allowing the evolution of crowding at a specific location to be tracked throughout the simulation. The regions were positioned at the points of flow convergence and at the exit approaches, where crowding, if it occurred, would be expected to concentrate.

Five measurement regions were defined at Parque Ardales, with a combined area of 147.2 m^2, as shown in Figure 5.4. MR_Exit1 (28.45 m^2) and MR_Exit2 (54.99 m^2) cover the approaches to the two exits. MR_Vial1-2 (21.96 m^2) is placed at the junction between Vial 2 and Vial 1, near the reception, where the flows from the upper zones merge before continuing towards the dominant exit; this is the principal convergence point of the site. MR_Vial2 (34.79 m^2) lies along Vial 2 in the upper part of the site, and MR_Pasillo4 (7.02 m^2), the smallest region, captures one of the narrow corridors connecting the bungalow zone to Vial 1.

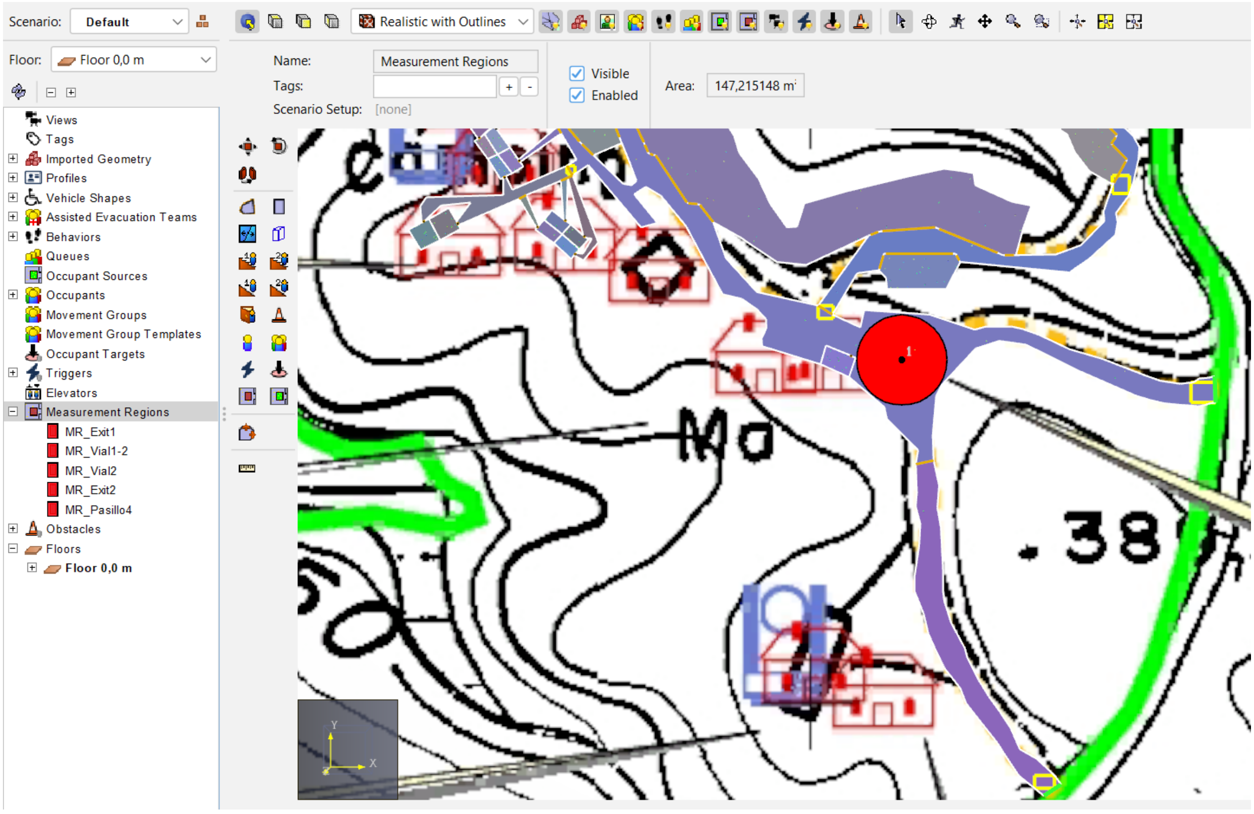

Figure 5.4. Measurement regions at Parque Ardales (highlighted), overlaid on the site model. The five regions cover the two exit approaches (MR_Exit1, MR_Exit2), the Vial 2-Vial 1 junction near the reception (MR_Vial1-2), the upper Vial 2 (MR_Vial2), and a bungalow connecting corridor (MR_Pasillo4).

Five measurement regions were likewise defined at Cabo Mayor, with a combined area of 155.9 m², as shown in Figure 5.5. MR_Exit (25.89 m²) and MR_Exit_Peatonal (7.24 m²) cover the approaches to the main vehicular exit and the secondary pedestrian exit respectively. MR_Vial1 (40.33 m²) is located on the road arriving from the lower part of the site, and MR_Vial2 (48.85 m²) on the road connecting to the upper zone. MR_Parking (33.64 m²) is placed at the parking area in the upper part of the site. As at Parque Ardales, the regions are positioned at the locations where flows from different zones merge and at the exit approaches, so that any developing congestion would be detected.

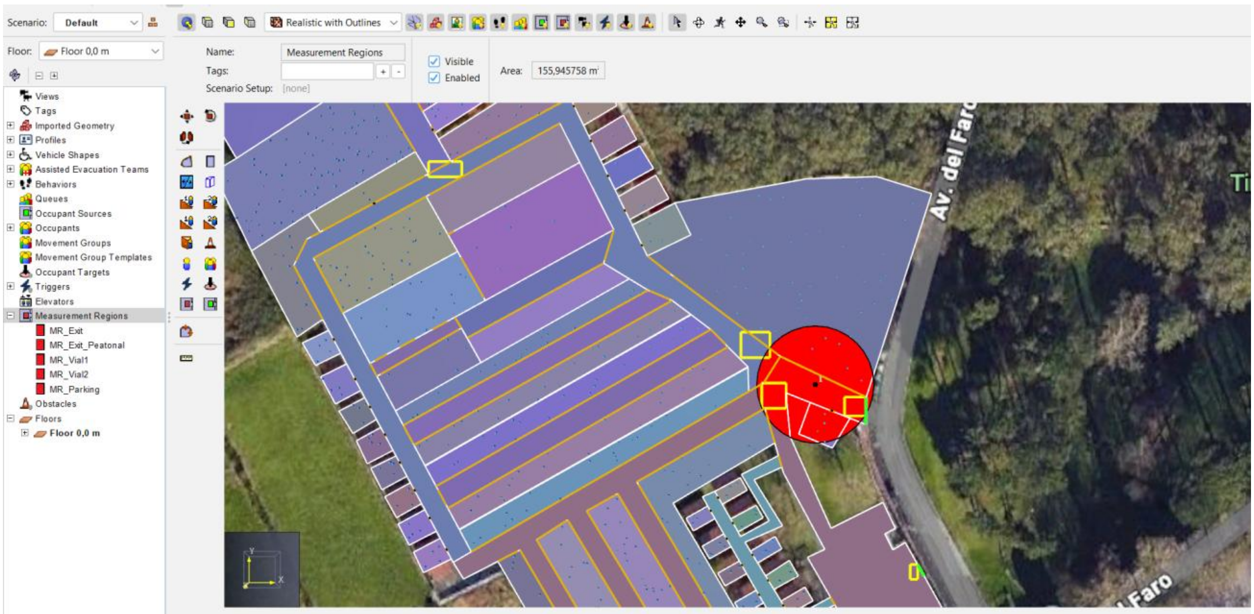

Figure 5.5. Measurement regions at Cabo Mayor (highlighted), overlaid on the satellite background. The five regions cover the two exit approaches (MR_Exit, MR_Exit_Peatonal), the lower and upper roads (MR_Vial1, MR_Vial2), and the parking area (MR_Parking).

5.5 Scenario Design

5.5.1 The Scenario Matrix

The simulation campaign is organized around a single baseline scenario from which a set of controlled variations is derived, each isolating the effect of one factor. The baseline, scenario S1, represents a daytime evacuation in which occupants move directly to the exits, with both exits available. From this reference case, three factors are varied independently.

The first factor is the time of day. Scenario S5 repeats the direct, both-exits configuration of S1 but under night-time conditions, applying the longer pre-movement distribution (category Ciii) and the 0.75 speed reduction described in Section 5.4. Comparing S5 with S1 isolates the effect of darkness and sleep on evacuation performance.

The second factor is the evacuation strategy. Scenarios S2 (day) and S6 (night) replace the direct evacuation with a muster-first protocol, in which occupants assemble at the reception point before proceeding to the exits. Comparing S2 with S1, and S6 with S5, isolates the cost of the assembly step.

The third factor is exiting availability. Scenarios S3 and S4 repeat the daytime direct configuration but with one exit closed: S3 closes the second exit, forcing all occupants through the first, while S4 does the reverse. Comparing these with S1 isolates the consequence of losing each exit and reveals any asymmetry between them.

A seventh scenario, S7, introduces family-group movement into the daytime direct configuration. Whereas S1 through S6 model every occupant as an independent agent, S7 organizes the population into family groups that move together, led by an adult, as detailed in Section 5.5.2. Comparing S7 with S1 isolates the effect of group cohesion on both evacuation time and local density. Because tourist campsites are occupied predominantly by families rather than by independent individuals, S7 represents the most realistic occupancy condition of the seven, and the comparison with S1 quantifies the degree to which the independent-agent assumption of the other scenarios departs from that reality.

The seven scenarios, identical in structure at both sites, are summarized in Table 5.4.

Scenario	Time of day	Strategy	Exits available	Movement
S1	Day	Direct	Both	Individual
S2	Day	Muster	Both	Individual
S3	Day	Direct	Exit 1 only	Individual
S4	Day	Direct	Exit 2 only	Individual
S5	Night	Direct	Both	Individual
S6	Night	Muster	Both	Individual
S7	Day	Direct	Both	Family groups

Table 5.4. The seven simulation scenarios. Each scenario was run at both campsites with five stochastic repetitions, giving 35 runs per site and 70 runs in total.

5.5.2 Family-Group Movement (S7)

In scenario S7, the occupant population is organized into family groups using Pathfinder's movement-group functionality. Each group is assigned an adult leader, and the remaining members follow the leader, with the option to follow the leader enabled and a maximum separation distance set at 2.0 m for families and 1.5 m for couples. Members of a group are restricted to originate in the same room, and inter-occupant social-distancing is disabled, so that group members move as a cohesive cluster rather than maintaining individual spacing.

Rather than imposing a single group type, the population was composed of several family compositions, to reflect the variety of party types present at a real campsite. At Parque Ardales, the 500 occupants were organized into 120 groups plus 10 ungrouped staff: 25 nuclear families of two adults and two children, 50 large families of two adults, three children, and one elderly member, and 45 adult couples. At Cabo Mayor, the 650 occupants were organized into 157 groups plus 11 ungrouped occupants (10 staff and one solo occupant): 34 nuclear families, 64 large families, 58 couples, and one couple accompanied by an elderly member (two adults and one elderly occupant). In both cases the group compositions preserve the same overall adult-child-elderly demographic split used in the individual-movement scenarios, so that S7 differs from S1 only in the cohesion of movement, not in the composition of the population.

5.5.3 Stochastic Protocol

Pathfinder's Steering mode is stochastic: each occupant's speed, body dimensions, and pre-movement delay are drawn from the distributions of Section 5.4, and the resulting trajectories vary between runs even for an identical model. To capture this variability rather than relying on a single realization, each scenario was run five times with independent random seeds, giving 35 runs per site and 70 runs across the campaign. The results reported in Chapter 6 are, unless otherwise stated, the mean across the five repetitions of a scenario, with the run-to-run dispersion reported alongside.

For the spatial density analysis, a worst-case run was additionally identified for each scenario, defined as the repetition exhibiting the highest single measurement-region peak density among the five. This worst-case run is used for the density contour maps in Chapter 6, so that the maps represent the most demanding crowding conditions observed rather than an averaged condition that would understate the peaks. The worst-case runs and their associated peak densities are listed in Table 5.5.

Site	Scenario	Run	Peak density (occs/m²)	Measurement region
Parque Ardales	S1	Run 4	0.44	MR_Vial1-2
	S2	Run 1	0.34	MR_Exit2
	S3	Run 4	0.35	MR_Exit1
	S4	Run 5	0.43	MR_Vial1-2
	S5	Run 5	0.33	MR_Vial1-2
	S6	Run 3	0.30	MR_Vial1-2
	S7	Run 4	0.64	MR_Vial1-2
Cabo Mayor	S1	Run 1	0.52	MR_Exit
	S2	Run 5	0.56	MR_Exit
	S3	Run 2	0.65	MR_Exit
	S4	Run 5	0.74	MR_Exit_Peatonal
	S5	Run 5	0.36	MR_Exit
	S6	Run 1	0.47	MR_Exit
	S7	Run 5	0.63	MR_Exit

Table 5.5. Worst-case run for each scenario at both sites, defined as the repetition with the highest single measurement region peak density among the five. The reported value is the peak density of that single worst-case run (not the scenario mean), and identifies the measurement region in which it occurs.

As noted in Section 5.4.5 and confirmed in Chapter 6, even the worst-case peak densities listed here remain an order of magnitude below the 4 occupants per square meter operational threshold; the table identifies the most demanding run for the purpose of the spatial density maps rather than indicating any approach to a critical crowding condition.

5.5.4 Initial run observations

Beyond the statistical and mode validations, each model was checked for physical integrity in every run of the campaign. The exit summaries of all 70 runs were examined to confirm that the full occupant population reached an exit in each run, with no occupants left stranded inside the model or trapped at an obstruction; the cumulative exit counts matched the configured occupancy (500 at Parque Ardales, 650 at Cabo Mayor) in every case. This whole population egress check is the most basic guarantee that the navigation mesh is fully connected and that no part of the geometry isolates its occupants. An early failure of exactly this kind, in which a small number of occupants became trapped at bungalow doorways of insufficient width, was detected during initial testing and resolved as described in Section 5.2.3, after which the check passed cleanly for all runs.

The evacuation animations were also reviewed visually for each scenario, to confirm that occupant trajectories were physically sensible: that occupants followed the road network rather than cutting through closed accommodation, that they chose reasonable routes towards the exits, and that no unphysical behavior (oscillation, backtracking, or clustering away from any exit) occurred. The trajectories were consistent with the expected evacuation patterns at both sites.

This visual inspection also surfaced an emergent behavior of the Steering algorithm worth documenting, in the daytime muster scenario (S2) at Cabo Mayor. In two of the five S2 runs, a single occupant completed the route to the secondary pedestrian exit (Exit_Peatonal) rather than returning to the main exit with the rest of the population. Examination of the trajectories indicates that the assembly area in front of the reception saturates locally under the daytime arrival rate, and that as the Steering algorithm searches for an unobstructed path, a few occupants are momentarily routed towards Exit_Peatonal; although almost all of them rejoin the flow to the main exit, in two runs one occupant completes the alternative route. The effect does not occur in the night-time muster scenario (S6), where the longer night-time pre-movement distribution staggers the arrivals at the assembly point and keeps the local density below the level at which this transient rerouting occurs. The impact on the results is negligible, shifting the S2 exit split from a complete 100/0 collapse to 99.8/0.2, but it is recorded here both because it is a genuine emergent property of the movement model rather than a configuration error, and because it nuances the muster-collapse finding reported in Chapter 6: the assembly step concentrates essentially all traffic on the main exit, but under daytime loading the concentration is not quite total.

Chapter 6. Results and Analysis

6.1 Parque Ardales

This section presents the evacuation simulation results for Camping Parque Ardales (PA), a 500 occupant facility. Seven scenarios were simulated with five Monte Carlo repetitions each (35 runs total), exploring the effects of time of day (day versus night), evacuation strategy (direct versus muster), exit availability (both exits, Exit 1 only, Exit 2 only), and group movement (family cohesion versus individual). All densities are reported in occupants per square meter (occs/m²) and evaluated against the operational threshold of 4 occs/m², above which congestion can escalate rapidly and pose safety risks (Oberhagemann, 2012; Helbing and Mukerji, 2012). Density contour maps are presented for day scenarios only (S1-S4 and S7), as night scenarios produce structurally lower peak densities and identical spatial routing patterns.

6.1.1 Master results and reproducibility

Table 6.1 summarizes the principal evacuation metrics across all seven scenarios. Total evacuation time ranges from 30.6 min (S1, day baseline) to 55.8 min (S6, night with muster). The coefficient of variation (CoV) remains below 7% in all scenarios, confirming adequate reproducibility with five repetitions per scenario.

Scenario	Description	TotalT (min)	SD (min)	CoV (%)	MeanCompT (min)	Mean Dist (m)	Exit Split (Exit/EP)
S1	Day/Direct	30.6	1.4	4.6	20.3	358	499/1
S2	Day/Muster	32.2	1.2	3.6	21.7	367	500/0
S3	Day/Direct/E1 only	32.3	1.5	4.6	21.0	403	0/500
S4	Day/Direct/E2 only	31.6	2.1	6.5	20.4	358	500/0
S5	Night/Direct	52.7	1.6	2.9	36.7	357	499/1
S6	Night/Muster	55.8	2.5	4.4	38.9	366	500/0
S7	Day/Direct/Group	34.9	1.2	3.4	24.2	472	499/1

Table 6.1. Master evacuation results for Parque Ardales (500 occupants, Steering mode). Times in minutes. Mean distance and exit split correspond to scenario-mean values.

Figure 6.1 shows the evacuation curves for all seven scenarios. The day scenarios (S1-S4 and S7) cluster in the 29-36 min range, while the night scenarios (S5-S6) extend to 53-56 min, visually confirming that time of day is the dominant source of variation. S7 (green curve) is clearly offset from the day cluster, reflecting the group movement penalty.

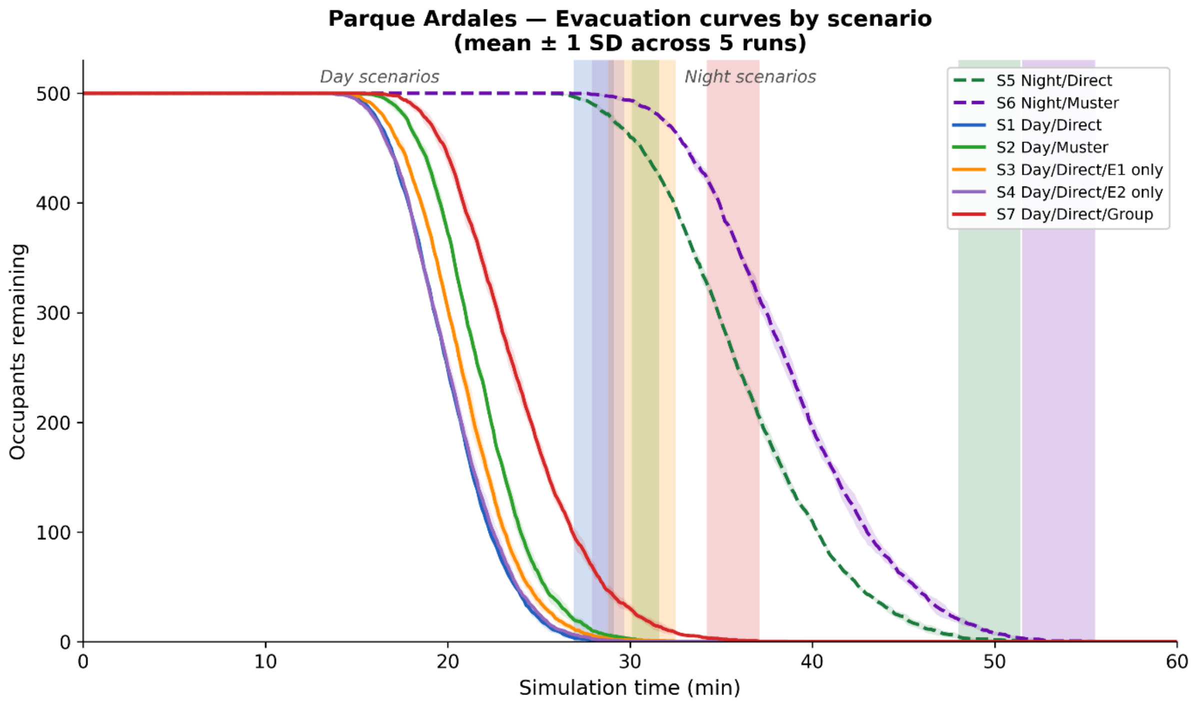

Figure 6.1. Evacuation curves for Parque Ardales, showing occupants remaining versus simulation time (mean ± 1 SD across 5 runs). Day scenarios cluster at left; night scenarios at right; S7 (group movement) is offset from the day cluster.

6.1.2 Time of day as the dominant source of variation

The night penalty dominates all other effects. S5 exceeds S1 by 22.1 min (+72%), driven by two compounding factors: the pre-movement median shifts from 14.3 min (PD 7974-6:2019 Category B) to 28.3 min (Category Ciii), a 2.0× multiplier; and walking speed reduces by 25% (night factor 0.75, per Labhiri, 2024, Section 5.5). The pre-movement shift alone accounts for approximately 14 min of the 22 min penalty, with the speed reduction contributing the remaining 8 min through longer active travel times.

Note on pre-movement parameters: the log-normal parameters used in this study (Location = 6.7435, Scale = 0.1487 for day; Location = 7.4367 for night) incorporate a dimensional correction to the values reported by Labhiri (2024, Appendix I). This correction is documented in Chapter 5 as an original methodological contribution of this thesis.

6.1.3 Exit usage and the single exit configuration

In the baseline scenarios (S1, S5), 499 of 500 occupants use Exit 2 (the emergency exit at Zona 2), with only one occupant, a Vial 4 resident positioned nearest to Exit 1, using the main entrance. This 499/1 split is preserved identically in S7 (group movement), confirming that the asymmetry is geometric, not behavioral. Exit 1 possesses substantial latent capacity (0.86 pers/s under full load in S3) that remains entirely unused under normal operation with two exits.

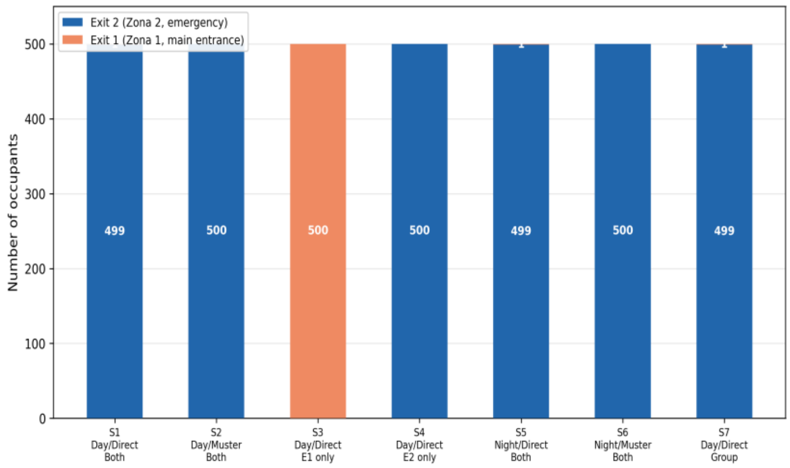

Figure 6.2. Exit usage by scenario. The 499/1 split between Exit 2 and Exit 1 is consistent across S1, S5, and S7, confirming a geometry-driven de-facto single-exit configuration.

6.1.4 Exit closure produces asymmetric penalties

Closing Exit 2 (S3, Exit 1 only) increases total evacuation time by 1.7 min (+5.6%), while closing Exit 1 (S4, Exit 2 only) adds only 1.0 min (+3.3%). The ratio of penalties (1.7×) contrasts sharply with the pre-closure usage ratio (499×), demonstrating that closure cost is governed by alternative path length, not by the number of displaced occupants.

Steady state throughput, measured as the slope of cumulative exits between the 50th and 450th occupant, is 0.86 pers/s for Exit 1 (S3) and 0.89 pers/s for Exit 2 (S4), a difference of 3.6% well within one standard deviation. The two exits have effectively identical physical capacity; the 499/1 baseline imbalance is driven by routing, not by capacity.

6.1.5 Muster strategy

The muster-first strategy adds 1.6 min to the day baseline (S2 versus S1, +5.3%) and 3.1 min at night (S6 versus S5, +5.9%). The day penalty closely matches the muster wait parameter (μ = 90 s = 1.5 min), indicating that most of the penalty is absorbed wait time with minimal additional routing cost. In all muster scenarios the exit split collapses to 500/0 (Exit 2 only), because the post-muster shortest path from Recepción always favors Exit 2.

6.1.6 Density analysis

Table 6.2 reports the scenario mean peak density in each Measurement Region for the day scenarios. All values remain well below the 4 occs/m² operational threshold. The highest mean peak density across all individual scenarios (S1-S4) is 0.37 occs/m² at MR_Vial1-2 in S1, an order of magnitude below the threshold. S7 (group movement) produces higher mean peaks across all MRs, reaching 0.50 occs/m² at MR_Vial1-2, but still well within the safe operating range.

MR	Area (m²)	S1	S2	S3	S4	S7
MR_Exit1	28.45	0.01	0.00	0.28	0.00	0.01
MR_Vial1-2	21.96	0.37	0.27	0.21	0.34	0.50

MR_Vial2	34.79	0.18	0.17	0.18	0.18	0.32
MR_Exit2	54.99	0.25	0.26	0.00	0.27	0.36
MR_Pasillo4	7.02	0.19	0.19	0.17	0.16	0.29

Table 6.2. Scenario-mean peak density per Measurement Region (occs/m²), day scenarios only. All values are below the 4 occs/m² operational threshold (Oberhagemann, 2012). S7 density values reflect the increased local crowding produced by family-group cohesion.

Methodological note: Two density metrics are employed. Table 6.2 reports Pathfinder's Measurement Region density, which computes the mean local density per occupant (Fruin, 1971, ellipse method) averaged over all occupants within the MR polygon at each 1.0 s interval (Thunderhead Engineering, 2024, Technical Reference Manual §7.2.3). The contour maps below use Pathfinder's floor contour visualization, which interpolates density spatially across the navigation mesh. The two metrics are not directly comparable in magnitude but provide complementary quantitative and spatial perspectives.

Figures 6.3 through 6.7 present the maximum instantaneous density contour for each day scenario (worst-case run, selected as the run with the highest single MR peak among the five repetitions; see Table 5.5 in Chapter 5). The color scale is fixed at 0-4 occs/m² across all maps.

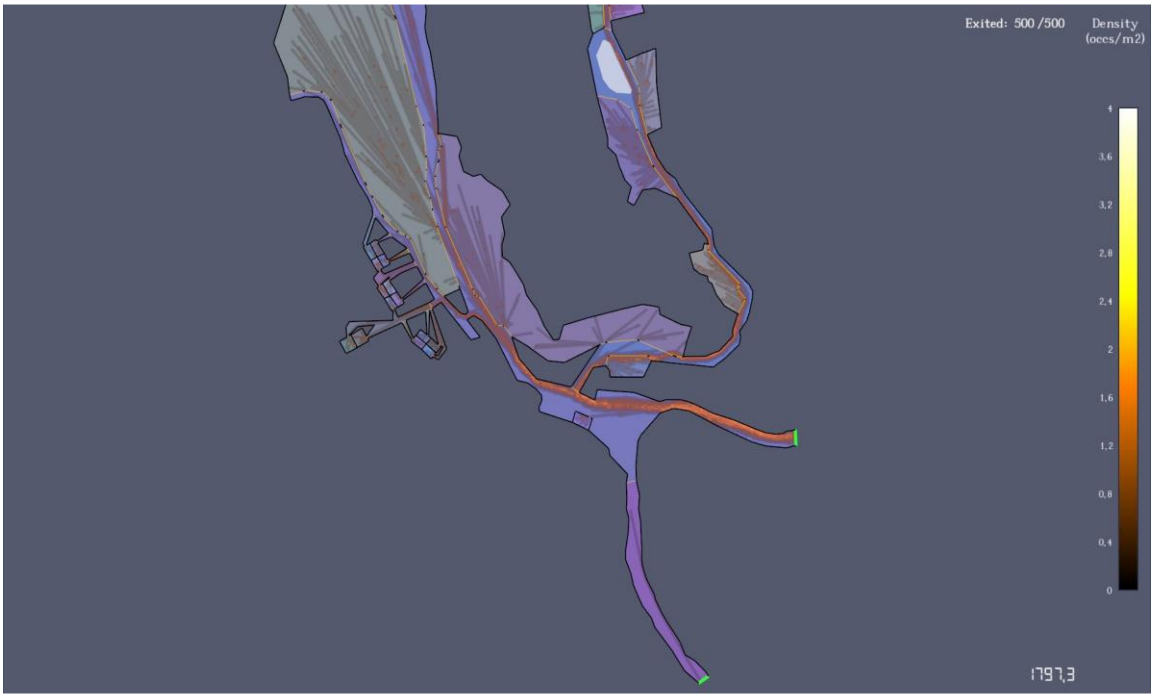

Figure 6.3. Maximum instantaneous density contour, S1 Day/Direct/Both exits (Run 4, worst-case). The dominant evacuation route toward Exit 2 is visible as a continuous band of elevated density (0.8-1.6 occs/m² locally). Exit 1 (lower left) shows negligible activity, consistent with the 499/1 exit split.

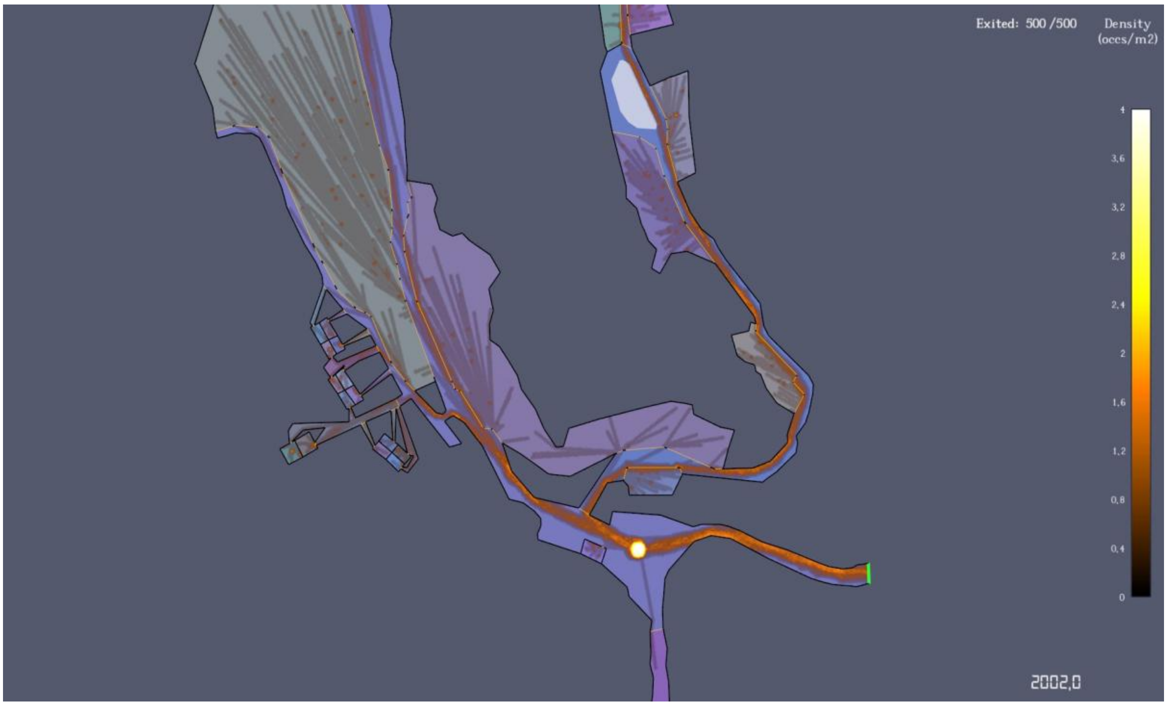

Figure 6.4. Maximum instantaneous density contour, S2 Day/Muster/Both exits (Run 1, worst-case). The muster strategy concentrates flow through a single corridor post-assembly, producing a localized hotspot near Recepción that exceeds the S1 baseline.

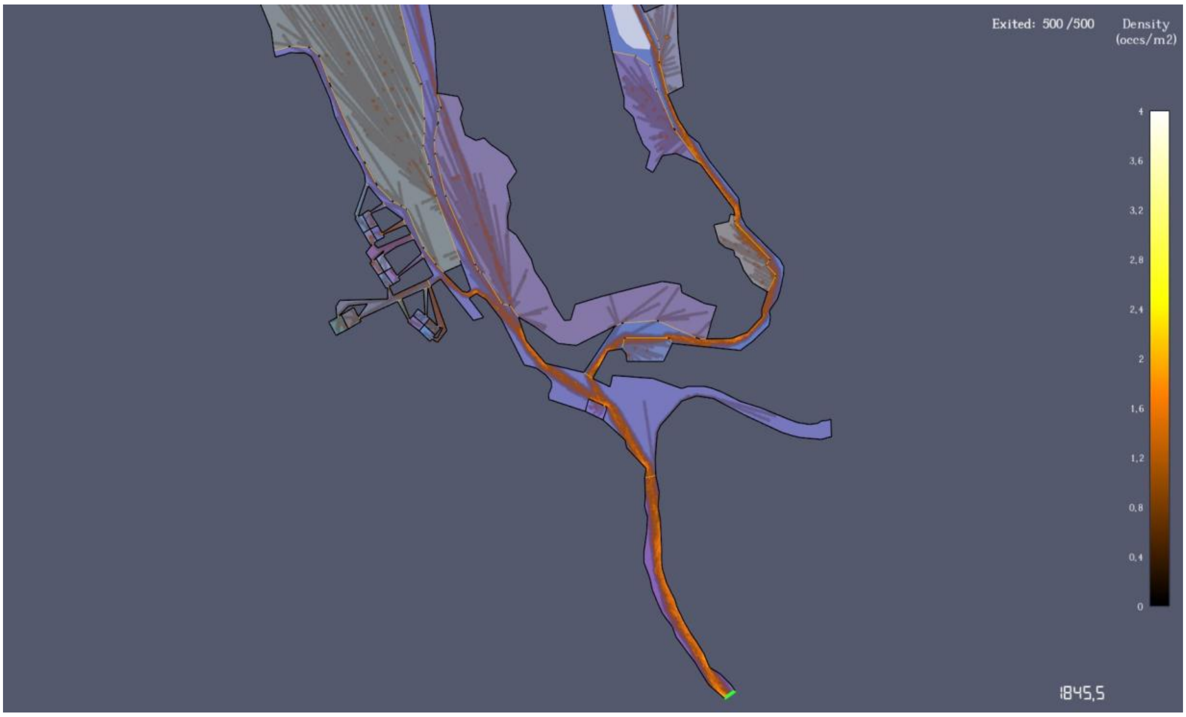

Figure 6.5. Maximum instantaneous density contour, S3 Day/Direct/Exit 1 only (Run 4, worst-case). With Exit 2 closed, evacuees are redirected through the southern vial network toward Exit 1, producing a continuous density band along the full alternative route.

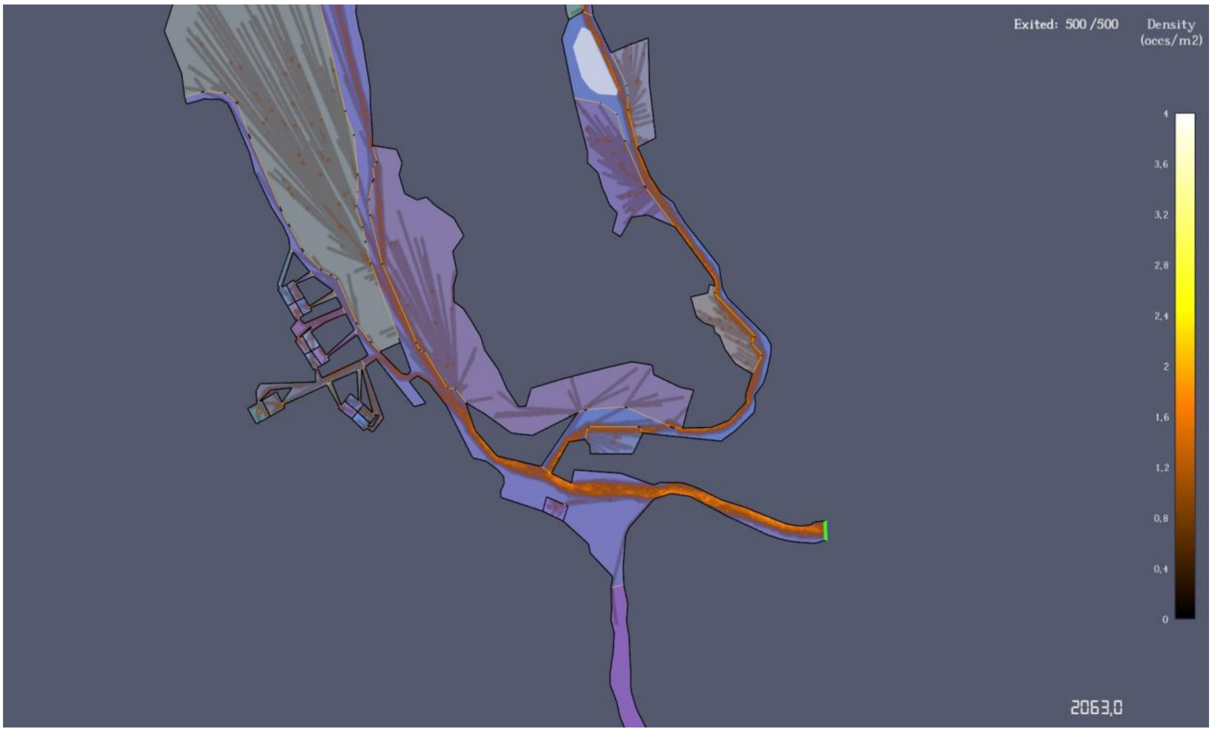

Figure 6.6. Maximum instantaneous density contour, S4 Day/Direct/Exit 2 only (Run 5, worst-case). The pattern is similar to S1 but with broader density bands, as the full 500 occupants converge on Exit 2 without any demand sharing.

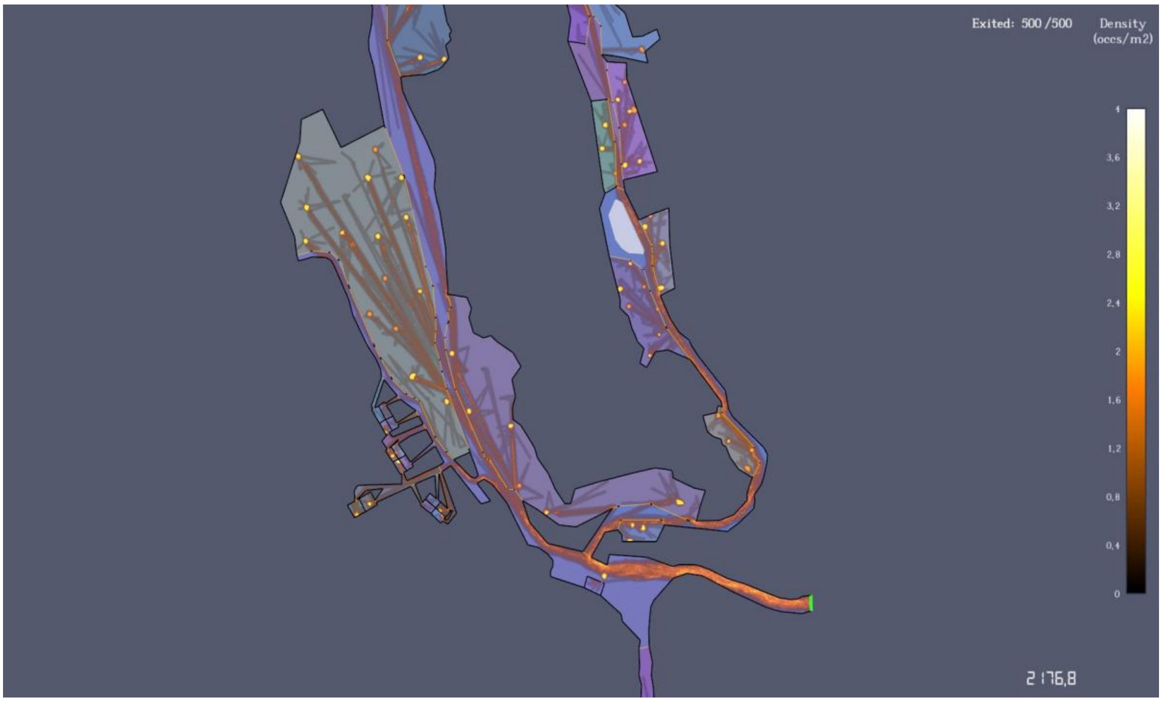

Figure 6.7. Maximum instantaneous density contour, S7 Day/Direct/Group movement (Run 4, worst-case). Group cohesion produces visibly wider and more intense density bands compared to S1, particularly along the main vial toward Exit 2 and in the central confluence zone.

Figures 6.8 through 6.12 present the accumulated space utilization (person-seconds per cell) for the same scenarios. The color scale is fixed at 0-250 occs·s for all PA scenarios.

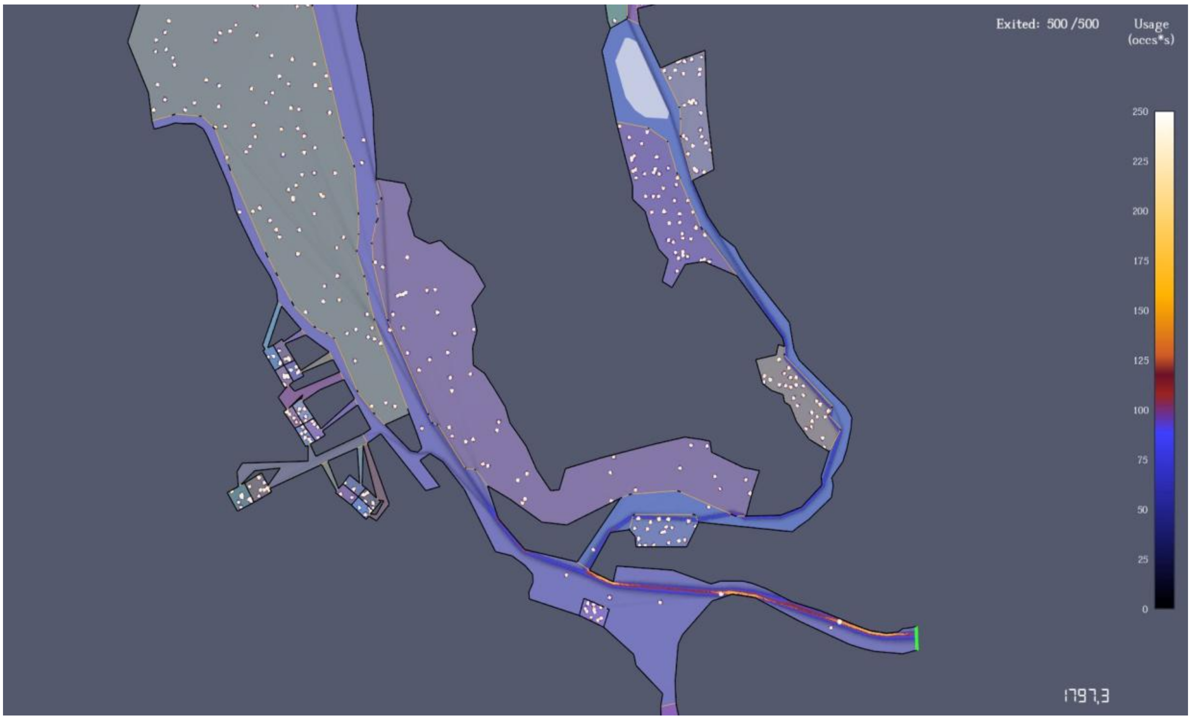

Figure 6.8. Accumulated space utilization, S1 Day/Direct/Both exits (Run 4). The dominant route toward Exit 2 concentrates the highest usage. Exit 1 and the southern tail show minimal accumulated traffic, confirming the de-facto single-exit configuration.

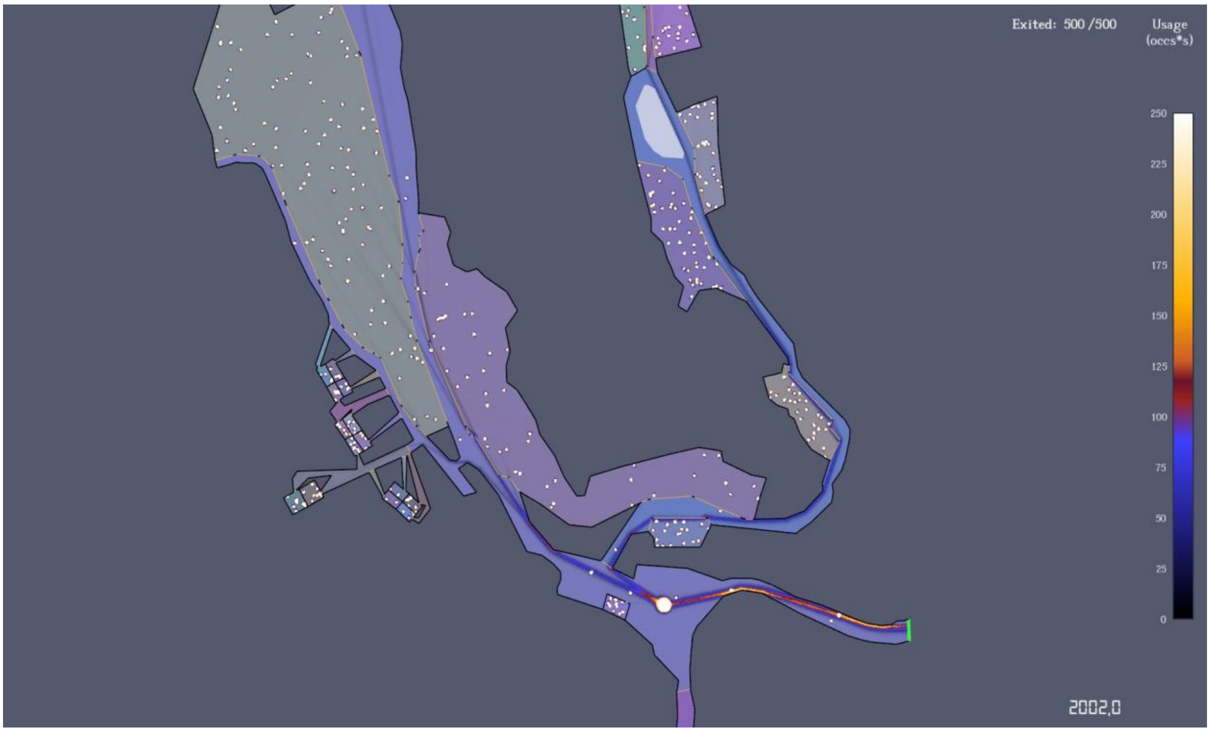

Figure 6.9. Accumulated space utilization, S2 Day/Muster/Both exits (Run 1). The muster point near Recepción generates a concentrated hotspot, and post-muster traffic is funneled toward Exit 2 exclusively.

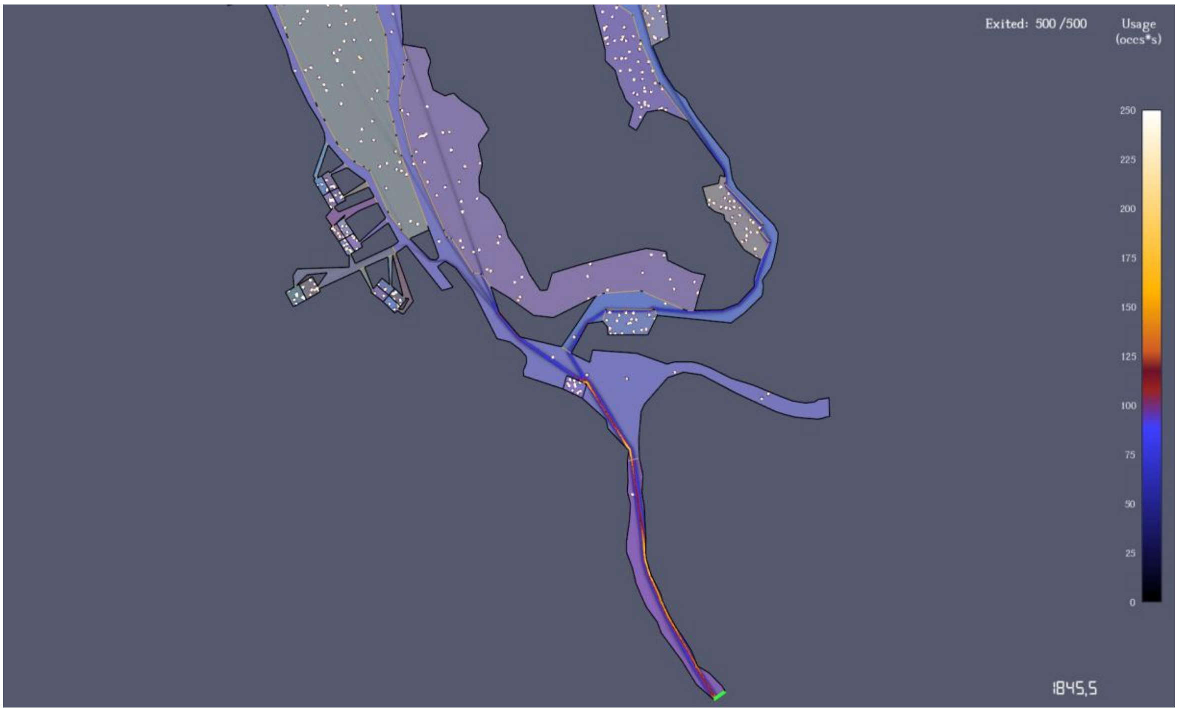

Figure 6.10. Accumulated space utilization, S3 Day/Direct/Exit 1 only (Run 4). Usage is redistributed toward the southern route, which becomes the sole evacuation corridor. The full-length activation of the alternative route explains the +45 m increase in mean distance.

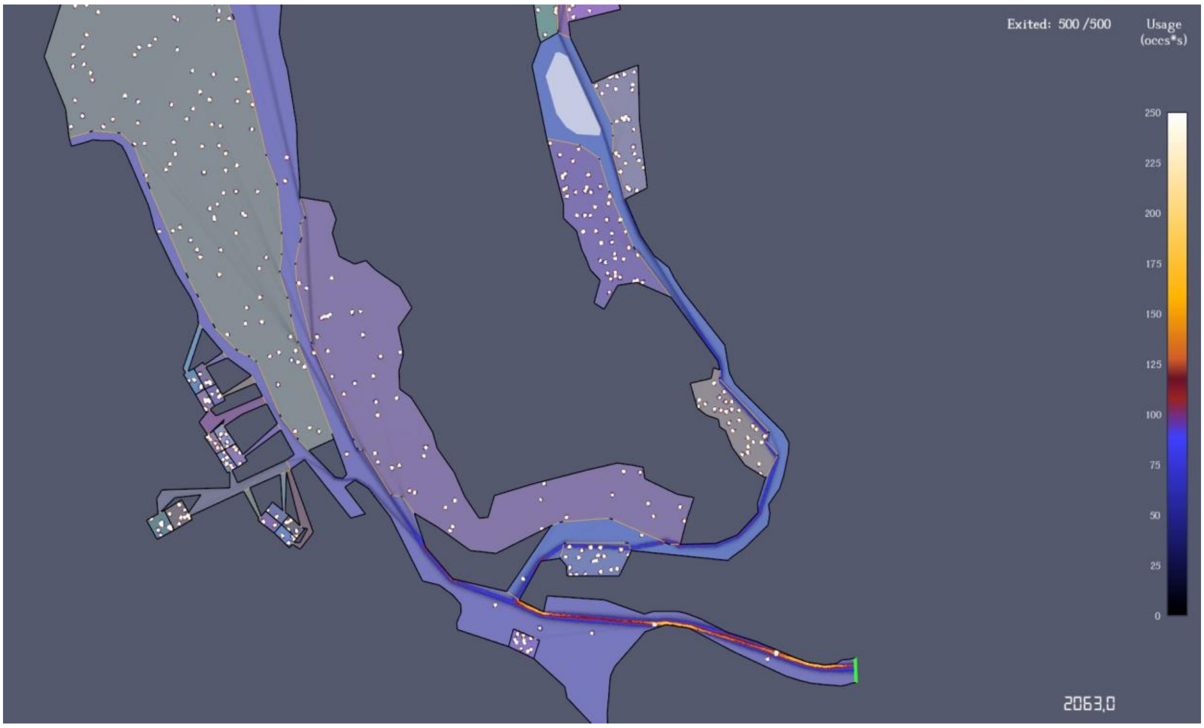

Figure 6.11. Accumulated space utilization, S4 Day/Direct/Exit 2 only (Run 5). Similar to S1 but with more uniform loading along the main vial, as the full 500 occupants use Exit 2.

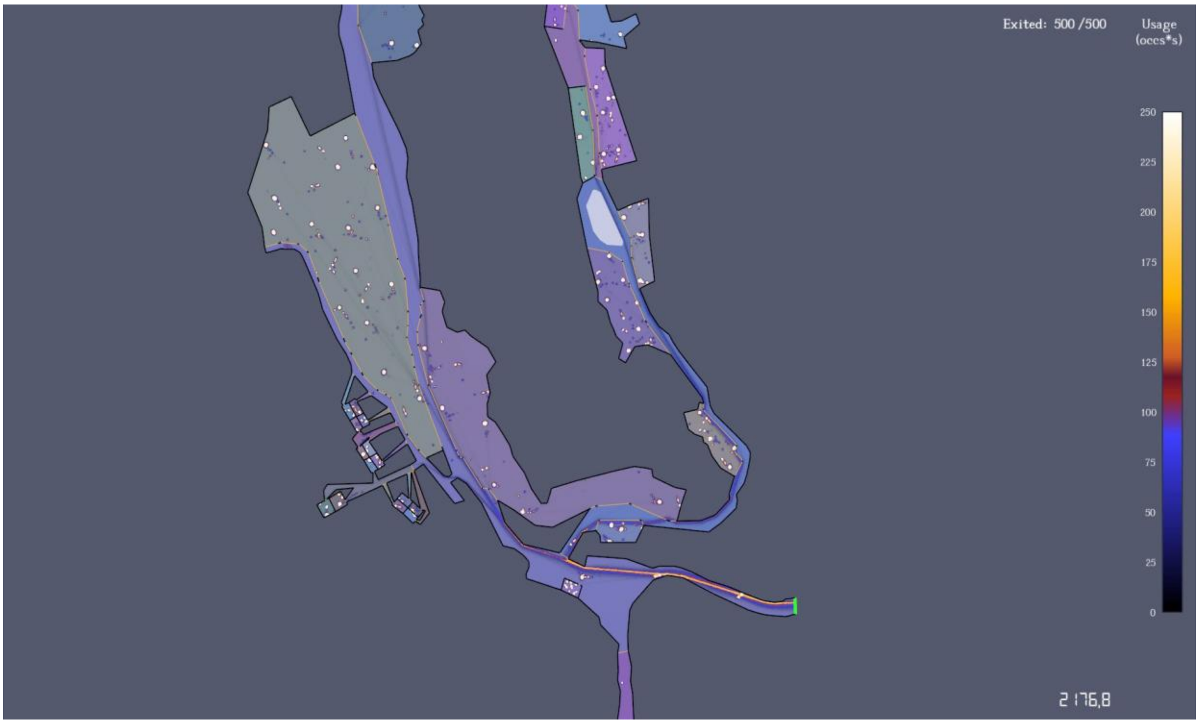

Figure 6.12. Accumulated space utilization, S7 Day/Direct/Group movement (Run 4). The spatial pattern is identical to S1 (same exits, same geometry), but usage values are higher because groups traverse cells more slowly, accumulating more person-seconds per cell.

6.1.7 Group movement (S7)

Scenario S7 introduces group movement based on families as a sensitivity analysis, with all other parameters identical to S1. Occupants are assigned to 120 movement groups (25 nuclear families of 4, 50 large families of 6, and 45 couples) plus 10 ungrouped staff. Group members follow their leader (an adult) and maintain spatial cohesion with a maximum inter-member distance of 2.0 m (1.5 m for couples).

The group penalty on total evacuation time is +4.3 min (+14.1%), the largest day scenario penalty after exit closure (S3, +1.7 min) and muster (S2, +1.6 min). Mean completion time increases by 3.9 min (+19.3%), and mean walking distance rises from 358 m to 472 m (+32%), the latter reflecting the oscillatory movement of group leaders maintaining cohesion with slower members.

The density impact is more pronounced. Figure 6.13 compares worst-case peak densities per MR between S1 (individual) and S7 (group). All transit zones experience substantial increases: MR_Vial1-2 rises from 0.44 to 0.64 occs/m² (+45%), MR_Vial2 from 0.18 to 0.44 (+144%), and MR_Pasillo4 from 0.19 to 0.41 (+116%). Despite these increases, no MR approaches the 4 occs/m² threshold.

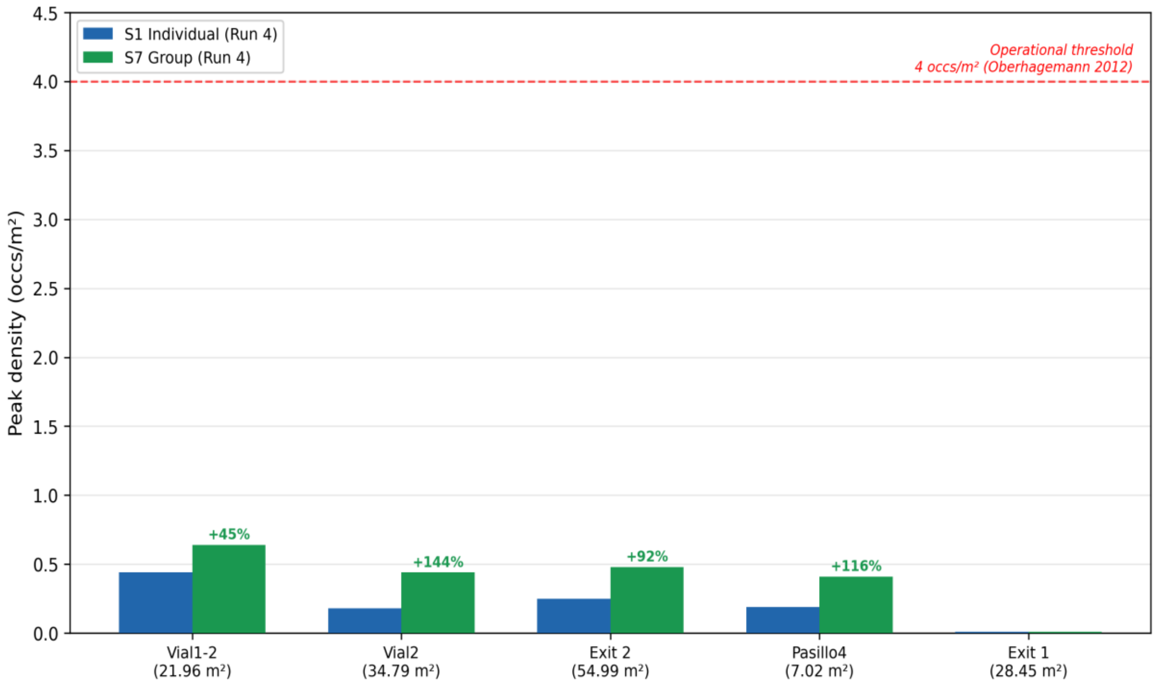

Figure 6.13. Comparison of worst-case peak density per Measurement Region, S1 (individual, blue) versus S7 (group, green). Percentage increases are annotated. The dashed red line marks the 4 occs/m² operational threshold (Oberhagemann, 2012).

A notable emergent property of group movement is the appearance of congestion time. In S1, zero kinematic congestion is recorded across all runs and MRs (velocity deficit = 0). In S7, the mean congestion time per occupant is 125 s, with only 3-6 of 500 occupants per run experiencing zero congestion. This congestion reflects the speed penalty imposed by group cohesion: faster adult leaders decelerate to maintain proximity with slower children and elderly members, which Pathfinder registers as kinematic congestion.

The profile-level completion times confirm this mechanism. In S7, adults complete evacuation in 22.9 min on average, children in 25.5 min, and elderly in 25.9 min, a compressed 3.0 min spread compared to the wider individual speed spread in S1. Group cohesion synchronizes members toward the slowest profile's pace, compressing inter-profile variability.

Caveat: group movement parameters (maximum distance, leader assignment) lack empirical calibration data (Thunderhead Engineering, 2026), and S7 should be interpreted as a sensitivity analysis exploring the direction and magnitude of the group effect, not as a validated prediction. Individual movement scenarios (S1-S6) likely underestimate both evacuation times and transit densities in a family dominated camping context, this finding is robust to reasonable parameter variations.

6.1.8 Synthesis

The Parque Ardales simulations yield six principal findings:

1. Night penalty dominates. The day-to-night transition adds 22 min (+72%), driven primarily by the 2.0× shift in pre-movement median (PD 7974-6:2019 Category B to Ciii) and secondarily by the 0.75× speed reduction. This is the single largest source of variation in the dataset and underscores early night-time alert as the primary intervention for reducing evacuation time.

2. De-facto single-exit configuration. PA operates as a single-exit camping despite having two physical exits, with 499 of 500 occupants using Exit 2 in all baseline and group scenarios. Exit 1 possesses identical physical capacity (0.86 vs 0.89 pers/s) but is geometrically disadvantaged. This latent capacity represents an opportunity for design intervention.

3. Exit closure asymmetry is driven by path, not demand. Closing the dominant exit (Exit 2) costs only 1.7 min because the alternative route, while longer, has ample capacity. The 1.7× penalty ratio contrasts with the 499× usage ratio, confirming that alternative path length, not displaced occupant count, governs closure cost.

4. Muster penalty is modest and partially absorbed. The 1.6 min muster overhead (+5.3%) closely tracks the mean wait parameter (1.5 min), indicating minimal additional routing cost. However, muster collapses the exit split to 500/0, eliminating any residual demand sharing.

5. Group movement produces the largest day scenario penalty. Family cohesion adds 4.3 min (+14.1%) to total evacuation time and increases transit densities by 45-144% across MRs. The individual movement model (S1-S6) underestimates both time and density in the realistic family camping context. Nevertheless, all densities remain well below the 4 occs/m² operational threshold.

6. PA is limited by travel time, not queueing limited. Peak densities in all 35 runs across all seven scenarios remain below 0.64 occs/m², an order of magnitude below the 4 occs/m² threshold. The mean walking distance of 358-472 m, not congestion at exits or corridors, is the binding constraint on evacuation time.

6.2 Cabo Mayor

Cabo Mayor (CM) is a 650 occupant camping facility in Santander whose layout differs from Parque Ardales in two structural respects: a shorter mean evacuation distance (~120 m versus ~360 m) and a functional two exit configuration in which both gates absorb meaningful traffic under baseline conditions. The same seven scenario protocol described in Section 6.1 was applied here, again with five stochastic repetitions per scenario (35 runs). Densities throughout this section are referenced to the 4 occs/m² operational threshold recommended by Oberhagemann (2012) and Helbing and Mukerji (2012). Contour maps cover day scenarios exclusively (S1-S4 and S7); night scenarios exhibit lower peak densities without altering the spatial distribution of flow.

6.2.1 Master results and reproducibility

Table 6.3 collects the key metrics for all seven CM scenarios. Evacuation times span from 23.5 min (S3) to 47.5 min (S6), a narrower absolute range than at PA (30.6-55.8 min), consistent with Cabo Mayor's shorter internal distances. Reproducibility is high: the mean CoV across scenarios is 2.7%, tighter than the 4.3% observed at Parque Ardales. The larger occupant pool (650 versus 500) dampens stochastic outlier effects on the total time metric, and all CoV values stay below 6%.

Scenario	Description	TotalT (min)	SD (min)	CoV (%)	MeanCompT (min)	Mean Dist (m)	Exit Split (Exit/EP)

S1	Day/Direct	23.6	0.7	3.0	16.3	118.6	509/141 (78/22%)
S2	Day/Muster	25.1	0.8	3.3	18.3	133.1	649/1 (99.8/0.2%)
S3	Day/Direct/Exit only	23.5	0.6	2.4	16.4	127.5	650/0 (100/0%)
S4	Day/Direct/EP only	24.6	1.3	5.3	16.8	151.3	0/650 (0/100%)
S5	Night/Direct	44.1	0.8	1.9	31.2	118.3	509/141 (78/22%)
S6	Night/Muster	47.5	0.7	1.5	34.8	132.8	650/0 (100/0%)
S7	Day/Direct/Group	24.4	0.3	1.2	18.9	277.2	513/137 (79/21%)

Table 6.3. Master evacuation results for Cabo Mayor (650 occupants, Steering mode). Times in minutes. EP = Exit_Peatonal. Exit split shows mean occupant count per exit and percentage in parentheses.

The evacuation curves in Figure 6.14 illustrate the scenario spread. Day conditions (S1-S4, S7) group tightly between 23 and 25 min, separated from the night band (S5-S6) by a gap of roughly 20 min. Unlike at PA, the S7 curve sits almost on top of the day cluster rather than forming a distinct offset, foreshadowing the small group penalty discussed in Section 6.2.7.

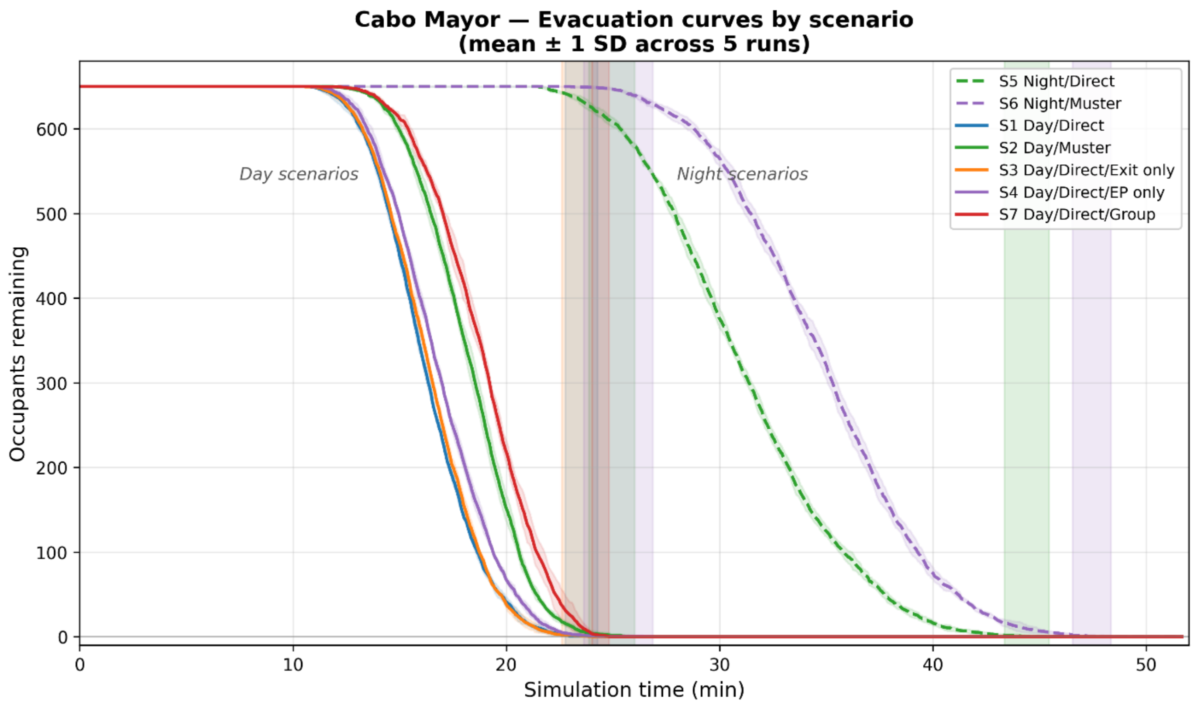

Figure 6.14. Occupants remaining versus simulation time for Cabo Mayor (mean ± 1 SD, 5 runs per scenario). Day and night bands are clearly separated. S7 overlaps the day cluster, indicating a minor group-movement effect at this camping.

6.2.2 Time of day as the dominant source of variation

Switching from day to night conditions increases total evacuation time by 20.5 min in the direct evacuation pair (S5 versus S1, +87%) and by 22.4 min in the muster pair (S6 versus S2, +89%). The mechanism is the same as at Parque Ardales: a doubled pre-movement median (14.1 to 28.3 min, PD 7974-6:2019 Categories B and Ciii) combined with the 0.75× speed factor for reduced night time visibility (Labhiri, 2024, Section 5.5). What changes is the relative weight of each component. Because CM's walking distances are roughly one third of PA's, the speed reduction contributes less in absolute terms, and the pre-movement shift accounts for a larger share of the penalty. This explains why the night-to-day Total Time ratio is steeper at CM (1.87) than at PA (1.73): in a short distance camping, the response to alarm phase, not the walk to the exit, dictates the evacuation timeline.

The log-normal pre-movement parameters (Location = 6.7435 / 7.4367 day/night, Scale = 0.1487) incorporate a dimensional correction applied to Labhiri's (2024) original values, detailed in Chapter 5.

6.2.3 Exit usage and the genuine two exit configuration

Under baseline conditions (S1), 509 occupants reach Exit (the main vehicular gate on the western perimeter) and 141 reach Exit_Peatonal (the pedestrian gate to the north east), a 78/22 split. This ratio is reproduced within ±1 occupant across all five runs of S1 and across the corresponding night scenario S5, confirming it as a deterministic consequence of shortest path routing from accommodation zones rather than a stochastic artifact. Occupants in the Parcela 7 and 8 clusters, located nearest to Exit_Peatonal, consistently choose that gate; the remaining occupants are closer to Exit via the central vial network.

The presence of two actively used exits is a defining structural contrast with Parque Ardales. Where PA channels 499 of 500 occupants through a single gate, CM distributes its 650 occupants across both exits in every direct evacuation scenario, providing inherent redundancy and reducing the load per exit by roughly one fifth.

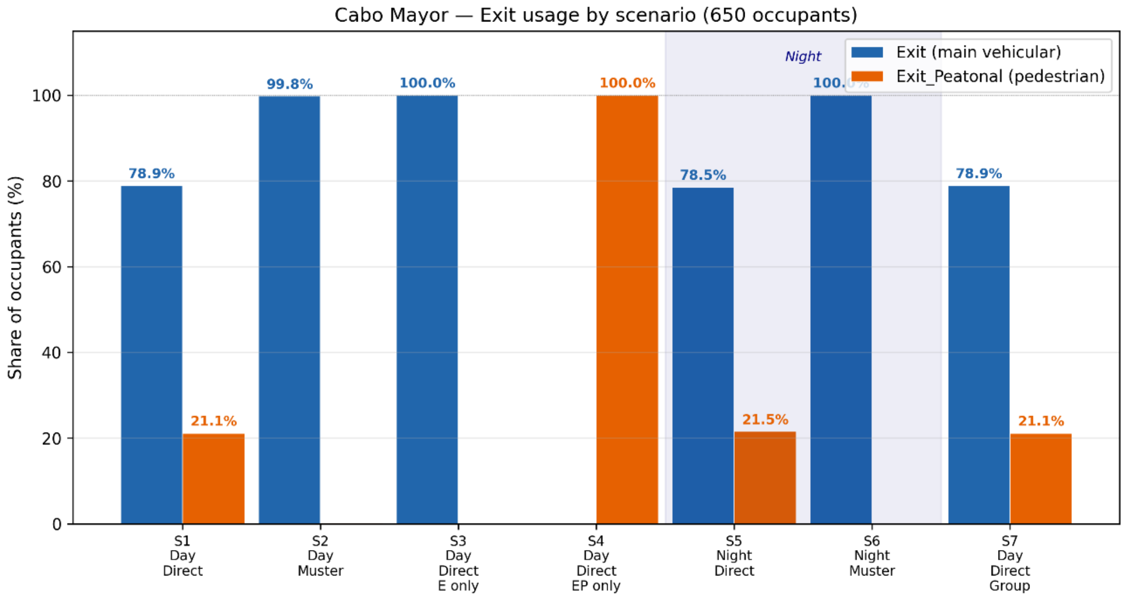

Figure 6.15. Percentage of occupants using each exit across scenarios. The 78/22 baseline split persists in all direct scenarios (S1, S5, S7). Muster scenarios collapse the split to 100/0 (S6) and 99.8/0.2 (S2), routing nearly all traffic through Exit despite Exit_Peatonal remaining open.

6.2.4 Exit closure asymmetry

Removing Exit_Peatonal from the network (S3, Exit only) produces a negligible 0.1 min reduction from the baseline (−0.4%). The 141 occupants who normally use that gate redirect through the vial network to Exit without meaningfully shortening their journeys or decreasing density at the exit. By contrast, shutting the dominant Exit (S4, Exit_Peatonal only) forces all 650 occupants onto a single, narrower pedestrian gate and raises total evacuation time by 1.0 min (+4.2%), with mean walking distance climbing from 118.6 m to 151.3 m (+28%).

This pattern is inverted relative to Parque Ardales. At PA, closing the dominant gate (Exit 2, used by 499 occupants) incurs a 1.7 min penalty while closing the nearly unused Exit 1 costs 1.0 min. The directional difference traces to the baseline split: when the minority exit serves only 22% of occupants, its removal displaces a small population over similar length alternatives; when the dominant exit serves nearly all occupants, its removal compels mass rerouting through a constrained alternative. Closure cost thus depends on the interaction between displaced demand and alternative path availability, not on traffic volume alone.

6.2.5 Muster strategy and the muster collapse phenomenon

Inserting a mandatory assembly step at Recepción before proceeding to the exits adds 1.5 min under day conditions (S2 versus S1, +6.3%) and 3.4 min at night (S6 versus S5, +7.7%). The day overhead slightly exceeds the 1.5 min mean muster-wait parameter ($\mu = 90$ s), indicating a small additional routing cost from the detour to the assembly point. The Recepción detour extends the mean walking distance by 14.5 m (S2 versus S1), roughly twice the detour observed at PA (+8.8 m), where the muster point sits closer to the main evacuation corridor.

The operationally significant result, however, is not the time overhead but the restructuring of exit usage. In both S2 and S6, every occupant exits through Exit. Exit_Peatonal registers zero or one passage across all ten muster runs, despite remaining physically accessible. After assembling at Recepción, the shortest onward path to any exit unambiguously favors this gate, so the post muster flow is channeled through a single corridor regardless of where occupants originated. This routing collapse converts the camping's two exit infrastructure into an effective single gate system whenever the muster protocol is enforced.

The density records quantify the equivalence. At MR_Exit, the mean peak density in S2 is 0.47 occs/m², virtually identical to S3 (0.49 occs/m²), the scenario in which Exit_Peatonal is physically locked. At MR_Exit_Peatonal itself, S2 registers 0.00 occs/m² mean peak, again matching S3. From the standpoint of gate zone loading, instructing occupants to assemble at Recepción has the same effect as removing the alternate exit from the model entirely. The pattern holds across all five runs of both muster scenarios as a fixed geometric consequence of the muster point's location relative to the two exits; the only departure is a single occupant who completes the Exit_Peatonal route in two of the five S2 runs, a transient saturation effect documented in Section 5.5.4 whose impact on the split is negligible (99.8/0.2).

6.2.6 Density analysis

Table 6.4 lists the mean peak density of each scenario at each Measurement Region for the day scenarios. The maximum value in the table is 0.69 occs/m² at MR_Exit_Peatonal in S4, where all 650 occupants converge on a single narrow gate. This concentration persists for an average of 35.8 s per run and represents the only instance in the CM dataset where any MR sustains a density above 0.43 occs/m² for more than a few seconds. Even so, it falls an order of magnitude short of the 4 occs/m² operational threshold (Oberhagemann, 2012). No timestep in any of the 35 runs records a density at or above 4 occs/m².

MR	Area (m²)	S1	S2	S3	S4	S7
MR_Exit	25.89	0.40	0.47	0.49	0.01	0.56
MR_Exit_Peatonal	7.24	0.14	0.00	0.00	0.69	0.23
MR_Vial1	40.33	0.10	0.18	0.19	0.23	0.20
MR_Vial2	48.85	0.20	0.23	0.21	0.14	0.37
MR_Parking	33.64	0.21	0.18	0.17	0.19	0.46

Table 6.4. Scenario-mean peak density per Measurement Region (occs/m²), day scenarios. The highest value (0.69 at MR_Exit_Peatonal in S4) remains far below the 4 occs/m² operational threshold. EP = Exit_Peatonal.

A note on density metrics: the tabulated values correspond to Pathfinder's Measurement Region density, a local density per occupant estimator based on Fruin's (1971) body ellipse method, averaged across all occupants inside the MR polygon at each 1.0 s interval (Thunderhead Engineering, 2024, Technical Reference Manual §7.2.3). The spatial contour maps shown below rely on a different algorithm that interpolates density across navigation mesh cells. Because the two methods differ in spatial resolution and averaging logic, their numerical outputs are not directly comparable; they are used here for complementary purposes (tabular quantification versus spatial visualization).

Figures 6.7 through 6.11 display the maximum instantaneous density contour for each day scenario, extracted from the worst-case run (the repetition exhibiting the highest single MR peak among the five: S1 Run 1, S2 Run 5, S3 Run 2, S4 Run 5, S7 Run 5). A uniform color scale of 0-4 occs/m² is applied throughout.

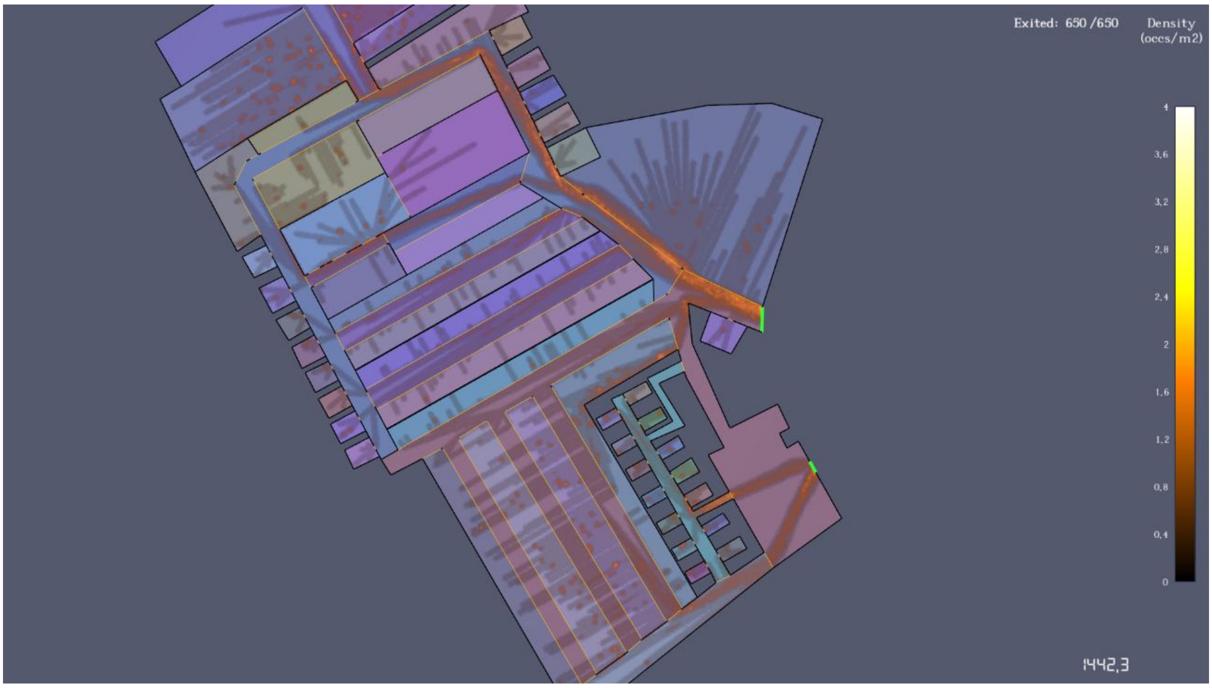

Figure 6.16. Maximum instantaneous density contour, S1 Day/Direct/Both exits (Run 1). Two active evacuation corridors are visible: the western vial toward Exit carries the majority of traffic, while a lighter band extends north-east toward Exit_Peatonal. The Libre_2 zone functions as the primary transit conduit for occupants originating in the eastern parcela cluster.

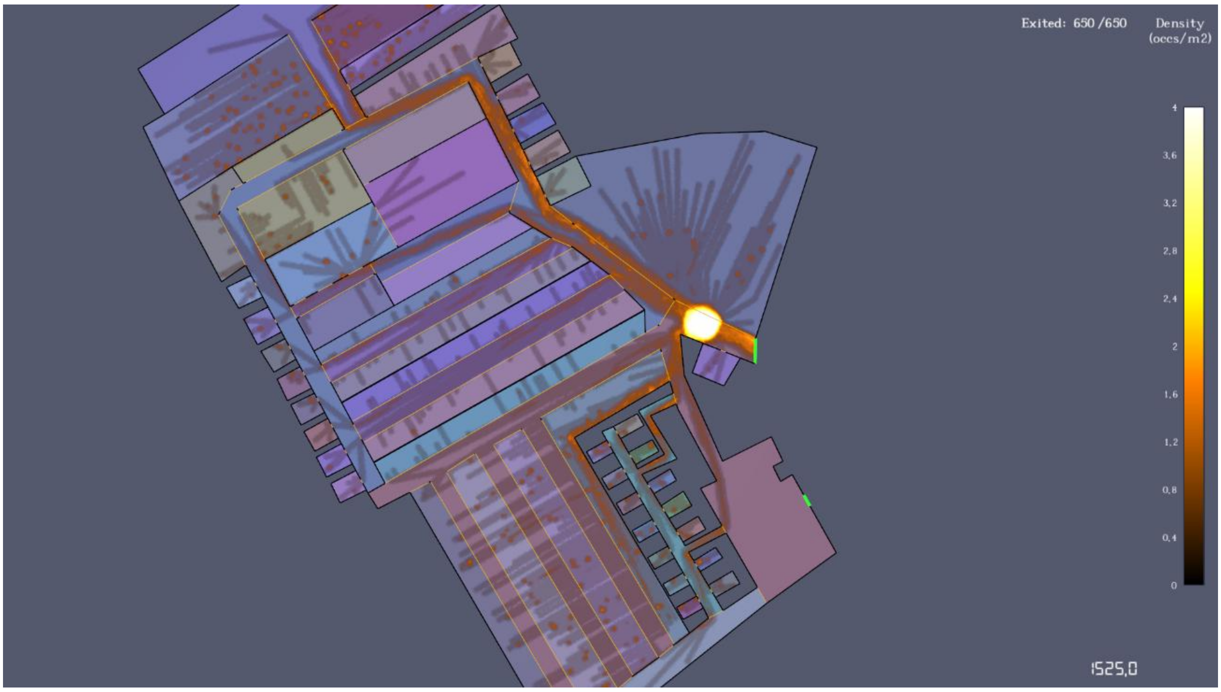

Figure 6.17. Maximum instantaneous density contour, S2 Day/Muster/Both exits (Run 5). The north-eastern corridor toward Exit_Peatonal has vanished, replaced by a single concentrated band along the western vial. A transient hotspot near Recepción marks the assembly phase. The spatial pattern is nearly indistinguishable from S3 (Exit-only closure), visually confirming the muster-collapse effect documented in Section 6.2.5.

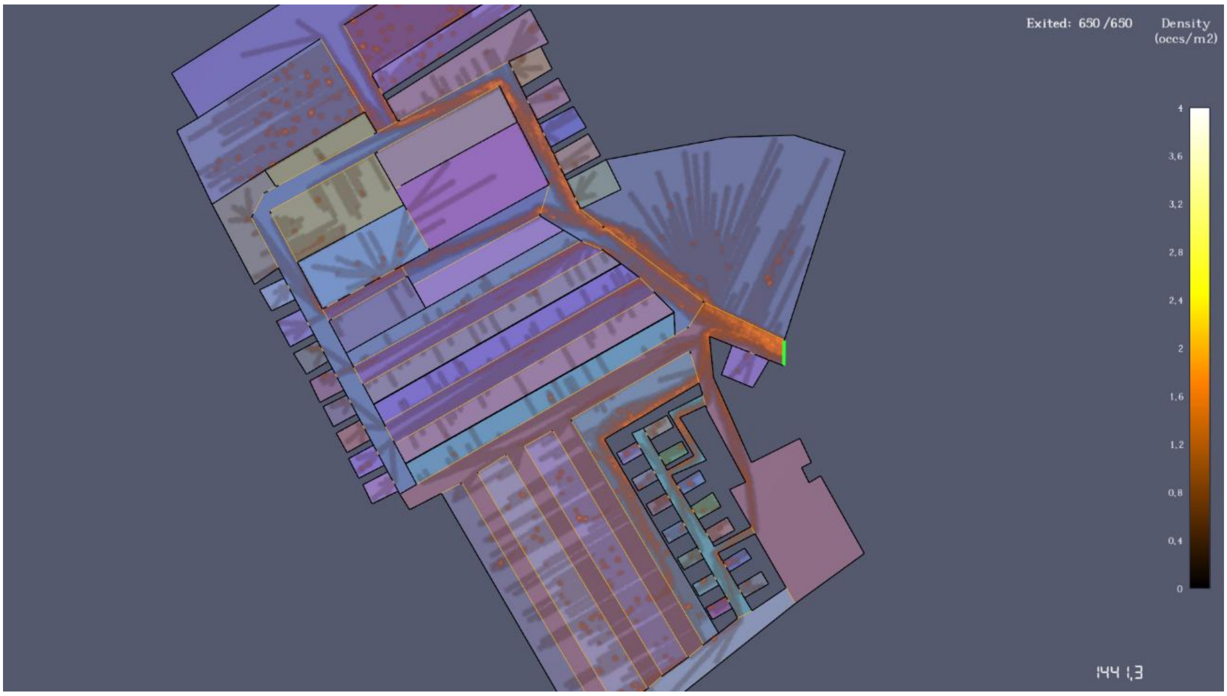

Figure 6.18. Maximum instantaneous density contour, S3 Day/Direct/Exit only (Run 2). Displaced north-eastern occupants reroute through Libre_2 and the central vial network, broadening the western density band relative to S1 but without generating new localized peaks. The similarity to S2 is evident.

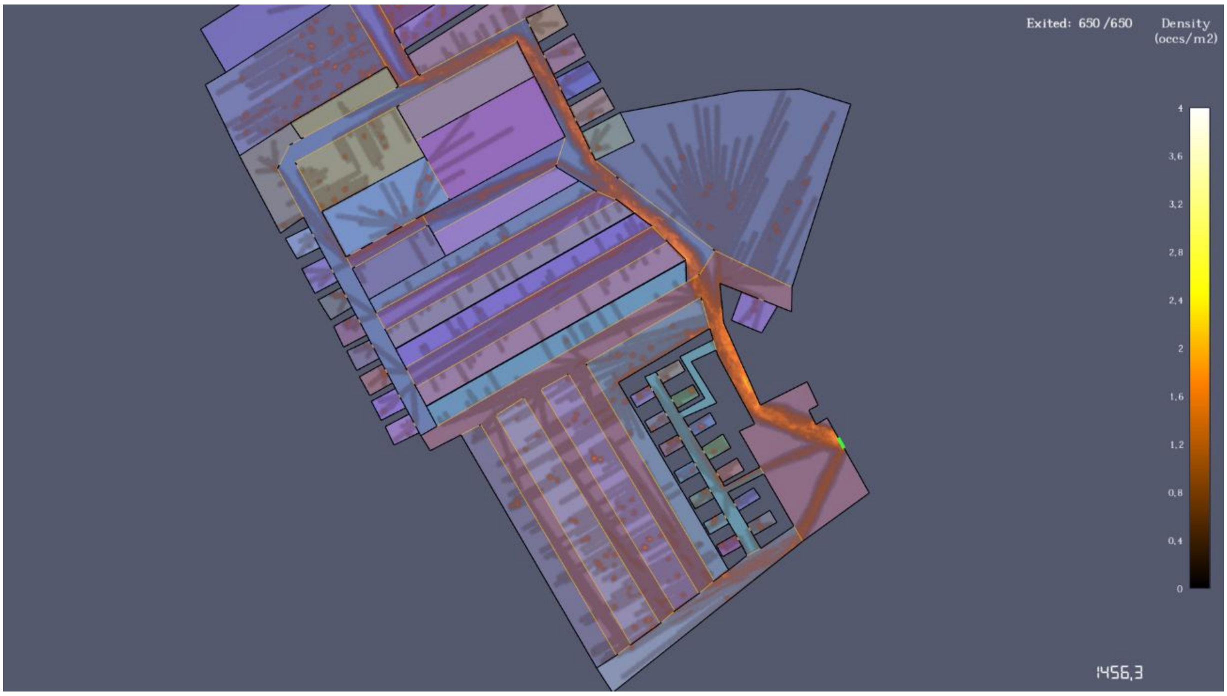

Figure 6.19. Maximum instantaneous density contour, S4 Day/Direct/Exit_Peatonal only (Run 5). With Exit sealed, all 650 occupants funnel toward the narrow pedestrian gate. MR_Exit_Peatonal records 0.74 occcs/m² in this run, the single highest density reading in the CM dataset. MR_Vial1 upstream also peaks at its maximum across scenarios (0.23 occs/m²), reflecting the bottleneck back-propagation.

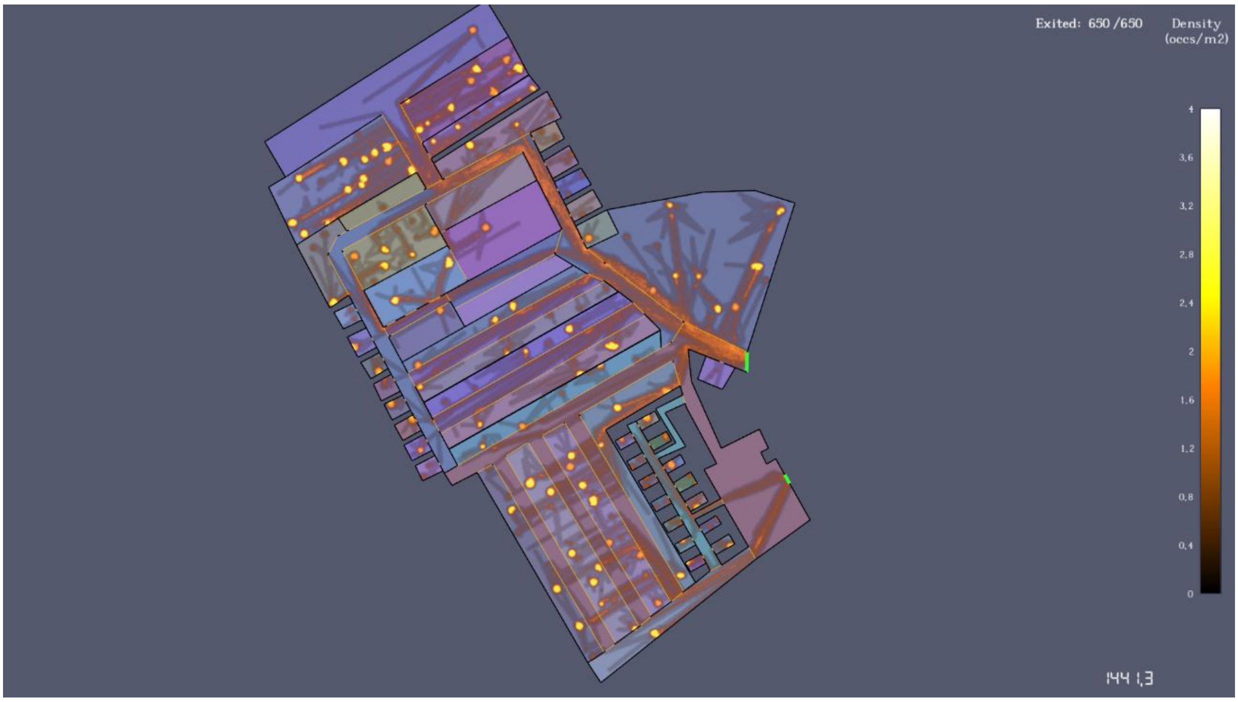

Figure 6.20. Maximum instantaneous density contour, S7 Day/Direct/Group movement (Run 5). The two-corridor routing of S1 is preserved, but density magnitudes are elevated throughout the vial network. MR_Exit reaches 0.63 occs/m² and MR_Parking 0.57 occs/m², both of which remain far below the operational threshold.

Figures 6.12 through 6.16 map accumulated space utilization (person-seconds per cell) for the same runs. The color scale is fixed at 0-300 occs·s across all CM maps.

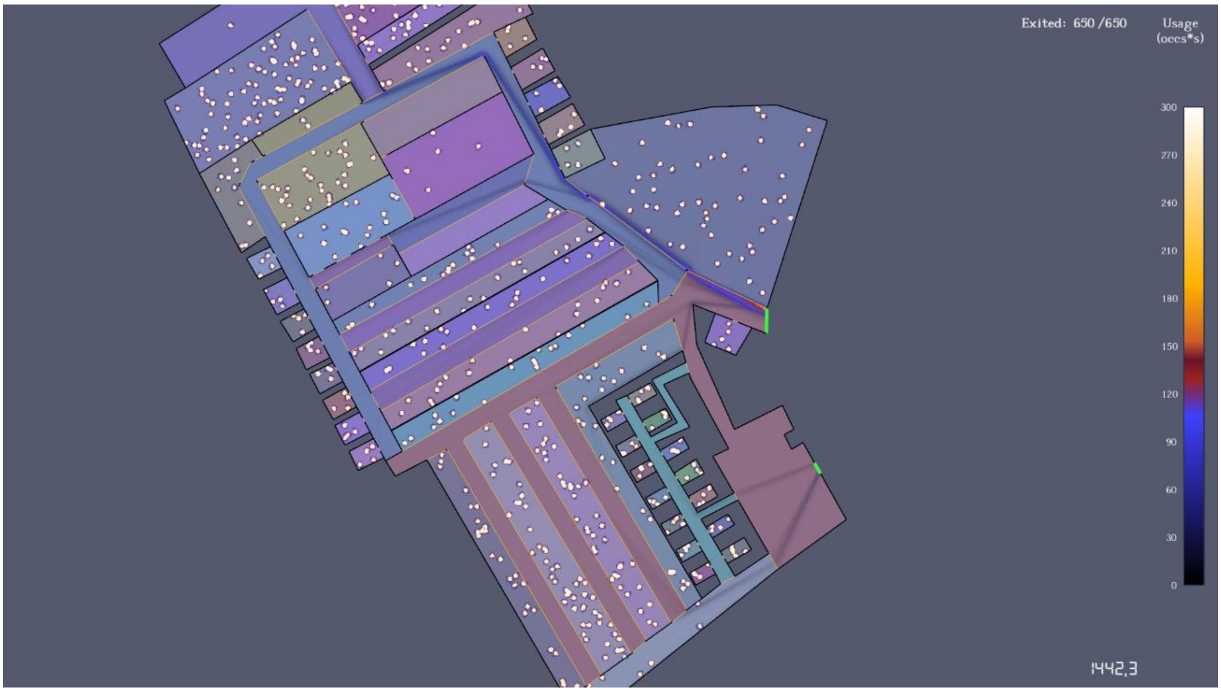

Figure 6.21. Accumulated space utilization, S1 Day/Direct/Both exits (Run 1). The dual-corridor pattern is clearly rendered: the western route to Exit shows high accumulated occupancy, while the north-eastern route to Exit_Peatonal carries a lighter but non-negligible load. Libre_2 stands out as a high-usage transit zone connecting the eastern parcelas to the central vial.

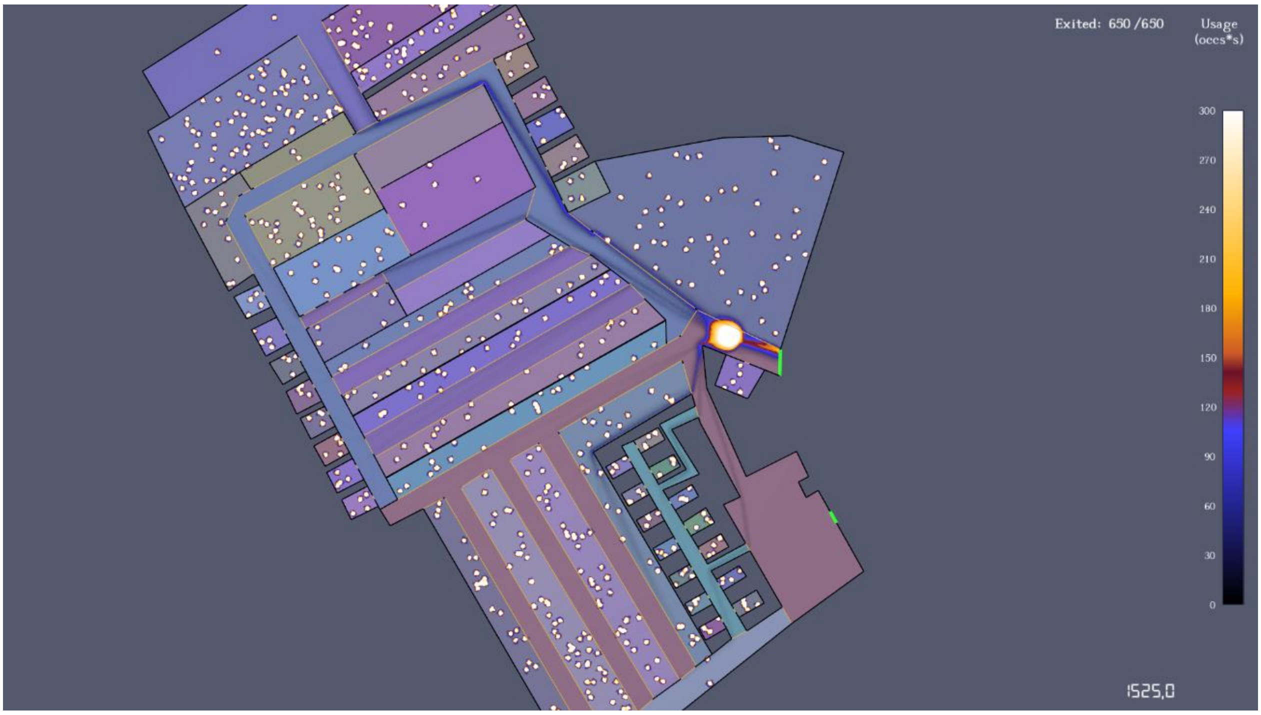

Figure 6.22. Accumulated space utilization, S2 Day/Muster/Both exits (Run 5). The Exit_Peatonal corridor disappears entirely. A concentrated hotspot at Recepción reflects the assembly dwell time, and the post-muster corridor to Exit carries a heavier person-second load than S1 owing to the increased per-occupant transit time through a single gate.

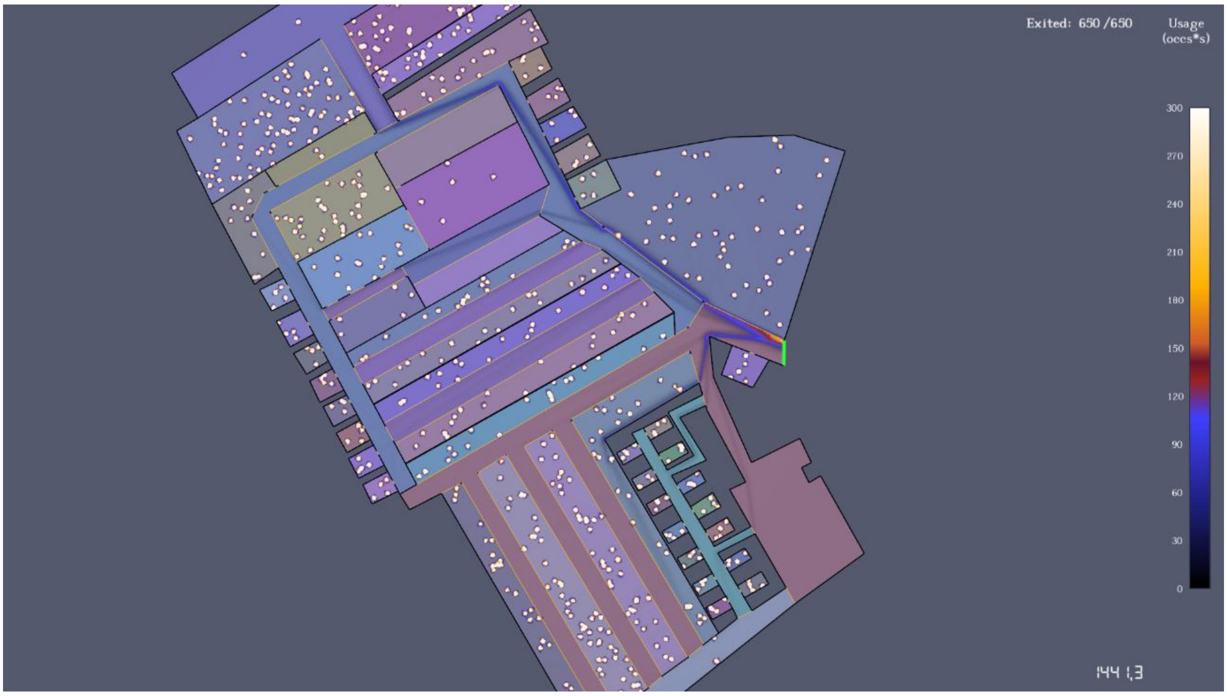

Figure 6.23. Accumulated space utilization, S3 Day/Direct/Exit only (Run 2). Traffic from the north-eastern sector redirects through Libre_2, producing higher accumulated usage along that corridor than in S1. The overall utilization footprint closely mirrors S2, reinforcing the functional equivalence between muster-collapse and physical exit closure.

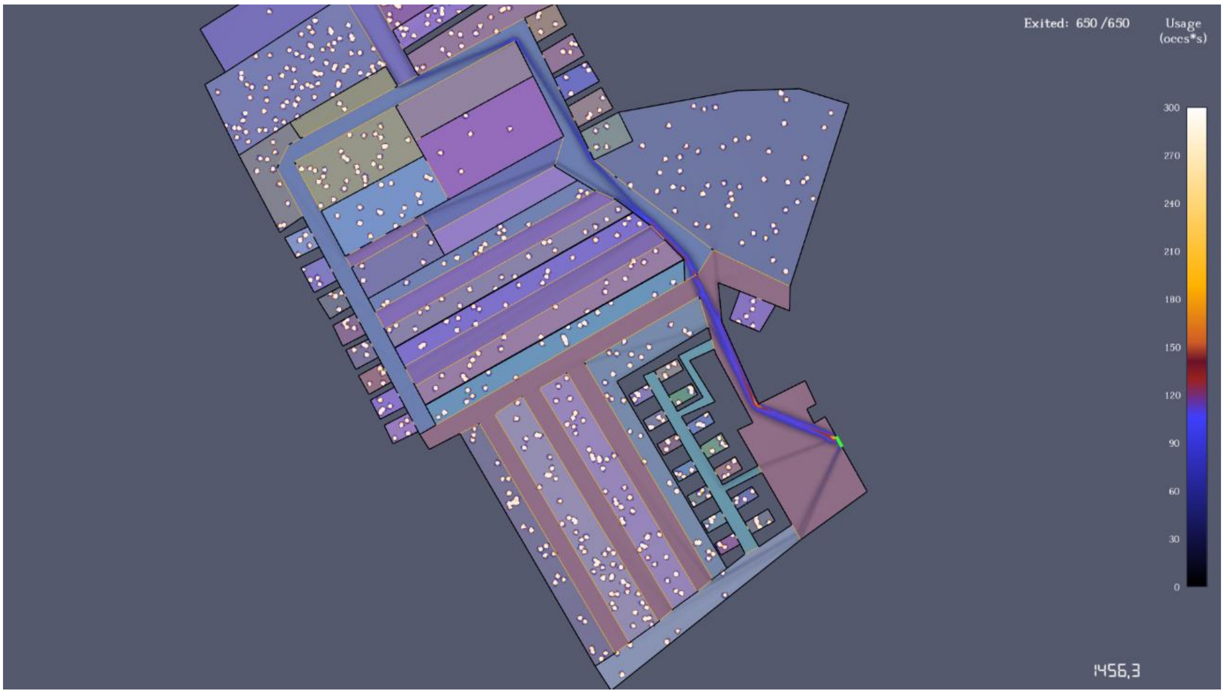

Figure 6.24. Accumulated space utilization, S4 Day/Direct/Exit_Peatonal only (Run 5). The entire traffic load converges on the north-eastern corridor. MR_Exit_Peatonal saturates the 300 occs·s color scale, consistent with all 650 occupants passing through a single narrow zone.

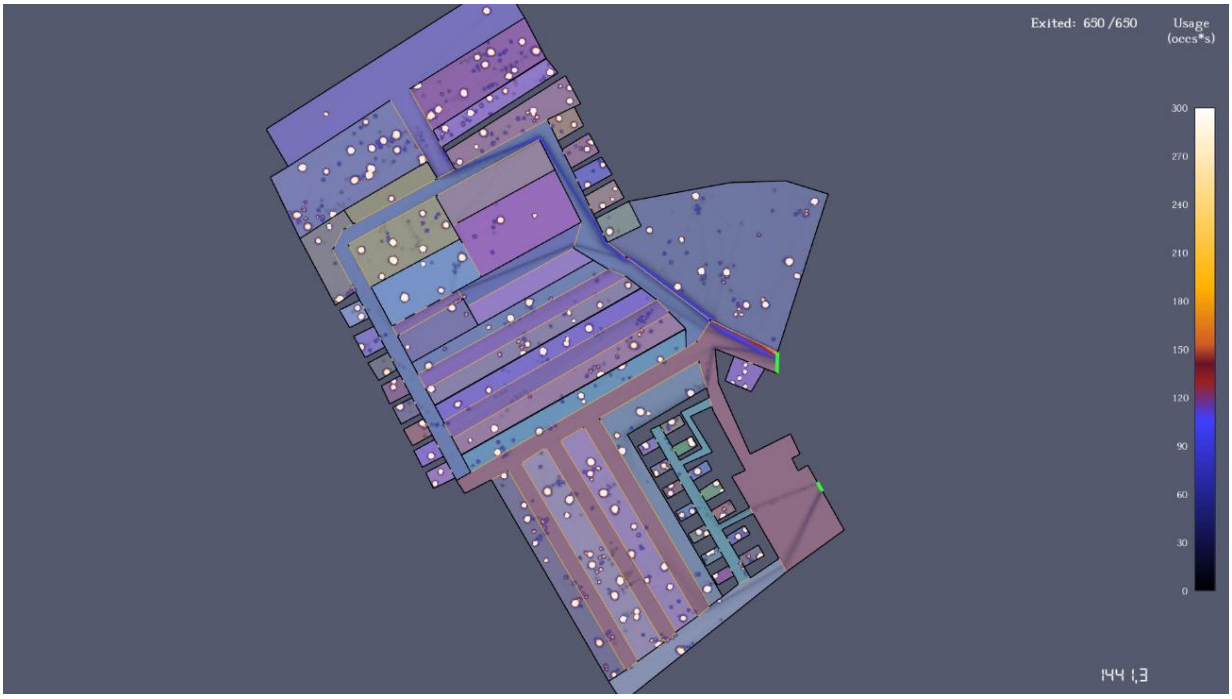

Figure 6.25. Accumulated space utilization, S7 Day/Direct/Group movement (Run 5). The routing footprint replicates S1, but the accumulated values are uniformly higher because group members traverse each cell at a reduced net speed, spending more time per unit area.

6.2.7 Group movement (S7)

S7 replicates the baseline S1 configuration with the addition of movement groups based on families. The 650 occupants are organized into 157 groups: 34 nuclear families (2 adults, 2 children), 64 large families (2 adults, 3 children, 1 elderly), 1 couple-and-elder group (2 adults, 1 elderly), and 58 couples, with 11 occupants left ungrouped (10 staff plus 1 solo). Leaders are adults; maximum inter-member spacing is 2.0 m for families and 1.5 m for couples.

Total evacuation time rises by 0.8 min to 24.4 min (+3.3%), the smallest incremental penalty of any scenario variation at CM. The contrast with PA is striking: the equivalent group penalty at Parque Ardales is 4.3 min (+14.1%), more than five times larger. The explanation lies in path length. CM's mean baseline distance of 118.6 m offers little scope for leader oscillation and wait-for-straggler behavior to accumulate time cost, whereas PA's 357.7 m baseline amplifies every instance of speed reduction over a longer corridor.

Mean walking distance, however, shows a disproportionately large increase: from 118.6 m (S1) to 277.2 m (+134%), far exceeding the +32% recorded at PA. The explanation is a profile level asymmetry. Adult group leaders cover 350 m on average because they pause, reverse, or loop back to maintain proximity to slower children (197 m) and elderly members (202 m). The population weighted mean is therefore inflated by the leader distances without reflecting an equivalent increase in actual route length. This makes the percentage change metric misleading if interpreted as a route elongation; it is more accurately described as a measure of cohesion related additional movement.

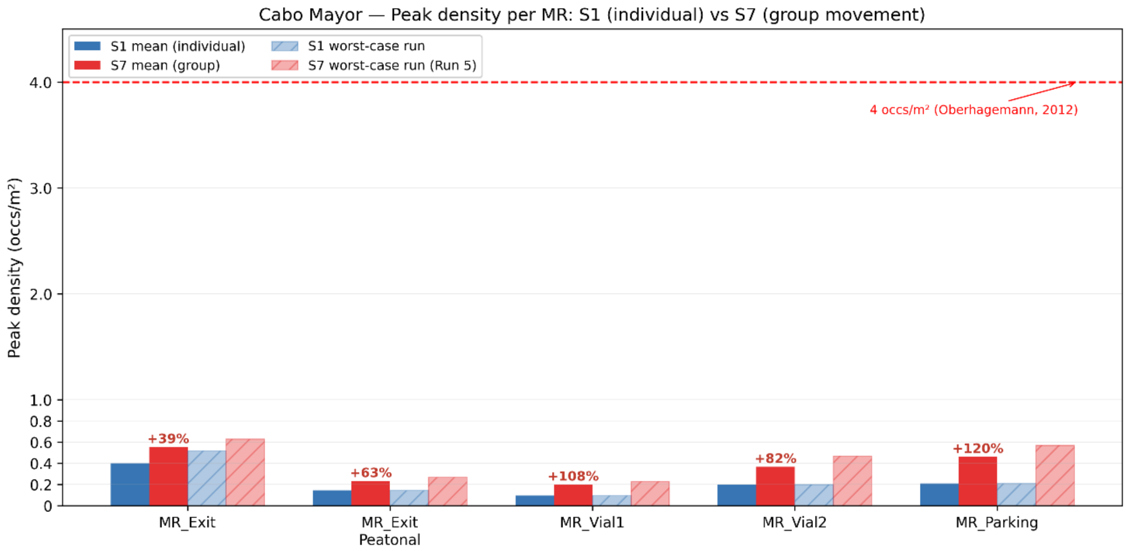

Figure 6.26. Worst-case peak density per Measurement Region, S1 (individual, blue) versus S7 (group, red). Solid bars show scenario-mean values; hatched bars show worst-case-run values. Percentage changes refer to mean values. The 4 occs/m² operational threshold (dashed red line, Oberhagemann, 2012) is included for scale.

Density increases in S7 range from +39% at MR_Exit to +120% at MR_Parking, with MR_Vial1 more than doubling (+108%). These percentages are large in relative terms, but the absolute values remain modest: the highest worst-case reading is 0.63 occs/m² at MR_Exit (Run 5), roughly one-sixth of the operational threshold.

Group cohesion also introduces kinematic congestion where none existed before. In S1, no occupant in any run experiences a non-zero congestion time. In S7, occupants spend an average of 120.5 s in congested movement, and fewer than 1% of occupants per run avoid congestion entirely. The congestion is not caused by spatial bottlenecks but by the speed mismatch within groups: adults decelerating to keep children and elderly within the leader radius register as congested in Pathfinder's velocity deficit accounting. The inter-profile completion spread confirms this reading: Adult 18.2 min, Child 19.5 min, Elderly 19.8 min, a 1.6 min range that is narrower than the S1 individual spread, consistent with cohesion compressing the group toward the slowest member's pace.

Interpretation caveat: the group parameters (leader assignment, maximum separation distance) are drawn from Pathfinder's default recommendations and are not empirically calibrated against observed family behavior during camping evacuations (Thunderhead Engineering, 2026). S7 should therefore be read as a sensitivity test illustrating the direction and approximate scale of the family cohesion effect, not as a point prediction. What the result does establish with confidence is that individual movement scenarios (S1-S6) underestimate both time and local density whenever families evacuate together, a condition that is the norm rather than the exception in tourist campings.

6.2.8 Synthesis

Six key results emerge from the Cabo Mayor analysis:

1. The day-night transition is the controlling variable. Night conditions extend the baseline evacuation by 20.5 min (+87%), dwarfing every other scenario effect. The ratio of night to day Total Time at CM (1.87) exceeds that at PA (1.73), because CM's short walking distances magnify the relative share of pre-movement time in the overall evacuation. Early detection and rapid alarm dissemination at night offer the single largest leverage point for reducing evacuation duration.

2. Both exits carry meaningful traffic under baseline conditions. The deterministic 78/22 split between Exit and Exit_Peatonal is preserved in all direct evacuation scenarios (S1, S3 by construction, S5, S7). This utilization of two gates provides built-in redundancy that Parque Ardales, with its 499/1 split, lacks entirely.

3. The muster protocol neutralizes the two exit advantage. Routing occupants through Recepción before releasing them to the exits funnels 100% of traffic through Exit, leaving Exit_Peatonal idle. The gate zone density under muster (0.47 occs/m² at MR_Exit in S2) matches the density under physical closure of Exit_Peatonal (0.49 occs/m² in S3). This muster-collapse is the most operationally significant finding at Cabo Mayor: it means that the muster protocol, as implemented, eliminates the camping's principal structural safety advantage.

4. Closure cost depends on displacement fraction and alternative quality, not raw traffic volume. Shutting the 22% usage Exit_Peatonal adds 0.1 min; shutting the 78%-usage Exit adds 1.0 min. The asymmetry is opposite to PA, where the dominant gate's closure costs 1.7 min and the marginal gate's closure costs 1.0 min. In both campings, the penalty tracks the interaction between the number of displaced occupants and the quality of their rerouting alternatives, not the pre-closure traffic count at the closed gate.

5. Group movement has a minor impact, scaling with distance. The +0.8 min group penalty (+3.3%) is 5.3 times smaller than at PA (+4.3 min, +14.1%), in close proportion to the 3.0× ratio of baseline walking distances. Density rises by 39-120% across MRs but stays below 0.63 occs/m² in the worst case, confirming that individual mode simulations underestimate crowding in a family context but that the underestimation does not approach dangerous levels at CM.

6. Evacuation performance at CM is governed by alarm response, not by physical capacity. No timestep in any of the 35 runs registers a density at or above the 4 occs/m² threshold. Zero kinematic congestion occurs in S1-S6. The binding constraint is pre-movement duration; the exit infrastructure has ample reserve capacity even under the most restrictive scenario (S4, single narrow gate, 0.69 occs/m² peak).

6.3 Comparative analysis

The preceding sections analyzed each camping in isolation. This section places the two datasets side by side to identify which evacuation dynamics are shared, which diverge, and what structural properties of the camping layout explain the differences. Table 6.5 summarizes the principal metrics; Figure 6.18 compares the scenario penalties as percentages of each camping's respective S1 baseline. The discussion is organized around five themes that emerged from the data: the balance between pre-movement and travel time, exit configuration and closure effects, the muster strategy, density patterns, and group movement. All observations remain strictly analytical; design recommendations derived from these findings are presented in Chapter 7.

Metric	Parque Ardales	Cabo Mayor
Capacity (occupants)	500	650
Mean distance S1 (m)	358	119
TotalT S1 (min)	30.6	23.6
MeanCompT S1 (min)	20.3	16.3
Night ratio (S5/S1)	1.73	1.87
Night penalty (min)	+22.1	+20.5

Exit split S1	499/1 (single-exit)	509/141 (78/22%)
Closure penalty, dominant exit	+1.7 min (+5.6%)	+1.0 min (+4.2%)
Closure penalty, marginal exit	+1.0 min (+3.3%)	+0.1 min (+0.4%)
Muster penalty day	+1.6 min (+5.3%)	+1.5 min (+6.3%)
Muster routing effect	None (already 500/0)	Collapse 78/22 → 100/0
Mean peak density S1-S4 (occs/m²)	0.37	0.69
Peak density location	MR_Vial1-2 (corridor)	MR_Exit_Peatonal (gate)
S7 group penalty	+4.3 min (+14.1%)	+0.8 min (+3.3%)
S7 congestion time (s/occ)	125	120.5
Threshold exceedance (4 occs/m²)	None (70 runs)	None (70 runs)

Table 6.5. Side-by-side comparison of key evacuation metrics for Parque Ardales (PA, 500 occupants) and Cabo Mayor (CM, 650 occupants). All times in minutes unless noted. Density values refer to the single highest scenario-mean MR peak across S1-S4. S7 data from the group-movement sensitivity analysis.

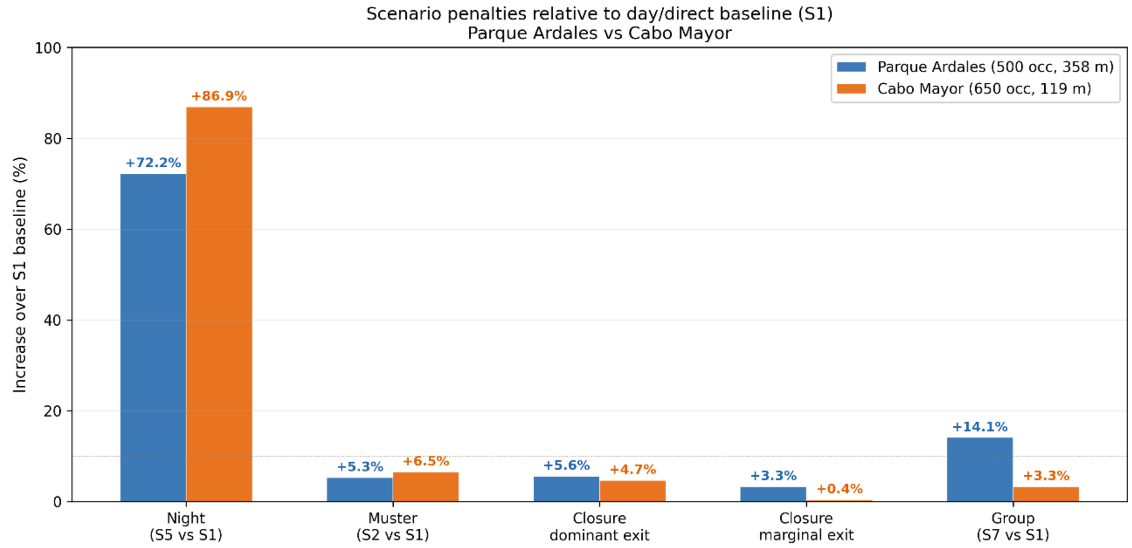

Figure 6.27. Scenario penalties as percentage increase over the respective S1 baseline for each camping. Night and muster penalties are of comparable magnitude at both sites. Closure asymmetry inverts direction between the two campings. The group-movement penalty diverges by a factor of 4.3, correlating with the 3.0× difference in baseline walking distance.

6.3.1 Evacuation time and the pre-movement versus travel time balance

Cabo Mayor evacuates 650 occupants in 23.6 min; Parque Ardales needs 30.6 min for 500. A facility with 30% more people finishes 23% sooner. The explanation is straightforward: mean walking distance at CM is 119 m, roughly one third of PA's 358 m. The time each occupant spends walking to the exit is correspondingly shorter, and because both campings share identical pre-movement distributions (same PD 7974-6 categories, same log-normal parameters), the only variable that separates their baselines is the spatial extent of the site.

This distance differential also reshapes the internal composition of the total evacuation time. At PA, the median pre-movement delay (14.1 min under day conditions) accounts for roughly 47% of the 30.6 min total, with the remaining 53% consumed by active travel. At CM, the same 14.1 min pre-movement median represents 61% of the 23.6 min total, leaving only 39% for travel. The implication is that CM's evacuation timeline is dominated by the response to alarm phase to a degree that PA's is not.

The night penalty confirms this asymmetry. In absolute terms the penalty is similar: +22.1 min at PA, +20.5 min at CM. In relative terms it is steeper at CM (+87%) than at PA (+72%), because the same absolute shift in pre-movement time (the median doubles from 14.1 to 28.3 min) represents a larger fraction of CM's shorter baseline. The night-to-day ratio of total evacuation times captures this neatly: 1.87 at CM versus 1.73 at PA. For any camping whose internal distances are short, the pre-movement phase becomes the rate-limiting step, and interventions that shorten alarm-response latency yield proportionally greater returns than at sprawling sites.

6.3.2 Exit configuration and the meaning of redundancy

Both campings have two physical exit gates. Only one has two functional exits. At PA, 499 of 500 occupants use Exit 2 in every baseline run, with a lone Vial 4 resident accounting for all Exit 1 traffic. At CM, 509 occupants use Exit and 141 use Exit_Peatonal, a stable 78/22 split. The architectural fact of possessing two gates does not, by itself, confer evacuation redundancy; what matters is whether the geometry of the accommodation zones distributes occupants across both gates under shortest-path routing.

The experiments where one exit is closed make the consequences of this distinction concrete. When PA's dominant exit (Exit 2) is closed (S3), the entire population must reroute through the alternative path to Exit 1, which is 45 m longer on average. The penalty is 1.7 min. When PA's marginal exit (Exit 1) is closed (S4), only one occupant is displaced, and the penalty is 1.0 min, driven not by demand redistribution but by the modest path length increase that closing any exit imposes on nearby occupants. The penalty ratio (1.7 to 1.0) is far smaller than the usage ratio (499 to 1), because the alternative route has ample capacity and the time cost is governed by path elongation, not queue formation.

At CM, the pattern inverts. Closing the dominant Exit (S4) forces all 650 occupants through Exit_Peatonal, adding 1.0 min. Closing the minority Exit_Peatonal (S3) displaces 141 occupants who find alternative routes of comparable length, which reduces evacuation time by 0.1 min. Here the penalty ratio (1.0 to 0.1 = 10×) is more proportional to the usage ratio (509 to 141 = 3.6×), though still nonlinear, because the displaced majority in S4 face a narrow gate with a longer approach.

The common lesson across both campings is that the time cost of losing an exit depends on two factors jointly: the number of occupants who must find a new route and the quality of the alternative path available to them. A large displacement onto a short alternative (CM S3: 141 occupants, +9 m mean reroute) costs almost nothing. A total displacement onto a longer alternative through a narrow gate (CM S4: 650 occupants, +33 m) costs more. A total displacement onto a long alternative with ample capacity (PA S3: 499 occupants, +45 m, but a wide gate at the end) falls between the two. Traffic volume at the closed gate before closure is a poor predictor of the penalty; geometric route analysis is required.

6.3.3 Muster strategy: wait-time absorption versus routing collapse

The muster protocol produces a time penalty of comparable magnitude at both campings: +5.3% at PA and +6.3% at CM. The similarity in percentage terms masks a fundamental difference in mechanism.

At Parque Ardales, the muster step is operationally transparent with respect to exit routing. Because 499 of 500 occupants already use Exit 2, and because the muster point at Recepción lies along the dominant evacuation corridor, the post-muster flow follows the same path it would have followed without the assembly step. The exit split moves from 499/1 to 500/0, a change of a single occupant. The entire muster penalty is therefore attributable to the wait time at the assembly point (μ = 90 s = 1.5 min), and the observed day penalty of 1.6 min matches this prediction closely. The muster step at PA is, in effect, a pure time insertion: it delays departure without altering the spatial flow pattern.

At Cabo Mayor, the muster step restructures the evacuation. The pre-muster 78/22 split collapses to 100/0 in S6 and in three of the five S2 runs, with the remaining two S2 runs at 99.8/0.2 (see Section 5.5.4); the collapse is effectively complete in all cases. The 141 occupants who would normally exit through Exit_Peatonal are rerouted through Exit after assembling at Recepción, because the post assembly shortest path unambiguously favors the principal gate. The muster point's proximity to Exit and distance from Exit_Peatonal make this outcome deterministic. The penalty therefore has two components: the wait time (similar to PA) and the loss of dual exit load sharing (specific to CM). The density data confirm the routing effect: MR_Exit's peak density rises from 0.40 occs/m² (S1) to 0.47 occs/m² (S2), statistically indistinguishable from 0.49 occs/m² in S3 where Exit_Peatonal is physically sealed. Meanwhile MR_Exit_Peatonal drops from 0.14 to 0.00 occs/m², identical to S3.

The contrast between the two campings establishes that the muster penalty is not a fixed property of the assembly protocol but a function of the muster point's geometric relationship to the exit network. Where the assembly point lies on the dominant corridor (PA), muster is benign. Where it lies near one exit and far from another (CM), muster can eliminate a camping's structural redundancy. This is the most operationally consequential finding of the comparative analysis.

6.3.4 Density patterns: corridor loading versus gate funneling

The spatial distribution of peak density differs systematically between the two sites. At PA, the highest densities occur in the interior transit corridors: MR_Vial1-2 records the global peak in S1 (0.37 occs/m² mean, 0.44 worst case) and in S7 (0.50 mean, 0.64 worst case). The exit zones themselves remain lightly loaded because Exit 2 is wide and the approach geometry permits occupants to spread laterally as they converge. The density profile along the evacuation route is therefore relatively uniform, with no single choke point concentrating flow.

At CM, the pattern is reversed. The interior vials are spacious relative to the traffic they carry (MR_Vial1 peaks at 0.10-0.23 occs/m² across scenarios), while the exit gates, particularly MR_Exit_Peatonal in S4 (0.69 occs/m² mean, 0.74 worst-case), act as funneling points where density spikes. The difference reflects the sites' geometries: PA has narrow interior corridors (MR_Vial1-2 area = 21.96 m²) leading to a wide exit zone (MR_Exit2 = 54.99 m²), whereas CM has wide interior corridors (MR_Vial1 = 40.33 m², MR_Vial2 = 48.85 m²) converging on more compact exit zones (MR_Exit = 25.89 m², MR_Exit_Peatonal = 7.24 m²).

Despite these contrasting spatial patterns, the quantitative conclusion is the same at both campings: all recorded densities fall an order of magnitude below the 4 occs/m² operational threshold (Oberhagemann, 2012; Helbing and Mukerji, 2012). Zero seconds of kinematic congestion are recorded in any of the 60 ungrouped runs (S1-S6) at either site. The velocity deficit, defined as $1 - V/SV$ where V is measured speed and SV is seek speed, is identically zero across all PA runs and below 0.004 across all CM runs. Both campings operate in a regime where walking time, not queue formation, determines the evacuation duration.

6.3.5 Group movement penalty as a function of walking distance

The S7 scenario provides a controlled comparison of the effects of family cohesion across two layouts with identical group movement parameters (MaxDistance = 2.0 m for families, 1.5 m for couples, FollowLeader enabled), but different spatial scales. At PA, the group penalty on total evacuation time is 4.3 min (+14.1%); at CM, it is 0.8 min (+3.3%). The 5.4× ratio of absolute penalties and the 4.3× ratio of percentage penalties both exceed the 3.0× ratio of baseline walking distances (358 m versus 119 m), indicating that group movement cost scales linearly with path length. The likely explanation is that longer corridors provide more opportunities for leader-straggler separation events, each of which triggers a pause and then regroup cycle that accumulates delay.

One metric does not scale with distance: the mean congestion time per occupant is 125 s at PA and 120.5 s at CM, a difference of less than 4%. This near equality reveals the mechanism. Congestion in group movement is not a spatial phenomenon (bottlenecks, queues) but a kinematic one: adult leaders decelerate to stay within the maximum-distance radius of slower children and elderly members, and Pathfinder registers the resulting velocity deficit as congestion time. Because the speed profiles are identical at both campings and the group compositions follow the same demographic split (50/40/10 adults/children/elderly), the per-occupant speed mismatch, and therefore the per-occupant congestion burden, is invariant to the site layout. What the layout controls is how much total time that per-occupant burden adds to the evacuation: more time at PA because the mismatch accumulates over a longer walk, less at CM because the walk ends sooner.

Density increases under group movement are proportionally similar at both campings: +45-144% across PA's MRs and +39-120% across CM's. The absolute maxima, however, are nearly identical: 0.64 occs/m² at PA (MR_Vial1-2, S7 Run 4) and 0.63 occs/m² at CM (MR_Exit, S7 Run 5). Both remain roughly one-sixth of the 4 occs/m² threshold. The implication for evacuation planning is twofold. First, the individual-movement assumption (S1-S6) systematically underestimates both time and density in any camping where families constitute the majority of occupants, which is the norm for tourist sites. Second, the magnitude of the underestimation depends on the site's spatial scale: compact campings like CM absorb the group penalty with minimal impact, while sprawling sites like PA incur a substantial time cost that should be factored into emergency planning margins.

The profile-level completion times add nuance to this picture. At PA, the Adult-Elderly gap in S7 is 3.0 min (22.9 versus 25.9 min), unchanged from the 3.0 min gap in S1 despite the 3.8-4.2 min upward shift across all profile times. At CM, the gap widens from 1.0 min in S1 to 1.6 min in S7 (18.2 versus 19.8 min), indicating that the group penalty is not distributed uniformly across profiles at this site. In both cases, however, the dominant effect is a roughly parallel upward shift of all completion times, driven by the increased path lengths and the leader-following deceleration that generates the congestion time documented above. The near-invariance of per-occupant congestion time across campings (125 s at PA, 120.5 s at CM) confirms that the speed mismatch within groups is a property of the demographic composition and the group algorithm parameters, not of the site layout.

Chapter 7. Conclusions and Future Work

7.1 Summary of Findings

This study set out to pursue five objectives (Section 4.2): construct validated Pathfinder models of two Spanish tourist campings, configure occupant behavior through empirically grounded parameter distributions, design a systematic scenario campaign, extract and compare quantitative evacuation indicators across both sites, and formulate operational recommendations for emergency planners. Chapters 5 and 6 addressed the first four objectives in full; the present chapter addresses the fifth. Before turning to recommendations (Section 7.2), this section explains the six principal findings that emerged from the seventy simulation runs.

Finding 1: both campings operate in a regime limited by travel time. Across all fourteen scenarios, the highest measurement region density recorded at any single run was 0.74 occ/m²

(CM S4 Run 5, MR_Exit_Peatonal), an order of magnitude below the 4 occ/m² operational threshold adopted in this study (Oberhagemann, 2012; Helbing & Mukerji, 2012). No sustained queueing formed at any exit, and the Pathfinder velocity deficit confirmed that seek velocity equaled actual velocity in virtually every measurement region at both sites. Evacuation time at these campings is therefore governed by how far occupants must walk and how long they wait before starting, not by how fast they can pass through exits. The practical implication is that interventions oriented by capacity, such as wider doors or additional lanes, yield diminishing returns, while pre-movement reduction offers the largest marginal gain (Objectives 4 and 5).

Finding 2: time of day is the dominant axis of variation. The night-to-day penalty was +22.1 min (+72.2%) at Parque Ardales (S5 vs. S1) and +20.5 min (+86.9%) at Cabo Mayor (S5 vs. S1), reducing the effect of every other scenario factor. This result is a direct consequence of the log-normal pre-movement distribution adopted from PD 7974-6:2019 (BSI, 2019), whose night median (28.3 min) is approximately twice the day median (14.1 min). Because both campings are limited by travel time, the pre-movement phase constitutes the majority of total evacuation time, and any factor that lengthens it propagates almost linearly into the final result (Objective 4).

Finding 3: the exit closure asymmetry inverts between sites. At Parque Ardales, closing the less used exit (Exit_1, used by 1 of 500 occupants under baseline conditions) imposed a +1.7 min penalty (S3 vs. S1), whereas closing the dominant exit (Exit_2, used by 499 of 500) would force all occupants onto a longer alternative path. This counterintuitive finding reflects the path structure of the site: the single occupant using Exit_1 originates from Vial4, and rerouting that occupant to Exit_2 adds distance, while the remaining 499 already use Exit_2 and are unaffected by Exit_1's closure. At Cabo Mayor, the asymmetry operates differently. Closing the main vehicular exit (S3) barely changed total time (23.5 min vs. 23.6 min, a reduction of 0.1 min) because Exit_Peatonal absorbed the full population without congestion, while closing Exit_Peatonal (S4) added only 1.0 min because the vehicular exit likewise had ample capacity. The contrast illustrates that closure penalties depend on the redistribution of walking distances, not on the fraction of occupants nominally using each exit (Objective 4).

Finding 4: the muster protocol at Cabo Mayor produces a routing collapse, but the time penalty is driven by wait time rather than by the collapse itself. Under direct evacuation scenarios (S1, S5), Cabo Mayor exhibited a stable 78/22 exit split between the vehicular exit and Exit_Peatonal. When muster was introduced (S2, S6), this split collapsed to approximately 100/0 because the muster point at the Recepción waste ground is geometrically adjacent to the main exit, pulling all occupants past it and away from Exit_Peatonal. This collapse phenomenon is an original finding of this study. However, exploratory testing of alternative muster point locations indicated that relocating the muster target did not meaningfully reduce the S2 penalty (approximately +1.5 min over S1). This suggests that the penalty is attributable to the muster wait time itself ($\mu = 90$ s) rather than to the routing distortion. The collapse is therefore best understood as a redundancy problem: under muster conditions, Cabo Mayor loses its backup exit without gaining any compensating time advantage. If the main exit were blocked during a muster scenario, the camping would have no alternative egress path, a vulnerability that does not exist under direct evacuation conditions (Objectives 4 and 5).

Finding 5: group movement penalties scale with mean walking distance. The S7 group scenario imposed a +4.3 min penalty (+14.1%) at Parque Ardales but only +0.8 min (+3.3%) at Cabo Mayor, a ratio of 5.4× in absolute terms and 4.3× in percentage terms. The mechanism is straightforward: group cohesion constrains faster members to the leader's pace, and the time lost accumulates over distance. Parque Ardales, with its longer internal vials and mean walking distance of 358 m (S1), amplifies this effect relative to Cabo Mayor's more compact layout. This finding implies that group movement penalties are not a fixed percentage overhead but a site dependent quantity that planners must evaluate for each geometry (Objective 4).

Finding 6: the unit conversion correction for pre-movement parameters is a methodological contribution with broader applicability. The log-normal pre-movement distributions specified by PD 7974-6:2019 (BSI, 2019) are defined with parameters in minutes, but Pathfinder's Initial Delay field accepts the Location and Scale parameters of the underlying log-normal in the same unit as the delay bounds. When the bounds are specified in seconds, the Location parameter must be converted accordingly. The correct transformation is $\mu seg = \mu min + \ln(60)$, with σ invariant under unit scaling, a property of the log-normal family (Ronchi & La Mendola, 2016). This study derived and validated the converted parameters (Annex C), confirmed them via Kolmogorov-Smirnov tests on per occupant output data (Section 5.4.2), and applied them consistently across all seventy runs. The correction is not specific to these two campings; it applies to any Pathfinder study that draws pre-movement times from PD 7974-6:2019 (Objective 2).

Taken together, these six findings compose a coherent picture: tourist camping evacuations in this occupancy range are dominated by pre-movement delays and walking distances, not by exit capacity or crowd density. The scenario factors that emergency planners can most readily control, namely nighttime alerting speed and muster point design, are precisely the ones that the simulation campaign identified as the largest levers. The recommendations that follow (Section 7.2) translate these findings into actionable measures.

7.2 Operational Recommendations

This section translates the analytical findings of Chapter 6 into prescriptive guidance for emergency planners. The recommendations are organized by scope: a universal priority that applies to both campings (Section 7.2.1), site specific measures for Parque Ardales (Section 7.2.2) and Cabo Mayor (Section 7.2.3), and generalizable principles that extend beyond the two sites studied (Section 7.2.4). Within each subsection, recommendations are ranked by expected impact.

7.2.1 Priority Recommendation: Reduce Nighttime Pre-Movement Time

The single most impactful intervention available to both campings is a reduction in the time elapsed between the start of a wildfire threat and the moment occupants begin walking toward an exit. The night-to-day penalty, +22.1 min at Parque Ardales and +20.5 min at Cabo Mayor, exceeds the combined effect of all other scenario variations (exit closure, muster, group movement). Because both sites operate in a travel-time-limited regime, any reduction in pre-movement time translates almost linearly into a reduction in total evacuation time.

Practical measures to achieve this reduction include the installation of audible alarm systems in all accommodation units (bungalows, parcelas, and free camping zones), the deployment of push notification infrastructure linked to regional wildfire alert systems, the training of staff in rapid alarm activation protocols, and the improvement of nighttime road visibility through low level pathway lighting along primary evacuation routes. The pre-movement distribution used in this study (PD 7974-6:2019, Category C*iii* for sleeping occupants) assumes that occupants receive no dedicated alerting beyond ambient cues. Any investment that shifts the effective occupant category from C*iii* toward a faster response category would compress the pre-movement distribution and reduce the night penalty substantially.

This recommendation takes priority over all geometric or procedural interventions because it addresses the dominant axis of variation identified in the simulation campaign. It applies equally to Parque Ardales and Cabo Mayor, and by extension to any tourist camping where nighttime occupancy is expected.

7.2.2 Site Specific Recommendations: Parque Ardales

Protect Exit_2 from obstruction. Parque Ardales is a de-facto single exit camping: 499 of 500 occupants use Exit_2 under baseline conditions, with only one occupant (originating from Vial4) routed to Exit_1. Any obstruction of Exit_2, whether from fallen vegetation, parked vehicles, or blockage due to fire, would force the entire population onto the longer alternative path through Exit_1, incurring a penalty of at least +1.7 min under daytime conditions and proportionally more at night. Operational protocols should designate Exit_2 as a critical asset and include it in pre-season clearance inspections.

Improve Exit_1 accessibility and signage. The current geometry routes only one occupant to Exit_1 because the shortest path calculation from every zone except Vial4 points to Exit_2. If Exit_1 were made genuinely accessible to occupants in the bungalow and autocaravana zones, through directional signage at key junctions, wider connecting pasillos, or the creation of a secondary path from the eastern zones, the camping would acquire true two exit redundancy. This would not only reduce the vulnerability to Exit_2 blockage but could also reduce baseline evacuation time by shortening mean walking distances for the eastern occupants. The physical isolation of the site, surrounded by natural parkland, constrains the feasibility of constructing entirely new exit points, but improvements to internal connectivity toward the existing Exit_1 are a realistic and cost effective measure.

The muster protocol is acceptable on time grounds. The muster penalty at Parque Ardales is +1.6 min (+5.3%) over the direct evacuation baseline, a modest cost that is justified by the operational benefits of accounting for all occupants before clearing the site. The muster point does not need to be eliminated; however, it should be sized adequately for 500 occupants and positioned at a verified safe distance from plausible wildfire approach paths. The Plan de Autoprotección (Ayuntamiento de Ardales, 2012) designates the open area in front of reception as the assembly point, which is consistent with the location modeled in this study.

7.2.3 Site-Specific Recommendations: Cabo Mayor

Redesign the muster protocol to preserve dual-exit redundancy. The muster collapse phenomenon identified in this study eliminates Cabo Mayor's principal structural advantage: a genuine two exit configuration with a stable 78/22 split under direct evacuation conditions. When muster is activated, the routing collapse to approximately 100/0 means that the camping's backup exit (Exit_Peatonal) goes unused, leaving no alternative egress path if the main vehicular exit were compromised. Exploratory testing confirmed that this time penalty is driven by the muster wait time itself rather than by the routing distortion, meaning that relocating the muster point does not reduce evacuation time. The recommendation is therefore not to relocate the muster point for time savings, but to redesign the protocol to restore redundancy. Two options merit consideration: (a) adopt a protocol with two stages in which occupants evacuate directly to the nearest exit and staff conduct a headcount at each exit separately, or (b) designate Exit_Peatonal as a secondary muster point for occupants in its catchment area, preserving the dual exit load distribution. Either approach retains the accountability function of muster while avoiding the failure point vulnerability that the current protocol creates.

Maintain accessibility of both exits during fire conditions. Cabo Mayor is robust to single exit failure under the scenarios tested: closing either exit imposed a penalty of at most +1.0 min because each exit alone has sufficient capacity for the full population. This robustness, however, depends on at least one exit remaining available. If both exits were threatened by the same fire approach direction, the camping would have no redundancy. Operational planning should account for the prevailing wind direction and fire spread axis when assigning exit priorities during an actual event.

No third exit is required on time grounds. Unlike Parque Ardales, where additional exit capacity serving the eastern zones would provide meaningful time and redundancy benefits, Cabo Mayor's current two exit configuration is adequate. The marginal benefit of a third exit would be small given the compact geometry and the absence of queueing at either existing exit. Investment is better directed toward the alerting infrastructure and muster protocol redesign recommended above.

7.2.4 Generalizable Principles

Three general lessons emerge from the comparative analysis that extend beyond Parque Ardales and Cabo Mayor to tourist campings more broadly.

First, camping evacuations in the occupancy range studied (500-650 persons) are limited by the time while walking rather than waiting time queuing. This means that the standard building evacuation intuition, in which exit width and number of exits are the primary design levers, does not transfer directly to open air camping layouts. The dominant lever is instead the pre-movement phase, and any investment in faster alerting infrastructure delivers a larger return than equivalent investment in exit capacity.

Second, muster point placement must be evaluated for its effect on exit routing distribution before being codified in a self-protection plan. The muster collapse phenomenon at Cabo

Mayor demonstrates that a muster point positioned near one exit can inadvertently convert a multi exit camping into a de-facto single exit one, eliminating redundancy without any compensating time benefit. Emergency planners should test candidate muster point locations in simulation, or at minimum assess the geometric relationship between the muster point and all available exits, before finalizing their placement.

Third, group movement penalties are not a fixed percentage overhead. They scale with the mean walking distance of the site, as demonstrated by the 5.4× absolute difference between Parque Ardales and Cabo Mayor. Campings with longer internal road networks should anticipate proportionally larger delays when families and tour groups evacuate together, and their evacuation time estimates should account for this relationship explicitly.

7.3 Limitations

The findings and recommendations presented in this study are subject to several limitations, each of which defines a boundary on the generalizability of the results. They are enumerated below together with an indication of the direction in which each limitation is expected to bias the results.

Five runs per scenario. The Monte Carlo sample size of five runs per scenario was sufficient to produce stable mean estimates (coefficient of variation 2.9-4.4% on total evacuation time), and the principal findings are well separated by their respective uncertainty bands. However, tail event metrics such as the Required Safe Egress Time (RSET) retain run-to-run variability of approximately ±5%, and confidence intervals on peak density values are wider than on time metrics. Increasing the sample to 20-50 runs would tighten these intervals and enable more robust statistical testing of secondary effects.

No vehicular component. Pathfinder is a simulator for pedestrians. Real camping evacuations involve cars, vans, and caravans sharing the same internal road network with pedestrians. The absence of vehicle modeling means that the simulated evacuation times are likely optimistic, because conflicts between vehicles and pedestrians, vehicle queuing at exit gates, and the time required to load vehicles are not captured. Labhiri (2024) incorporated a SUMO traffic simulation component to address this gap at a macroscopic level, and Wahlqvist et al. (2021) developed the WUI-NITY platform for coupled pedestrian and vehicle modeling. Extending the present study with a vehicular component would increase realism, particularly for Parque Ardales, whose isolated location makes evacuation by foot to a safe zone impractical for most occupants.

Simplified demographic profiles. Occupants were modeled using three demographic categories (Adult, Child, Elderly) with truncated-normal speed distributions. This simplification omits individuals with mobility impairments, occupants with cognitive disabilities, and nationality specific behavioral differences such as language barriers or unfamiliarity with the site layout. The effect of this simplification is likely to underestimate the tail of the evacuation-time distribution, because the slowest and most vulnerable occupants are not represented.

No fire-spread coupling. All scenarios assume a clean evacuation trigger: occupants receive an alarm and begin their pre-movement phase without any progressive route blockage, smoke effects on visibility, or speed reductions due to heat. In a real wildfire event, the available exit set may change during the evacuation as fire fronts advance, and smoke may reduce walking speed in certain zones. The clean trigger assumption means that the exit closure scenarios (S3, S4) are best interpreted as bounding cases rather than as realistic representations of fire driven blockage, which would be gradual and spatially heterogeneous.

Static geometry. The Pathfinder models use a fixed navigation mesh throughout each simulation. Time varying obstacles, such as fallen trees, collapsed structures, or vehicles abandoned in evacuation routes, are not represented. This means that the density and flow patterns reported reflect best case geometric conditions. In a real event, localized obstructions could create transient bottlenecks that the simulations do not predict.

Muster wait time calibrated by analogy. The muster wait-time distribution (day $\mu = 90$ s, $\sigma = 30$ s; night $\mu = 144$ s, $\sigma = 48$ s) was adapted from Labhiri (2024) with downward adjustments for the smaller occupant populations in this study. No camping specific empirical data on muster wait times exist in the published literature. The night-to-day ratio of 1.6 was preserved from the source study, but the absolute values remain an assumption. If actual muster wait times were longer than assumed, the muster penalties reported in Chapter 6 would be underestimates.

Near capacity occupancy only. Both campings were modeled at near capacity occupancy (500 and 650 occupants, respectively). Low-season or partial-occupancy scenarios, in which fewer occupants share the same exit infrastructure, were not simulated. Under reduced occupancy the travel-time-limited finding would be reinforced, because lower densities further reduce any queueing effects, but the absolute evacuation times and the relative scenario penalties may differ.

7.4 Future Work

The limitations identified in Section 7.3 define a natural agenda for future research. The following lines of work are listed in approximate order of priority, balancing scientific value against practical feasibility.

Larger Monte Carlo samples. Increasing the number of runs per scenario from five to 20-50 would tighten confidence intervals on all reported metrics, enable formal hypothesis testing (e.g., paired t-tests on scenario differences), and improve the reliability of tail-event estimates such as the 95th-percentile RSET. This extension requires no additional model development, only computational time, and is the most straightforward path to strengthening the statistical foundation of the results.

Coupled pedestrian and vehicle modeling. Integrating a traffic simulation component, either through the WUI-NITY platform (Wahlqvist et al., 2021) or through a Pathfinder-SUMO coupling similar to Labhiri's (2024) approach, would capture the pedestrian vehicle conflicts that dominate real camping evacuations. This extension is particularly important for Parque

Ardales, where the site's isolation means that occupants must ultimately leave by vehicle, and the internal road network is shared between pedestrians walking to the muster point and vehicles departing through Exit_2.

Fire-spread integration. Coupling the pedestrian model with a wildfire propagation model, such as FARSITE or Phoenix, would replace the current clean trigger assumption with a time evolving hazard that progressively blocks routes and reduces visibility. This would transform the exit closure scenarios from discrete bounding cases into dynamic representations of fire driven route loss, yielding more realistic time of evacuation estimates and enabling the identification of critical fire approach directions for each camping.

Empirical pre-movement data collection. The pre-movement distributions used in this study were adapted from PD 7974-6:2019 (BSI, 2019), which was developed for building evacuations rather than open air camping environments. Collecting empirical pre-movement data through controlled evacuation drills at real camping sites, or through post-event surveys following actual wildfire evacuations, would provide camping specific distributions that could either validate or replace the adapted PD 7974-6 values. Such data would be a significant contribution to the field, given that no published camping specific pre-movement measurements currently exist.

Geometric interventions at Parque Ardales. The present study identified Parque Ardales as a de-facto single-exit camping whose physical isolation constrains the feasibility of constructing entirely new exit points. A focused follow-up study could model specific geometric interventions, such as a new secondary exit on the eastern perimeter serving the bungalow and autocaravana zones, or an improved internal path connecting these zones to the existing Exit_1. These interventions would test whether the de-facto single-exit pattern can be broken through realistic infrastructure modifications, and quantify the resulting reduction in evacuation time and improvement in redundancy.

Scaling to other tourist infrastructure types. The travel-time-limited finding and the muster collapse phenomenon may apply beyond traditional campings to other tourist infrastructure types, including holiday parks, glamping sites, and festival grounds. Applying the same seven scenario methodology to sites with different geometries, occupancy densities, and exit configurations would test the generalizability of the principal findings and potentially establish a typology of tourist infrastructure evacuation regimes.

Alignment with WUITIPS and UCPM-2027. The European Union's UCPM-2027 program and the associated WUITIPS project are developing standardized tools and protocols for wildland and urban interface evacuation planning. As these deliverables become publicly available, the methodology developed in this study could be aligned with the European-scale toolset, potentially contributing the camping specific simulation approach and the comparative framework as a module within the broader WUITIPS platform. This alignment would extend the practical reach of the present work beyond the two campings studied and into the European emergency planning ecosystem.

Chapter 8. Bibliography

Ayuntamiento de Ardales. (2012). *Plan de Autoprotección del Camping Parque Ardales*. Ayuntamiento de Ardales, Málaga.

Balkan Insight. (2024, July 23). Five years on, Greece remembers Mati wildfire victims. *Balkan Insight*. https://balkaninsight.com/

Bellas, R., Galdo, M., Barreira, L., Gómez, M., & Vilán, J. A. (2026). Fire and evacuation simulation in a leisure and spa resort using FDS and Pathfinder. *Safety Science*, *170*, Article 106366. https://doi.org/10.1016/j.ssci.2023.106366

British Standards Institution. (2019). *PD 7974-6:2019. Application of fire safety engineering principles to the design of buildings. Part 6: Human factors: Life safety strategies — Occupant evacuation, behaviour and condition (Sub-system 6)*. BSI.

European Commission Joint Research Centre. (2022). *Forest fires in Europe, Middle East and North Africa 2021* (JRC Technical Report). Publications Office of the European Union. https://doi.org/10.2760/034135

European Commission Joint Research Centre. (2023). *Forest fires in Europe, Middle East and North Africa 2022* (JRC Technical Report). Publications Office of the European Union. https://doi.org/10.2760/091540

Folk, L. H., Kuligowski, E. D., Gwynne, S. M. V., & Gales, J. A. (2019). A provisional conceptual model of human behavior in response to wildland-urban interface fires. *Fire Technology*, *55*(5), 1619-1647. https://doi.org/10.1007/s10694-019-00821-z

Fruin, J. J. (1971). *Pedestrian planning and design*. Metropolitan Association of Urban Designers and Environmental Planners.

Gwynne, S. M. V., & Boyce, K. E. (2016). Engineering data. In M. J. Hurley (Ed.), *SFPE handbook of fire protection engineering* (5th ed., pp. 2429-2551). Springer. https://doi.org/10.1007/978-1-4939-2565-0_64

Helbing, D., & Molnár, P. (1995). Social force model for pedestrian dynamics. *Physical Review E*, *51*(5), 4282-4286. https://doi.org/10.1103/PhysRevE.51.4282

Helbing, D., & Mukerji, P. (2012). Crowd disasters as systemic failures: Analysis of the Love Parade disaster. *EPJ Data Science*, *1*(1), Article 7. https://doi.org/10.1140/epjds7

Hunter, J. D. (2007). Matplotlib: A 2D graphics environment. *Computing in Science & Engineering*, *9*(3), 90-95. https://doi.org/10.1109/MCSE.2007.55

Johnson, N. L., Kotz, S., & Balakrishnan, N. (1994). *Continuous univariate distributions* (Vol. 1, 2nd ed.). Wiley.

Korhonen, T., Hostikka, S., Heliövaara, S., & Ehtamo, H. (2008). FDS+Evac: An agent based fire evacuation model. In W. W. F. Klingsch, C. Rogsch, A. Schadschneider, & M. Schreckenberg (Eds.), *Pedestrian and evacuation dynamics 2008* (pp. 109-120). Springer. https://doi.org/10.1007/978-3-642-04504-2_8

Labhiri, A. (2024). *Informing wildfire evacuation guidelines in touristic areas* [Master's thesis, Lund University]. International Master of Science in Fire Safety Engineering (IMFSE).

Labhiri, A., Ronchi, E., & Rohaert, A. (2024). A scoping review of tourist evacuation behavior in wildfire scenarios. *Safety Science*, *175*, Article 106516. https://doi.org/10.1016/j.ssci.2024.106516

Lovreglio, R., Ronchi, E., Kinsey, M. J., & Adalsteinsson, E. T. (2023). Modeling the evacuation of a large humanitarian settlement: A case study using Pathfinder. *Safety Science*, *160*, Article 106058. https://doi.org/10.1016/j.ssci.2022.106058

McKinney, W. (2010). Data structures for statistical computing in Python. In S. van der Walt & J. Millman (Eds.), *Proceedings of the 9th Python in Science Conference* (pp. 56-61). https://doi.org/10.25080/Majora-92bf1922-00a

Ministerio del Interior. (2007). Real Decreto 393/2007, de 23 de marzo, por el que se aprueba la Norma Básica de Autoprotección de los centros, establecimientos y dependencias dedicados a actividades que puedan dar origen a situaciones de emergencia. *Boletín Oficial del Estado*, 72, 12841-12850.

Moussaïd, M., Perozo, N., Garnier, S., Helbing, D., & Theraulaz, G. (2010). The walking behaviour of pedestrian social groups and its impact on crowd dynamics. *PLoS ONE*, *5*(4), Article e10047. https://doi.org/10.1371/journal.pone.0010047

Oberhagemann, D. (2012). *Static and dynamic crowd densities at major public events* (Technical Report TB 13-01). Vereinigung zur Förderung des Deutschen Brandschutzes e. V. (vfdb).

Pheasant, S., & Haslegrave, C. M. (2006). *Bodyspace: Anthropometry, ergonomics and the design of work* (3rd ed.). CRC Press. https://doi.org/10.1201/9781420043693

Ronchi, E., Gwynne, S. M. V., Rein, G., Intini, P., & Wadhwani, R. (2019). An open multi-physics framework for modeling wildland-urban interface fire evacuations. *Safety Science*, *118*, 868-880. https://doi.org/10.1016/j.ssci.2019.06.009

Ronchi, E., & La Mendola, S. (2016). *Sensitivity analysis of evacuation model results using the Kolmogorov-Smirnov test* (Report No. LUTVDG/TVBB-3215-SE). Department of Fire Safety Engineering, Lund University.

Ronchi, E., & Nilsson, D. (2016). Modeling total evacuation strategies for high-rise buildings. *Building Simulation*, *9*(2), 165-177. https://doi.org/10.1007/s12273-015-0261-0

Ronchi, E., Wahlqvist, J., Gwynne, S. M. V., Lovreglio, R., & Kuligowski, E. D. (2023). Verification and validation of evacuation models for wildland-urban interface fire evacuation. *Fire Technology*, *59*(3), 1261-1290. https://doi.org/10.1007/s10694-023-01377-5

Salas, J. (2024, March 12). Spain broke its own wildfire record in 2022, burning nearly 245,000 hectares. *El País English*. https://english.elpais.com/

San-Miguel-Ayanz, J., Durrant, T., Boca, R., Maianti, P., Libertà, G., Artés-Vivancos, T., Oom, D., Branco, A., de Rigo, D., Ferrari, D., Pfeiffer, H., Grecchi, R., & Nuijten, D. (2024). *Forest fires in Europe, Middle East and North Africa 2023* (JRC Technical Report). Publications Office of the European Union. https://doi.org/10.2760/318925

Thornton, C., O'Konski, R., Hardeman, B., & Swenson, D. (2011). Pathfinder: An agent-based egress simulator. In R. D. Peacock, E. D. Kuligowski, & J. D. Averill (Eds.), *Pedestrian and evacuation dynamics* (pp. 889-892). Springer. https://doi.org/10.1007/978-1-4419-9725-8_94

Thunderhead Engineering. (2024). *Pathfinder technical reference manual* (Version 2024.1). Thunderhead Engineering Consultants, Inc. https://www.thunderheadeng.com/pathfinder

Thunderhead Engineering. (2026). *Movement groups* [Online documentation]. Thunderhead Engineering Consultants, Inc. https://www.thunderheadeng.com/pathfinder

Wahlqvist, J., Ronchi, E., Gwynne, S. M. V., Kinateder, M., Rein, G., Mitchell, H., Bénichou, N., Ma, C., Kimball, A., & Baker, G. (2021). The simulation of wildland-urban interface fire evacuation: The WUI-NITY platform. *Safety Science*, *136*, Article 105145. https://doi.org/10.1016/j.ssci.2020.105145

Annex A. Alignment with the United Nations Sustainable Development Goals

This annex describes the alignment of the present study with the United Nations Sustainable Development Goals (SDGs) adopted in the 2030 Agenda for Sustainable Development. The project contributes directly to two SDGs and indirectly to one additional one.

SDG 11: Sustainable Cities and Communities

Target 11.5 aims to significantly reduce the number of deaths and the number of people affected by disasters, including water-related disasters, with a focus on protecting the poor and people in vulnerable situations. This project contributes directly to this target by providing quantitative evacuation performance data for two tourist campings located in wildfire-prone areas of Spain. The simulation campaign identifies site-specific vulnerabilities, such as the de-facto single-exit configuration at Parque Ardales and the muster-collapse phenomenon at Cabo Mayor, that would not be detected through paper-based emergency planning alone. The operational recommendations formulated in Chapter 7, including the prioritization of nighttime alerting systems, the protection of critical exit infrastructure, and the redesign of muster protocols to preserve exit redundancy, are directly actionable by local authorities and campsite operators to reduce the human impact of wildfire emergencies.

Target 11.b calls for an increase in the number of cities and human settlements adopting integrated policies and plans toward resilience to disasters, in line with the Sendai Framework for Disaster Risk Reduction. The methodology developed in this study, a systematic seven-scenario simulation campaign applied comparatively across two sites, provides a replicable framework that municipalities and civil protection authorities can adopt to evaluate and improve the Self-Protection Plans (Planes de Autoprotección) required under Real Decreto 393/2007.

SDG 13: Climate Action

Target 13.1 calls for strengthening resilience and adaptive capacity to climate-related hazards and natural disasters in all countries. Wildfire frequency and severity in southern Europe are increasing as a consequence of climate change, with the European Forest Fire Information System recording over 500,000 hectares burned in the EU in 2023 alone (San-Miguel-Ayanz et al., 2024). This project contributes to climate adaptation by developing simulation tools and evidence-based recommendations that improve the preparedness of tourist infrastructure, a sector particularly exposed to climate-driven wildfire risk due to the overlap between peak fire season and peak tourism season in the Mediterranean basin.

SDG 3: Good Health and Well-Being

Target 3.d aims to strengthen the capacity of all countries for early warning, risk reduction, and management of national and global health risks. While this target is primarily oriented toward epidemiological risks, the principles of early warning and risk reduction apply directly to wildfire evacuation. The principal finding of this study, that nighttime pre-movement time is the dominant determinant of total evacuation time at both campings, identifies early alerting infrastructure as the single highest-leverage intervention for protecting human life. The recommendation to install audible alarm systems in all accommodation units translates this finding into a concrete public health measure.

Annex B. Project Timeline

This annex presents the project timeline as a Gantt chart. The project was developed over approximately nine months, from October 2025 to June 2026, corresponding to the 6 ECTS credits allocated to the Final Degree Project in the GITI curriculum (approximately 150 hours of student work). The work was organized into five sequential phases with partial overlaps where the nature of the tasks permitted concurrent progress. May is subdivided into two half-month periods to reflect the transition between the simulation campaign (Phase 3) and the post-processing and analysis (Phase 4).

Task	Oct	Nov	Dec	Jan	Feb	Mar	Apr	May (1st)	May (2nd)	Jun
Phase 1: Tool familiarization and literature review										
Pathfinder installation and familiarization										
Literature review (pedestrian modeling, pre-movement, WUI)										
Site selection and data collection										
Phase 2: Geometry capture and model construction										
PA model: background importation and geometry										
CM model: background importation and geometry										
Occupant profile and pre-movement calibration										
Phase 3: Profile calibration, scenario definition, and simulation campaign										
Scenario design (S1-S7) and verification										
Simulation campaign execution (70 runs)										
Phase 4: Post-processing, analysis, and comparative synthesis										
Python post-processing and figure generation										
Per-camping and comparative analysis										
Phase 5: Recommendations, thesis drafting, and defense preparation										
Thesis drafting (Chapters 1-8, Annexes)										
Defense preparation										

Table B.1. Project Gantt chart. Colored cells indicate active work periods. Phase rows (green background) show the aggregate span; task rows show individual activities within each phase.

Annex C. Derivation of the Log-Normal Pre-Movement Parameters

The pre-movement time T is modeled as a log-normal random variable, meaning that ln(T) is normally distributed. If T is expressed in minutes, the distribution is characterized by two parameters on the logarithmic scale: the Location parameter $\mu\_min = E[\ln(T\_min)]$, the mean of the natural logarithm of the time in minutes; and the Scale parameter $\sigma = SD[\ln(T\_min)]$, the standard deviation of the natural logarithm.

Pathfinder's Initial Delay field operates in seconds, so the variable must be expressed as $T\_sec = 60 \cdot T\_min$. The two log-scale parameters transform as follows.

Location parameter (μ)

Taking the natural logarithm of the unit conversion:

$$\ln(T\_sec) = \ln(60 \cdot T\_min) = \ln(60) + \ln(T\_min)$$

Taking expectations of both sides:

$$\mu\_sec = E[\ln(T\_sec)] = \ln(60) + E[\ln(T\_min)] = \mu\_min + \ln(60)$$

With $\ln(60) \approx 4.0943$, the Location parameter increases additively by this amount when converting from minutes to seconds.

Scale parameter (σ)

Since ln(60) is a constant, adding it to ln(T_min) shifts the distribution of the logarithm without changing its dispersion:

$$\sigma\_sec = SD[\ln(T\_sec)] = SD[\ln(60) + \ln(T\_min)] = SD[\ln(T\_min)] = \sigma\_min$$

The Scale parameter is therefore invariant under the change of time unit.

Applied values

Applying the transformation to the minute-scale descriptions of PD 7974-6:2019 categories B (day) and Ciii (night) yields the second-based parameters entered into Pathfinder, summarised in Table C.1.

State	μ (min)	μ (s) = μ_min + ln(60)	σ (invariant)	Bounds (s)
Day (Cat B)	2.6492	6.7435	0.1487	600-1200
Night (Cat Ciii)	3.3424	7.4367	0.1487	1200-2400

Table C.1. Log-normal pre-movement parameters in minutes and seconds. The Location parameter increases by ln(60) ≈ 4.0943 under the unit conversion; the Scale parameter is invariant. Bounds correspond to the 1st and 99th percentiles.

These second-scale parameters correspond to a median pre-movement time of approximately 848 s (14.1 min) for the daytime distribution and 1697 s (28.3 min) for the night-time distribution. The 1st and 99th percentiles of the fitted distributions coincide with the configured bounds (600 and 1200 s for day; 1200 and 2400 s for night), confirming the internal consistency of the parametrization. The realized distributions were verified by Kolmogorov-Smirnov test in Section 5.4.2.

Annex D. Complete Occupant Profile Parameters

This annex compiles all parameter distributions used to configure the occupant profiles in both Pathfinder models. The parameters documented here correspond to the values entered in the Profile and Behavior dialogs of Pathfinder 2026.1.211 and are identical at both campings. Truncation bounds for speed and shoulder width correspond to the 5th and 95th percentiles, following the anthropometric convention of Pheasant and Haslegrave (2006). Pre-movement time bounds correspond to the 1st and 99th percentiles, following PD 7974-6:2019 (BSI, 2019). The percentile convention difference is deliberate: each variable adopts the convention of its source standard.

D.1 Walking Speed

Walking speed was configured in the Profile > Speed field as a truncated Normal distribution. Night speeds were obtained by multiplying all day parameters (mean, SD, min, max) by a factor of 0.75, following Labhiri (2024, Section 5.5). The Kolmogorov-Smirnov test on the Adult Day sample from CM S1 Run 1 ($n = 332$) returned $D = 0.036$, not rejected at $\alpha = 0.05$.

Parameter	Distribution	Mean	SD	Min	Max	Unit	Source
Adult Day	Trunc. Normal	1.25	0.18	0.95	1.55	m/s	Labhiri (2024); PD 7974-6
Child Day	Trunc. Normal	0.90	0.18	0.60	1.20	m/s	Labhiri (2024); PD 7974-6
Elderly Day	Trunc. Normal	0.80	0.18	0.50	1.10	m/s	Labhiri (2024); PD 7974-6
Adult Night	Trunc. Normal	0.94	0.135	0.71	1.16	m/s	Day × 0.75
Child Night	Trunc. Normal	0.675	0.135	0.45	0.90	m/s	Day × 0.75
Elderly Night	Trunc. Normal	0.60	0.135	0.38	0.83	m/s	Day × 0.75

Table D.1. Walking speed parameters by profile and time of day. All distributions are truncated Normal. Night parameters are Day × 0.75. Bounds correspond to the 5th and 95th percentiles.

D.2 Shoulder Width

Shoulder width was configured in the Profile > Shoulder Width field as a truncated Normal distribution. The same values apply to both day and night scenarios, as body dimensions do not change with lighting conditions.

Profile	Distribution	Mean	SD	Min (P5)	Max (P95)	Unit	Source
Adult	Trunc. Normal	0.510	0.0426	0.44	0.58	m	Pheasant & Haslegrave (2006)
Child	Trunc. Normal	0.420	0.0182	0.39	0.45	m	Pheasant & Haslegrave (2006)
Elderly	Trunc. Normal	0.500	0.0243	0.46	0.54	m	Pheasant & Haslegrave (2006)

Table D.2. Shoulder width parameters by profile. Bounds correspond to the 5th and 95th percentiles of the anthropometric data from Pheasant and Haslegrave (2006).

D.3 Height

Height was configured in the Profile > Height field as a Uniform distribution between the minimum and maximum values listed below. Height affects the visual representation of occupants in the Pathfinder results viewer but does not influence the movement algorithm in Steering mode.

Profile	Distribution	Min	Max	Unit	Source

Adult	Uniform	1.60	1.85	m	Pheasant & Haslegrave (2006)
Child	Uniform	1.30	1.60	m	Pheasant & Haslegrave (2006)
Elderly	Uniform	1.55	1.75	m	Pheasant & Haslegrave (2006)

Table D.3. Height parameters by profile. Uniform distribution.

D.4 Pre-Movement Time

Pre-movement time was configured in the Behavior > Initial Delay field as a log-normal distribution. The Location and Scale parameters are defined on the natural-logarithm scale. The conversion from the minute-based parameters of PD 7974-6:2019 to the second-based parameters required by Pathfinder follows the transformation $\mu\_s = \mu\_min + \ln(60)$, with Scale ($\sigma$) invariant. The full derivation is documented in Annex C. The same distribution applies to all three demographic profiles within each time-of-day condition.

Condition	PD 7974-6 Cat.	Distribution	Location	Scale	Min (P1)	Max (P99)	Median	Unit
Day (awake)	B	Log-normal	6.7435	0.1487	600	1200	848	s
Night (asleep)	Ciii	Log-normal	7.4367	0.1487	1200	2400	1697	s

Table D.4. Pre-movement time parameters by time of day. Log-normal distribution with bounds at the 1st and 99th percentiles of PD 7974-6:2019, Categories B (day) and Ciii (night), management level M2-M3. Median = exp(Location).

D.5 Muster Wait Time

The muster wait time was configured as a Wait action in the Behavior sequence for scenarios S2 and S6. It represents the time spent at the assembly point before proceeding to the exit. The night-to-day ratio of 1.6 was preserved from Labhiri (2024). The absolute values are lower than Labhiri's to reflect the smaller occupant populations (500 and 650 vs. 900) and the compact assembly areas of the two campings studied.

Condition	Distribution	Mean	SD	Min	Max	Unit	Source
Day	Trunc. Normal	90	30	30	180	s	Adapted from Labhiri (2024)
Night	Trunc. Normal	144	48	60	360	s	Day × 1.6 ratio

Table D.5. Muster wait-time parameters by time of day. Truncated Normal distribution.

D.6 Demographic Composition

The table below summarizes the demographic breakdown at each camping. The approximate 50/40/10 split (Adult/Child/Elderly) was maintained at both sites, following Labhiri (2024). Minor deviations arise from the fixed family compositions assigned to individual bungalows, particularly at Cabo Mayor.

Site	Total	Adult	Child	Elderly	Adult %	Child %	Elderly %
Parque Ardales	500	253	198	49	50.6	39.6	9.8
Cabo Mayor	650	332	263	55	51.1	40.5	8.5

Table D.6. Occupant demographic composition by site.

Annex E. Detailed Per-Run Simulation Results

This annex reports the principal evacuation metrics for each individual simulation run across both campings and all seven scenarios. Each scenario was executed five times with independent random seeds, yielding 35 runs per site and 70 runs in total. The values reported here are computed directly from the per-occupant CSV files exported by Pathfinder. TotalT is the exit time of the last occupant (RSET). MeanCompT is the mean exit time across all occupants. Mean Dist is the mean walking distance. Mean Active is the mean active movement time (excluding pre-movement delay). Mean Cong is the mean congestion time per occupant, defined as the cumulative time during which an occupant's actual velocity was below its seek velocity.

E.1 Parque Ardales (500 occupants)

Scenario	Run	TotalT (min)	MeanCompT (min)	Mean Dist (m)	Mean Active (s)	Mean Cong (s)
S1	1	30.19	20.27	357.9	361.0	3.0
S1	2	32.45	20.32	357.5	369.8	3.0
S1	3	31.39	20.31	357.8	358.9	3.0
S1	4	29.95	20.17	357.8	363.7	3.0
S1	5	28.78	20.31	357.7	362.2	3.0
S2	1	33.37	21.63	366.1	350.4	11.6
S2	2	31.77	21.81	366.6	362.1	13.7
S2	3	32.94	21.74	366.7	356.9	12.9
S2	4	32.38	21.61	366.5	355.7	12.3
S2	5	30.42	21.72	366.8	358.3	11.6
S3	1	33.32	20.95	402.7	404.7	3.0
S3	2	34.2	20.92	403.2	402.9	2.9
S3	3	32.54	21.12	403.0	410.8	3.0
S3	4	30.76	20.98	402.9	412.4	3.0
S3	5	30.91	21.08	403.3	406.8	3.0
S4	1	29.55	20.47	357.7	360.6	3.0
S4	2	32.83	20.3	357.5	362.0	3.0
S4	3	31.73	20.29	357.7	359.1	3.0
S4	4	29.73	20.43	357.6	363.8	3.0
S4	5	34.38	20.43	357.4	365.0	3.0
S5	1	51.0	36.61	356.4	474.2	3.8
S5	2	54.99	36.84	356.5	484.6	3.9
S5	3	53.08	36.61	356.6	479.7	3.8
S5	4	51.55	36.48	356.5	477.4	3.8
S5	5	52.93	36.88	356.7	483.4	3.9
S6	1	56.68	38.92	366.0	475.8	16.2
S6	2	54.9	38.5	366.4	467.2	16.0
S6	3	53.99	39.39	365.7	478.1	16.7
S6	4	59.8	39.04	365.5	468.9	15.3
S6	5	53.86	38.86	366.2	472.3	16.1
S7	1	33.38	24.05	469.8	587.9	121.1
S7	2	33.95	24.46	478.5	608.8	133.6
S7	3	35.63	24.25	466.6	592.2	125.6
S7	4	36.28	24.31	477.7	603.7	126.6
S7	5	35.13	23.88	467.3	581.0	115.8

Table E.1. Per-run evacuation metrics for Parque Ardales, 7 scenarios × 5 runs = 35 simulations.

E.2 Parque Ardales — Scenario Summaries

Scenario		TotalT (min)	MeanCompT (min)	Mean Dist (m)		
S1	Mean	30.55	20.28	357.7		
	SD	1.26	0.06			
S2	Mean	32.18	21.70	366.5		
	SD	1.03	0.07			
S3	Mean	32.35	21.01	403.0		
	SD	1.34	0.08			
S4	Mean	31.64	20.38	357.6		
	SD	1.84	0.07			
S5	Mean	52.71	36.68	356.5		
	SD	1.39	0.15			
S6	Mean	55.85	38.94	366.0		
	SD	2.22	0.29			
S7	Mean	34.87	24.19	472.0		
	SD	1.07	0.20			

Table E.2. Scenario-level means and standard deviations for Parque Ardales.

E.3 Cabo Mayor (650 occupants)

Scenario	Run	TotalT (min)	MeanCompT (min)	Mean Dist (m)	Mean Active (s)	Mean Cong (s)
S1	1	24.04	16.29	118.5	120.2	3.0
S1	2	22.94	16.31	118.7	121.1	3.0
S1	3	24.3	16.31	118.6	120.0	3.0
S1	4	24.09	16.23	118.6	120.1	3.0
S1	5	22.77	16.23	118.7	120.5	3.0
S2	1	23.88	18.42	133.6	140.3	29.7
S2	2	25.56	18.22	132.9	134.1	23.3
S2	3	26.02	18.21	132.9	133.4	23.6
S2	4	24.72	18.34	132.9	132.6	22.4
S2	5	25.41	18.08	133.0	132.5	22.5
S3	1	23.51	16.38	127.6	131.5	3.1
S3	2	24.02	16.38	127.4	129.4	3.0
S3	3	22.59	16.43	127.7	129.9	3.0
S3	4	23.81	16.37	127.3	129.7	3.0
S3	5	23.65	16.4	127.3	130.8	3.0
S4	1	26.87	16.89	151.3	156.1	3.0
S4	2	24.22	16.84	151.4	154.9	3.0
S4	3	23.65	16.86	151.2	152.9	3.0
S4	4	23.89	16.87	151.3	155.0	3.0
S4	5	24.27	16.73	151.3	154.7	3.0
S5	1	44.33	31.17	118.1	157.8	3.9
S5	2	43.52	31.18	118.1	158.8	3.9
S5	3	43.34	31.39	118.3	158.3	3.8
S5	4	43.75	31.02	118.2	158.8	3.9
S5	5	45.43	31.14	118.8	156.6	3.8
S6	1	47.23	35.03	132.9	176.2	31.7
S6	2	48.0	35.0	132.8	177.0	32.8
S6	3	46.55	34.58	132.7	170.3	26.5
S6	4	48.34	34.85	132.8	175.2	30.3
S6	5	47.59	34.75	132.7	174.0	28.7
S7	1	24.25	19.04	281.0	285.0	124.3
S7	2	24.6	18.83	275.1	277.0	118.4
S7	3	24.29	18.8	279.1	273.6	115.6
S7	4	24.82	18.93	274.4	281.0	122.8
S7	5	24.02	18.79	276.2	276.1	121.6

Table E.3. Per-run evacuation metrics for Cabo Mayor, 7 scenarios × 5 runs = 35 simulations.

E.4 Cabo Mayor — Scenario Summaries

Scenario		TotalT (min)	MeanCompT (min)	Mean Dist (m)		
S1	**Mean**	**23.63**	**16.27**	**118.6**		
	SD	**0.64**	**0.04**			
S2	**Mean**	**25.12**	**18.25**	**133.1**		
	SD	**0.75**	**0.12**			
S3	**Mean**	**23.52**	**16.39**	**127.5**		
	SD	**0.49**	**0.02**			
S4	**Mean**	**24.58**	**16.84**	**151.3**		

	SD	1.17	0.06			
S5	Mean	44.07	31.18	118.3		
	SD	0.76	0.12			
S6	Mean	47.54	34.84	132.8		
	SD	0.62	0.17			
S7	Mean	24.40	18.88	277.2		
	SD	0.28	0.09			

Table E.4. Scenario-level means and standard deviations for Cabo Mayor.

Annex F. Python Analysis Scripts

This annex reproduces the principal Python scripts used for the post-processing of Pathfinder simulation outputs and the generation of figures. All scripts use Python 3.x with pandas (McKinney, 2010), NumPy, Matplotlib (Hunter, 2007), and SciPy. The scripts are organized by function: scenario aggregation, evacuation curve generation, measurement-region density processing, and exit-usage visualization.

F.1 Scenario Aggregation

This script reads the per-occupant CSV files exported by Pathfinder for each run and computes per-run statistics (TotalT, MeanCompT, mean distance, mean congestion time), then aggregates them across runs to produce scenario-level means, standard deviations, and coefficients of variation. The per-run output forms the basis of Annex E.

```
import pandas as pd
import numpy as np
import os, glob

SITE = "CM"           # or "PA"
N_OCCUPANTS = 650     # or 500
DATA_DIR = f"./{SITE}_Occupants"
SCENARIOS = [f"S{i}" for i in range(1, 8)]
N_RUNS = 5

records = []
for scen in SCENARIOS:
    run_stats = []
    for r in range(1, N_RUNS + 1):
        fname = f"{DATA_DIR}/{SITE}_{scen}_R{r}_Occ.csv"
        df = pd.read_csv(fname)
        et = df["exit time(s)"].values
        at = df["active time(s)"].values
        dist = df["distance (m)"].values
        cong = df["congestion time total(s)"].values

        run_stats.append({
            "scenario": scen, "run": r,
            "TotalT_s": np.max(et),
            "MeanCompT_s": np.mean(et),
            "MeanDist_m": np.mean(dist),
            "MeanActive_s": np.mean(at),
            "MeanCong_s": np.mean(cong),
        })
    records.extend(run_stats)

df_all = pd.DataFrame(records)

# Per-run table (Annex E)
df_all["TotalT_min"] = df_all["TotalT_s"] / 60
df_all["MeanCompT_min"] = df_all["MeanCompT_s"] / 60
df_all.to_csv(f"{SITE}_per_run_results.csv", index=False)

# Scenario aggregates
agg = df_all.groupby("scenario").agg(
    TotalT_mean=("TotalT_s", "mean"),
```

```
        TotalT_std=("TotalT_s", "std"),
        MeanCompT_mean=("MeanCompT_s", "mean"),
        MeanDist_mean=("MeanDist_m", "mean"),
    ).reset_index()
    agg["CoV"] = agg["TotalT_std"] / agg["TotalT_mean"] * 100
    print(agg.to_string(index=False))
```

F.2 Evacuation Curves with Stochastic Bands

This script generates the evacuation curves shown in Chapter 6 (Figures 6.1 and 6.14). For each scenario, the five per-run curves of occupants remaining versus time are computed at 1.0 s resolution, then the mean and standard deviation are plotted with shading. Vertical background bands show the range of total evacuation time (last occupant) across the five runs.

```
import pandas as pd
import numpy as np
import matplotlib.pyplot as plt

SITE = "CM"
N = 650
DATA_DIR = f"./{SITE}_Occupants"

scenarios = {
    "S1": {"label": "S1 Day/Direct",       "color": "#1f77b4", "ls": "-
"},
    "S2": {"label": "S2 Day/Muster",       "color": "#2ca02c", "ls": "-
"},
    "S3": {"label": "S3 Day/Direct/E1",    "color": "#ff7f0e", "ls": "-
"},
    "S4": {"label": "S4 Day/Direct/E2",    "color": "#9467bd", "ls": "-
"},
    "S5": {"label": "S5 Night/Direct",     "color": "#2ca02c", "ls": "--
"},
    "S6": {"label": "S6 Night/Muster",     "color": "#9467bd", "ls": "--
"},
    "S7": {"label": "S7 Day/Group",        "color": "#d62728", "ls": "-
"},
}

t_max = 3500
time_axis = np.arange(0, t_max + 1, 1.0)
results = {}

for sid, props in scenarios.items():
    curves = []
    totals = []
    for r in range(1, 6):
        df = pd.read_csv(f"{DATA_DIR}/{SITE}_{sid}_R{r}_Occ.csv")
        et = df["exit time(s)"].values
        remaining = np.array([np.sum(et > t) for t in time_axis])
        curves.append(remaining)
        totals.append(np.max(et))

    curves = np.array(curves)
    results[sid] = {
        "mean": np.mean(curves, axis=0),
        "std": np.std(curves, axis=0),
        "total_min": np.min(totals),
        "total_max": np.max(totals),
```

```
        "props": props,
    }

fig, ax = plt.subplots(figsize=(10, 6))
t_min = time_axis / 60.0

for sid in ["S5", "S6", "S1", "S2", "S3", "S4", "S7"]:
    r = results[sid]
    p = r["props"]
    ax.axvspan(r["total_min"]/60, r["total_max"]/60,
               alpha=0.15, color=p["color"], zorder=0)
    ax.plot(t_min, r["mean"], label=p["label"],
            color=p["color"], ls=p["ls"], lw=1.8, zorder=2)
    ax.fill_between(t_min, r["mean"] - r["std"],
                    r["mean"] + r["std"],
                    color=p["color"], alpha=0.12, zorder=1)

ax.set_xlabel("Simulation time (min)")
ax.set_ylabel("Occupants remaining")
ax.set_title(f"{SITE} — Evacuation curves (mean ± 1 SD)")
ax.legend(loc="upper right")
ax.grid(True, alpha=0.3)
plt.tight_layout()
plt.savefig(f"{SITE}_evacuation_curves.png", dpi=300)
```

F.3 Measurement-Region Density Processing

This script processes the measurement-region CSV files exported by Pathfinder. Each CSV contains time-series data for all five measurement regions at 1.0 s intervals, with a three-row header (MR name, metric, unit). The script extracts peak density and time-to-peak for each MR in each run and aggregates across runs to produce the scenario-mean peak density tables reported in Chapter 6 (Tables 6.2 and 6.4).

```
import pandas as pd
import numpy as np
import os

SITE = "CM"
MR_DIR = f"./{SITE}_MR"
SCENARIOS = [f"S{i}" for i in range(1, 8)]
N_RUNS = 5

# MR CSV format: 3 header rows, 1.0 s interval
# Row 0: MR names, Row 1: metric, Row 2: unit
# Read with header=[0,1], skip row 2

records = []
for scen in SCENARIOS:
    for r in range(1, N_RUNS + 1):
        fname = f"{MR_DIR}/{SITE}_{scen}_R{r}_MR.csv"
        if not os.path.exists(fname):
            continue
        df = pd.read_csv(fname, header=[0, 1], skiprows=[2])
        # Column names are tuples: (MR_name, metric)
        # Filter density columns
        density_cols = [c for c in df.columns
                        if "density" in str(c[1]).lower()
                        or "Density" in str(c[1])]
```

```
        for col in density_cols:
            mr_name = col[0].strip()
            series = pd.to_numeric(df[col], errors="coerce")
            peak = series.max()
            t_peak = series.idxmax()
            records.append({
                "scenario": scen, "run": r,
                "MR": mr_name,
                "peak_density": peak,
                "t_peak_s": t_peak,
            })

df_density = pd.DataFrame(records)

# Scenario-mean peak density per MR
pivot = df_density.groupby(["scenario", "MR"]) \
    .agg(peak_mean=("peak_density", "mean"),
         peak_std=("peak_density", "std")) \
    .reset_index()
pivot.to_csv(f"{SITE}_peak_density_by_scenario.csv", index=False)
print(pivot.to_string(index=False))
```

F.4 Exit-Usage Bar Chart

This script generates the exit-usage comparison charts (Figures 6.2 and 6.15) showing the number of occupants using each exit per scenario at both campings. The dominant exit is shown in navy and the secondary exit in orange, following the color convention adopted throughout Chapter 6.

```
import matplotlib.pyplot as plt
import numpy as np

# Data from master results (scenario means)
scenarios = ["S1", "S2", "S3", "S4", "S5", "S6", "S7"]

# PA exit splits: Exit_2 / Exit_1
pa_exit2 = [499, 500, 0, 500, 499, 500, 499]
pa_exit1 = [1, 0, 500, 0, 1, 0, 1]

# CM exit splits: Exit / Exit_Peatonal
cm_exit  = [509, 649, 650, 0, 509, 650, 513]
cm_ep    = [141, 1, 0, 650, 141, 0, 137]

fig, (ax1, ax2) = plt.subplots(1, 2, figsize=(12, 5))
x = np.arange(len(scenarios))
w = 0.35

# PA
ax1.bar(x - w/2, pa_exit2, w, label="Exit 2", color="#1f4e79")
ax1.bar(x + w/2, pa_exit1, w, label="Exit 1", color="#ed7d31")
ax1.set_xticks(x)
ax1.set_xticklabels(scenarios)
ax1.set_ylabel("Occupants")
ax1.set_title("Parque Ardales — Exit usage")
ax1.legend()

# CM
ax2.bar(x - w/2, cm_exit, w, label="Exit", color="#1f4e79")
```

```
ax2.bar(x + w/2, cm_ep, w, label="Exit Peatonal", color="#ed7d31")
ax2.set_xticks(x)
ax2.set_xticklabels(scenarios)
ax2.set_title("Cabo Mayor — Exit usage")
ax2.legend()

plt.tight_layout()
plt.savefig("exit_usage_comparison.png", dpi=300)
```